DEPARTMENT OF COMMERCE
SINCLAIR WEEKS, Secretary

WEATHER BUREAU
F. W. REICHELDERFER, Chief

MONTHLY WEATHER REVIEW

JAMES E. CASKEY, JR., Editor

Volume 86
Number 7

JULY 1958

Closed September 15, 1958
Issued October 15, 1958

THE ERROR IN NUMERICAL FORECASTS DUE TO RETROGRESSION OF ULTRA-LONG WAVES

PAUL M. WOLFF, CDR, U. S. NAVY[1]

Joint Numerical Weather Prediction Unit, Suitland, Md.

[Manuscript Received April 25, 1958; revised June 3, 1958]

ABSTRACT

Error charts for the numerical barotropic forecasts prepared at the Joint Numerical Weather Prediction Unit since October 1957 have revealed retrogressive patterns of very long wavelength. These errors are shown to be due to changes in the large-scale components predicted by the numerical model. These components are actually quasi-stationary in the atmosphere. Forecasts prepared with an approximation to these components held unchanged show significantly increased accuracy. Finally, some of the difficulties in developing a more acceptable physical approach to this problem are outlined.

1. INTRODUCTION

Beginning in October 1957 500-mb. barotropic forecasts by the Joint Numerical Weather Prediction Unit were prepared on a hemispheric basis with boundaries in the Tropics. The smaller area of previous forecasts had boundaries in meteorologically active locations, and it was widely anticipated that this expansion would be accompanied by a large reduction in gross error. Instead, the new error patterns were of very long wavelength and showed westward motion during the forecast.

Figure 1 is a 48-hour error chart in which the type of error treated here is prominent. The scale of the pattern is much greater than that of the corresponding 48-hour observed height changes. The largest scale error is positive over the central Pacific Ocean and negative over the eastern Atlantic and western Europe. The persistence in location of these errors from day to day has been so high that the variations in shape and intensity due to other causes are not large enough to cause a reversal of sign in these areas. That is, while the magnitude

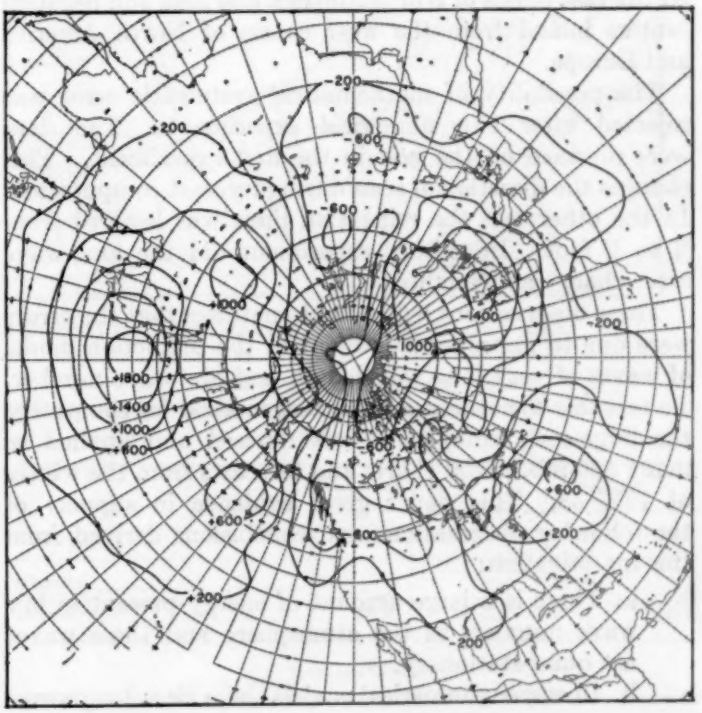

FIGURE 1.—48-hour error in feet. JNWP Unit operational forecast from 0000 GMT, January 16, 1958.

[1] Any opinions expressed by the author are his own and do not necessarily reflect the views of the Navy Department. Author's present affiliation: Navy Numerical Weather Problems Group, Fleet Weather Central, Suitland, Md.

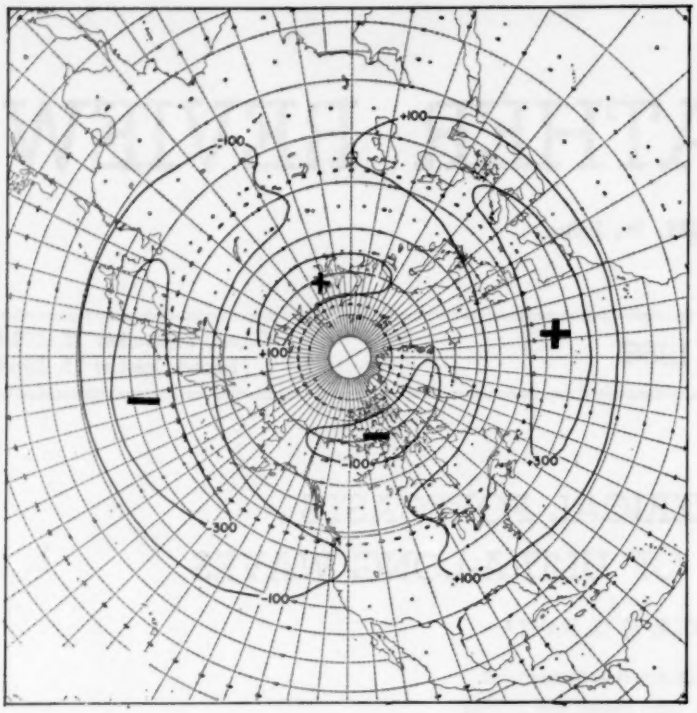

FIGURE 2.—Wave number one, in feet. Initial data, 0000 GMT, January 6, 1958.

of the error over the Pacific varies it always has a positive sign in the 48-hour forecasts. Similarly the sign of the error on the west coast of northern Europe has always been negative.

Some other persistent errors of smaller scale and slightly less persistence should also be noted in figure 1. These patterns are continental in scale and have positive centers off the east coasts of North America and Asia and negative centers inland from the west coasts of North America and Europe.

The possibility of mathematical systematic error was rejected after two numerical experiments. The data were reversed on the grid in the first experiment. This changes the direction of scan during forecast computation. In the other test the relaxation limit was lowered from ½ to ¼ foot. In neither experiment did the long-wave error change appreciably.

These observations led to the hypothesis that the errors were due to improper treatment in the prediction model of waves of very long wavelength and low wave number. To test this hypothesis a numerical method for computing the large-scale component was devised and applied to many 500-mb. initial charts and forecasts from the winter of 1957–58. This paper gives evidence in support of the following observations and conclusions derived from this investigation:

a. There is a large amount of energy present in low wave numbers in the atmosphere and these waves are quasi-stationary.

b. In current numerical models these ultra-long waves are moved westward at very great speeds and altered in shape and intensity.

c. Numerical forecasts made with these components held stationary are consistently superior to those prepared without this modification.

2. METHOD OF COMPUTATION

The sinusoidal form has been frequently assumed for atmospheric wave disturbances and the Fourier representation was chosen in this investigation for ease in machine computation. The form used was

$$\Phi(\lambda)=A_0+\sum_{n=1}^{n=\infty}(A_n\cos n\lambda+B_n\sin n\lambda)$$

where Φ=height of 500-mb. surface

λ=longitude in radians

n=wave number

Computations of A_n and B_n were made for wave numbers one through five for each initial chart and 48-hour forecast for January and February 1958. Due to an insufficient number of grid points, the computations for wave numbers higher than one were terminated at latitude 70° N.

3. DESCRIPTION OF WAVE ONE IN THE ATMOSPHERE

Of the components computed, wave number one had the greatest intensity. For these 60 winter days there were two pairs of centers on each initial chart of wave number one. Since the Fourier computation enforces symmetry in each pair, it is sufficient to describe the negative center—the positive center completing the pair, being the mirror image of the negative one.

The lower latitude centers were fixed in phase with the negative center over the western Pacific Ocean. These centers varied in intensity from 300 to 850 ft.

There was another pair of centers in higher latitudes. These centers were almost randomly distributed in phase. They varied in intensity from 150 to 1,000 ft. Figure 2 shows wave one for 0000 GMT, January 6, 1958. This was the weakest wave number one pattern observed in the two-month period.

4. DISTORTION OF WAVE NUMBER ONE IN THE NUMERICAL FORECASTS

The basic equation of the forecast model requires the individual conservation of vorticity. From this same consideration Rossby [1] derived his famous equation governing the motion of long waves on a zonal current. The phase-speed is given by the relation:

$$C=U-\frac{\beta L^2}{4\pi^2}$$

where U is the mean zonal wind, β is the variation of the Coriolis parameter with latitude, and L is the wavelength.

From this formula it is found that the maximum value of U observed in the atmosphere will give eastward displacement only for wave number five and higher. There-

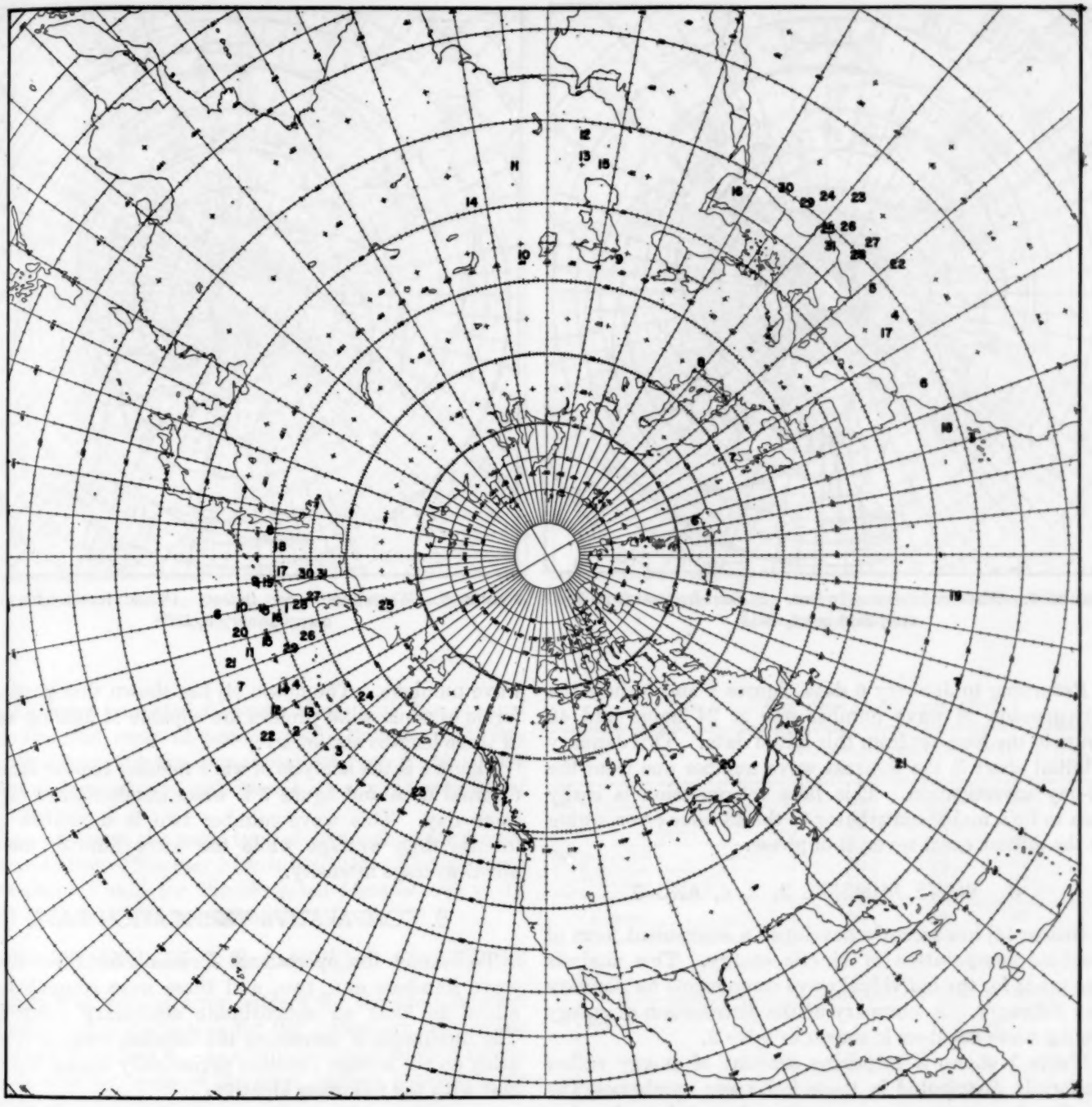

FIGURE 3.—Southern negative center, initial and 48-hour forecast positions identified by day for January 1958.

fore in this numerical model wave numbers one through four will be moved rapidly westward. In his computation of "influence functions" this effect was dismissed by Charney [2] with the statement ". . . these [very long waves] are associated with little of the total energy."

Figure 3 shows the initial and 48-hour forecast position of the southern negative center of wave number one for January 1958. The initial positions are all clustered in the western Pacific, illustrating the almost stationary nature of these waves. The forecast centers have been moved southward slightly and westward at high speed. Table 1 summarizes the treatment of both centers in the 48-hour forecasts.

TABLE 1.—*Wave one average values*

	January		February	
Southern Centers				
	D 00	D 48	D 00	D 48
Latitude	48	35	44	30
Longitude	168E	014E	172W	69E
Intensity	570 ft.	280 ft.	460 ft.	240 ft.
Northern Centers				
Latitude	73	73	68	69
Intensity	480 ft.	620 ft.	440 ft.	600 ft.

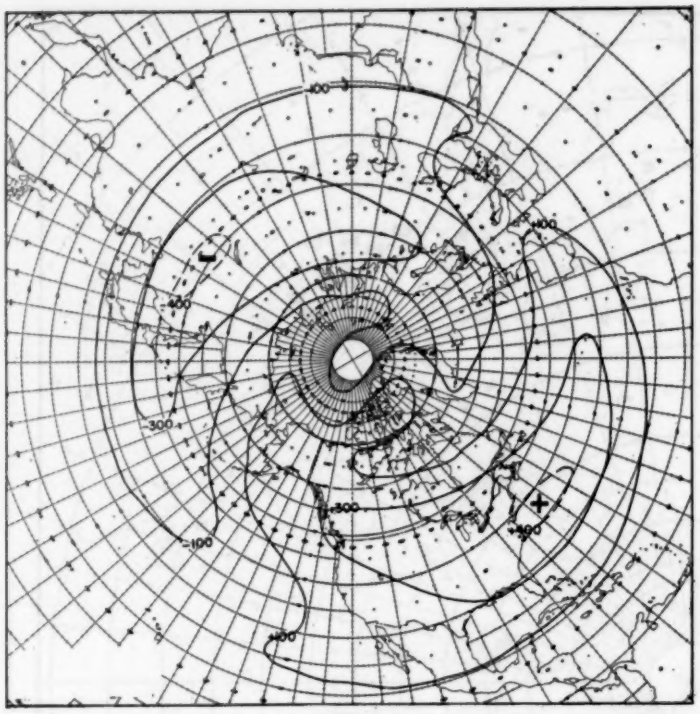

FIGURE 4.—Wave number one, in feet. 24-hour forecast from 0000 GMT, January 6, 1958.

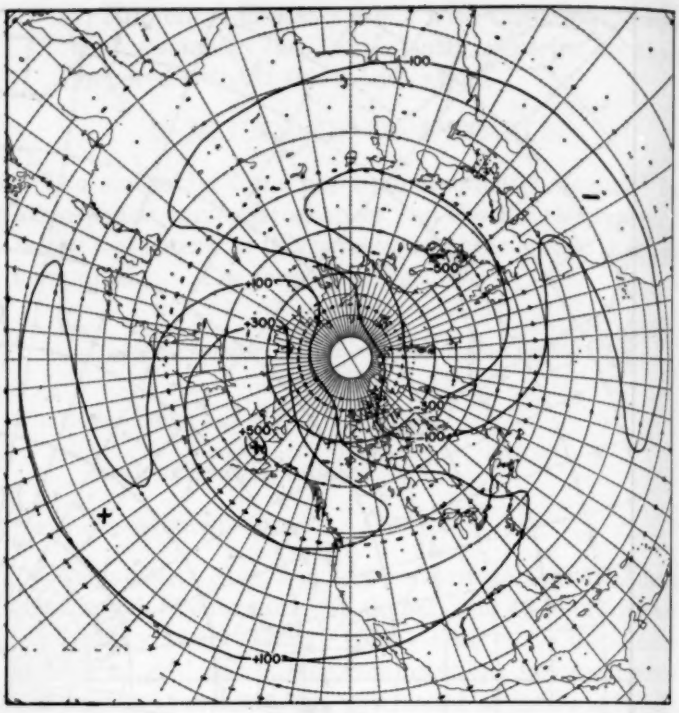

FIGURE 5.—Wave number one, in feet. 48-hour forecast from 0000 GMT, January 6, 1958.

Returning to January 6 data, figures 4 and 5 show the retrogression of wave number one at 24 hours and 48 hours in the forecast from this initial data. This January 6 initial chart is the weakest wave number one from the 60-day investigation. This false retrogression is easily seen to be a major contributor to the 48-hour error, owing to the almost exact reversal of phase.

5. WAVE NUMBERS 2, 3, 4, AND 5

Bristor [3] has recently developed a convenient form of machine computation of kinetic energy. This analysis was made for the individual wave components for January and February. A summary of the distribution of energy among wave numbers is shown in table 2.

Table 2 shows a surprising amount of energy rather uniformly distributed in these low wave numbers. The familiar long waves (wave number circa 5) have less important intensity.

The barotropic model occasionally held one or two of these waves stationary but spurious retrogression was the normal behavior. The slower westward motion in the forecast was somewhat balanced by the shorter wavelength so that reversal of phase was again possible in these wave numbers. Thompson [4] has shown that particular forms of zonal wind profiles are capable of holding waves of these lengths stationary.

Figure 6 is the analysis of wave number two for January 6 initial data and figure 7 is wave number three for the same day. This wave number two is somewhat more intense than average while the wave number three is about average intensity.

TABLE 2.—*Average kinetic energy (units proportional to knots²)*

	Total perturbation KE	Wave number					
		1	2	3	4	5	6 and up
January	426	77	53	41	59	39	157
February	486	66	40	45	60	30	245

6. COMPARATIVE VERIFICATION DATA

To correct the operational forecasts for these effects, wave numbers one, two, and three were computed and added to form an approximate stationary component. The mechanics of correcting the forecast consists of operating on the stream function periodically during the forecast with the following identity.

$$\psi_c = \psi_\gamma + S_{00} - S_\gamma$$

where ψ_c is corrected stream
ψ_γ is forecast stream at time γ
S_{00} is initially computed stationary components
S_γ is stationary component at time γ

This correction was applied to a series of forecasts and was incorporated in the operational computations on April 10, 1958. To avoid excessive stabilization of the flow pattern at the high latitudes, the stabilization of wave numbers 1, 2, and 3 was terminated at latitudes 75° N., 65° N., and 55° N., respectively.

A series of forecasts was corrected for waves one, two and three. Table 3 lists the root mean square errors in

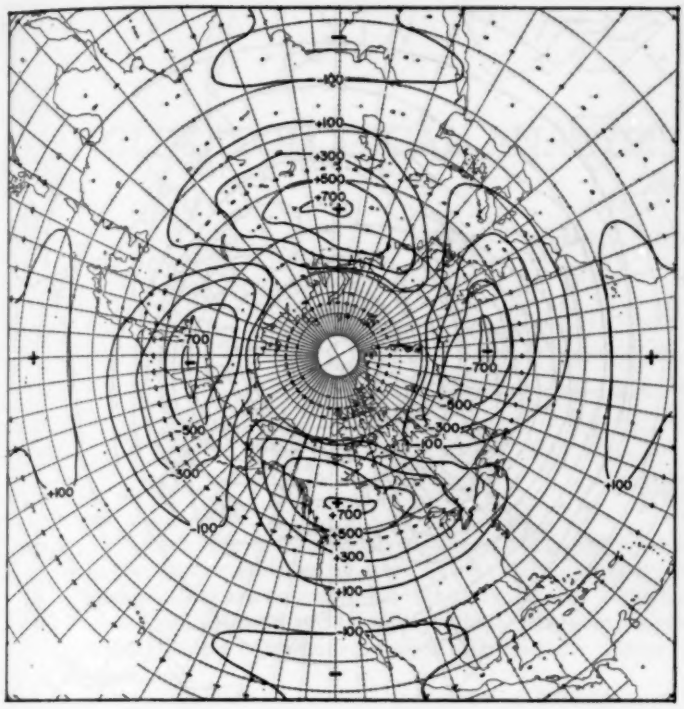

FIGURE 6.—Wave number two, in feet. Initial data, 0000 GMT, January 6, 1958.

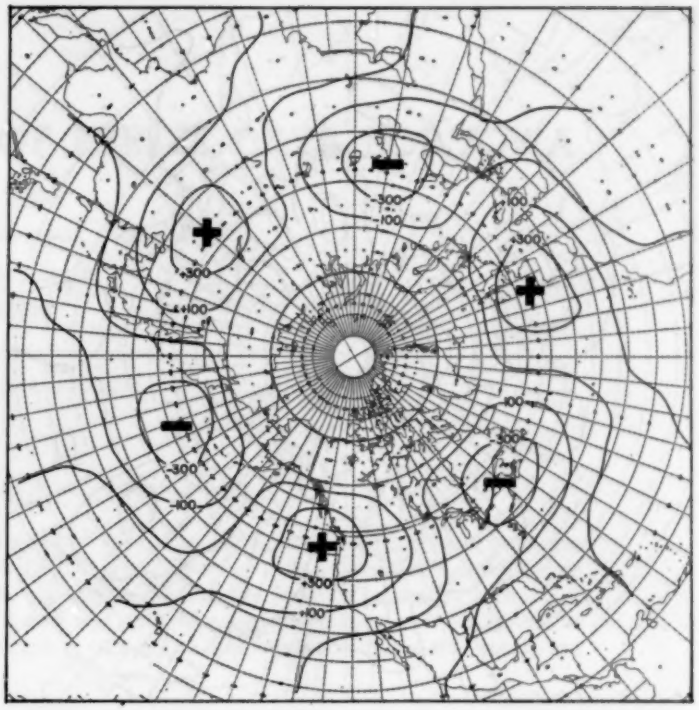

FIGURE 7.—Wave number three, in feet. Initial data, 0000 GMT, January 6, 1958.

feet for these corrected forecasts along with the original error and the error of persistence.[2] Petterssen [5] has recently suggested the comparison of root mean square errors of forecast and persistence as a valid scheme of verification.

Figure 8 shows the same type of comparison for a forecast made from 1200 GMT March 31, 1958. These curves show positive skill for the corrected forecast out to 72 hours compared with persistence.

7. IMPROVEMENT IN THE EMPIRICAL PROCEDURE

Figure 9 shows the error pattern for the same forecast as figure 1 after correction for the stationary component as defined in section 6. In addition to the marked reduction in error the scale of the error pattern is much more acceptable.

Although these results may appear impressive, further improvement is expected from a different method of defining the stationary component. The symmetry of the Fourier computation must introduce local errors even while effecting an over-all improvement. The discontinuity at 70° N. Lat. may produce gradient errors in high latitudes. Since the removal of the errors arising from spurious retrogression of the ultra-long waves, certain systematic errors of treatment of the zonal profile have become relatively more prominent. Improvements in the definition of the stationary component should be ac-

[2] Essentially similar results were obtained by L. Carstensen who isolated the stationary component by repeated smoothing and subtracted a tendency computed from this component at each time step in the forecast.

TABLE 3.—*Root mean square errors (feet)*

Day	Persistence	Operational	WV1	WV1, 2, and 3
Jan 8	325	406	278	230
Jan 10	324	377	251	201
Jan 12	296	411	293	229
Jan 14	309	414	296	252
Jan 16	352	482	319	217
Feb 8	272	339	262	181
Feb 12	310	372	339	217
Feb 16	303	479	320	227
Average	311	410	295	219

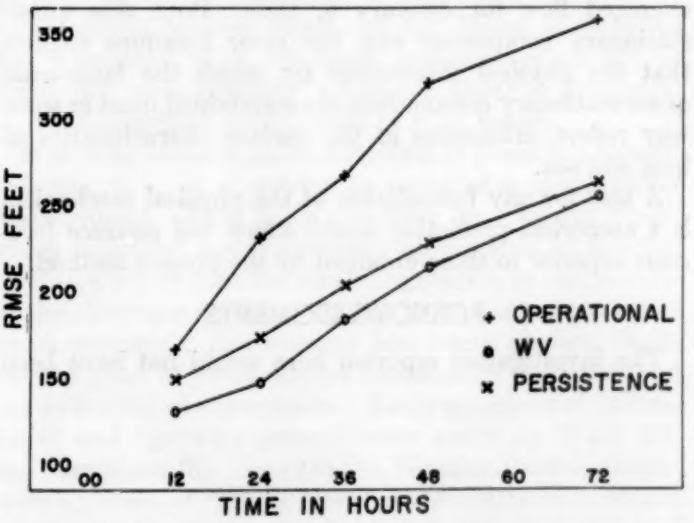

FIGURE 8.—Root mean square error curves for forecasts from 1200 GMT, March 31, 1958.

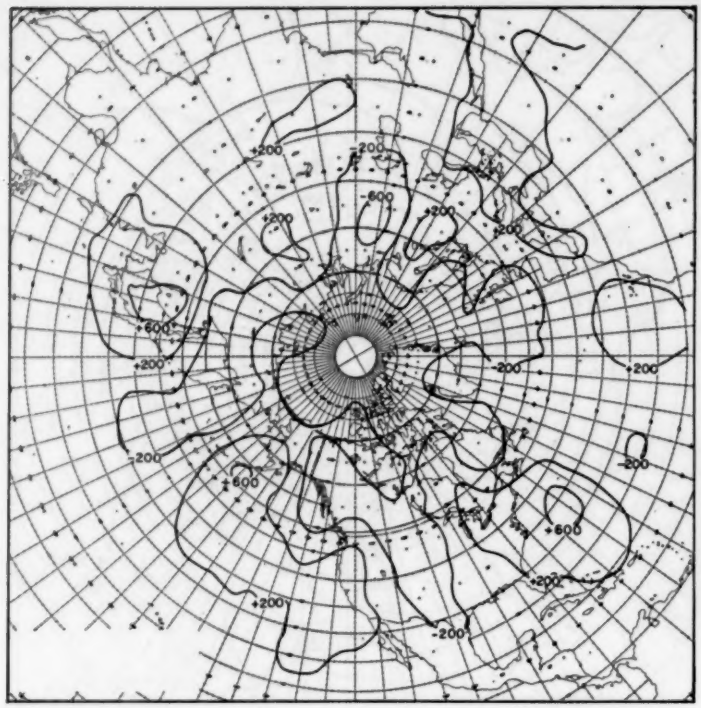

FIGURE 9.—48-hour error in feet. Operational JNWP Unit forecast corrected for waves number 1, 2, and 3 from 0000 GMT, January 16, 1958.

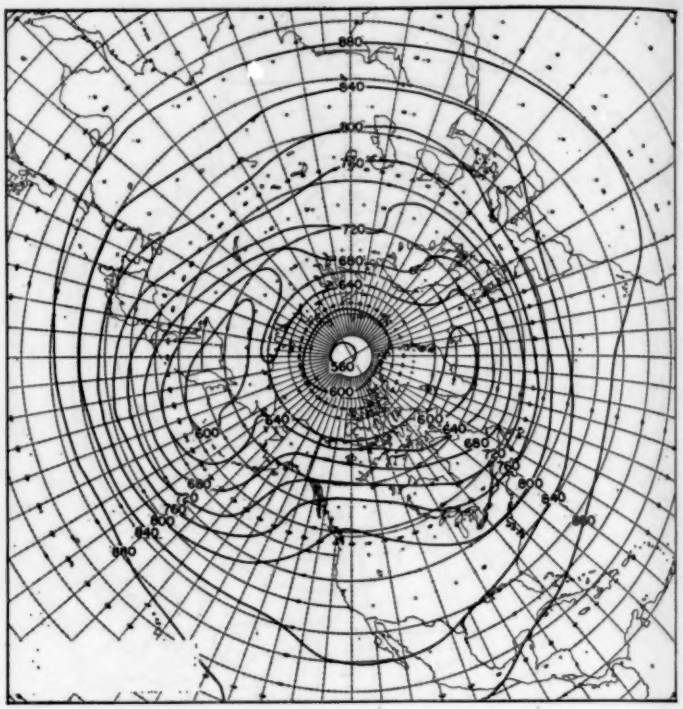

FIGURE 10.—Zonally averaged heights plus waves number 1, 2, and 3 from 0000 GMT, January 6, 1958.

companied by some method of removing systematic profile errors.

8. IMPROVEMENT IN THE PHYSICAL MODEL

The empirical corrections now employed should obviously be replaced by terms in the equations which describe the mechanism by which energy is transferred to and from these waves and the fields which hold them stationary in the atmosphere.

Figure 10 is the long-wave component plus the zonally averaged flow for January 6, 1958. Both this quasi-stationary component and the error locations suggest that the physical mechanism by which the large-scale quasi-stationary components are maintained must in some way reflect differences in the surface characteristics of land and sea.

A test for any formulation of the physical mechanism is a numerical prediction model which will produce forecasts superior to those obtained by the present method.

ACKNOWLEDGMENTS

The investigation reported here would not have been possible except for the continued encouragement and guidance of Lt. Col. Philip Thompson, Head of the Development Section, JNWP Unit. The author is also indebted to LCDR W. E. Hubert, who noted the regular retrogression of the 12-hour error patterns in October 1957 and also read the completed manuscript. R. E. Walker, AG2, USN, assisted in the many computations involved.

REFERENCES

1. C.-G. Rossby and collaborators, "Relation between Variations in the Intensity of the Zonal Circulation of the Atmosphere and the Displacements of the Semi-Permanent Centers of Action," *Journal of Marine Research*, vol. 2, No. 1, 1939, pp. 38–55.
2. J. G. Charney, "On a Physical Basis for Numerical Prediction of Large-Scale Motions in the Atmosphere," *Journal of Meteorology*, vol. 6, No. 6, December 1949, pp. 371–385.
3. C. L. Bristor, Unpublished manuscript, JNWP Unit Technical Series.
4. P. D. Thompson, "The Propagation of Permanent-Type Waves in Horizontal Flow," *Journal of Meteorology*, vol. 5, No. 4, August 1948, pp. 166–168.
5. S. Petterssen, "On Verification of Prognostic Charts," University of Chicago, *Scientific Report* No. 9, 1956, 14 pp.

CLIMATOLOGICAL ANALYSIS OF FREEZE DATA FOR IOWA

H. C. S. THOM

Office of Climatology, U. S. Weather Bureau, Washington, D. C.

and

R. H. SHAW

Agronomy Department, Iowa State College, Ames, Iowa

[Manuscript received March 14, 1958; revised June 5, 1958.]

ABSTRACT

A set of freeze thresholds is defined which replaces the loosely defined element "killing frost." Freeze series are tested and found to be random. This makes it possible to fit frequency distributions. It is hypothesized that these distributions are normal and a test of significance verifies this. A hypothesis that the variance parameter is constant over Iowa is tested and found to be true. It is shown that spring and fall freeze are independent and this results in a simple form of freeze-free period distribution. The calculation of probabilities of freeze and freeze-free season are explained.

1. INTRODUCTION

There seems to have been little statistical treatment of frost or freeze data prior to the excellent works of Reed and Tolley [7, 8] in 1916. Previous writers on this subject for the most part were content to give means with little explanation of their significance. Few seemed to recognize the role of the random variable in computing means or in climatology in general, and randomness was usually looked on only as giving rise to errors in physical measurements which were to be avoided if possible.

About the time of the publication of the Reed and Tolley papers, the technique of linear correlation was being introduced rapidly in applied climatology. Here was a "magic" tool which depicted relationships and seemingly avoided the randomness that was so difficult to treat. Correlation immediately absorbed the energies of many able climatologists in attempts to solve problems for which the use of the technique was largely inappropriate. Many did not recognize the random character of the sample correlation coefficient and frequently interpreted correlations erroneously. Probably more in climatology than in other fields, the correlation technique tended to displace more objective statistical methods and to delay progress.

In contrast Reed and Tolley's papers show a remarkable understanding of the statistical method and its application in climatology. Indeed, one is amazed at their surprisingly modern slant in this discussion of over 40 years ago. Yet these papers seem to have drawn little attention, for work carried out 20 and more years later had not yet taken advantage of Reed and Tolley's contributions. Even much of the work being done today is not up to the high standard set by these able climatologists.

2. KILLING FROST VERSUS FREEZE

While the occurrence of the temperature at a point in time and space can be measured and expressed as a definite value with particular interest, there are also critical values below which effects of interest are the same. Thus, if we are interested in the freezing of water as a simple physical event, we might say that water freezes at 32° F. or any temperature lower than 32°, therefore 32° is a critical value for water. The interpretation of frost or freeze in meteorology is similar in that an effect produced by a critical value is also produced by any temperature lower than the critical value. Hence we define a freeze as the occurrence of a minimum temperature of specified value or lower, which can produce some special freezing effect. A 32° freeze is therefore the occurrence of a minimum temperature of 32° or lower and more generally a t-degree freeze is the occurrence of minimum temperature of $t°$ or lower.

It is to be noted that our definition of freeze is a numerical one; i. e., it is defined in terms of a thermometer measurement. This is in contrast to "killing frost" which is defined non-numerically as the frost or freezing condition which kills the staple vegetation in the vicinity of the observing station. As has been pointed out many times previously this element has many obvious faults not the least of which are its looseness of definition and the difficulties of observation. Early criticisms of "killing frost" and "growing season" were made by Ward [12] and Landsberg [6]. In 1948 the Weather Bureau discontinued the use of "killing frost" as a climatic element and substituted the freeze thresholds 32°, 28°, 24°, 20°, and 16° F. These were arrived at in consultation with agronomists and horticulturists.

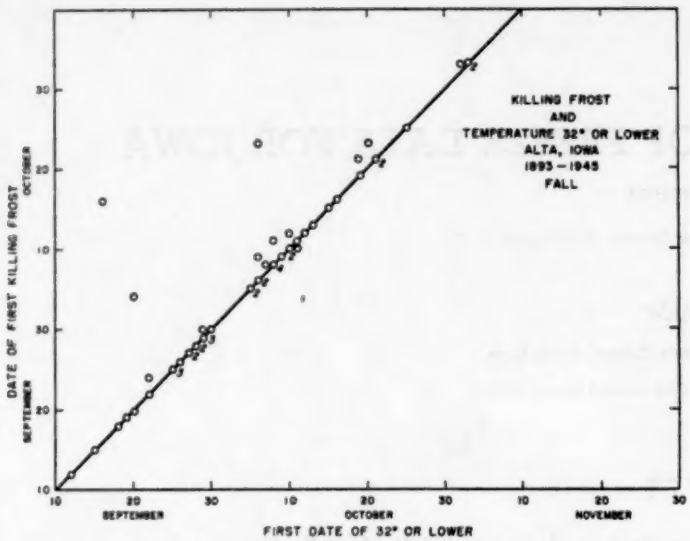

FIGURE 1.—Killing frost dates plotted against dates of 32° F. threshold in fall, Alta, Iowa.

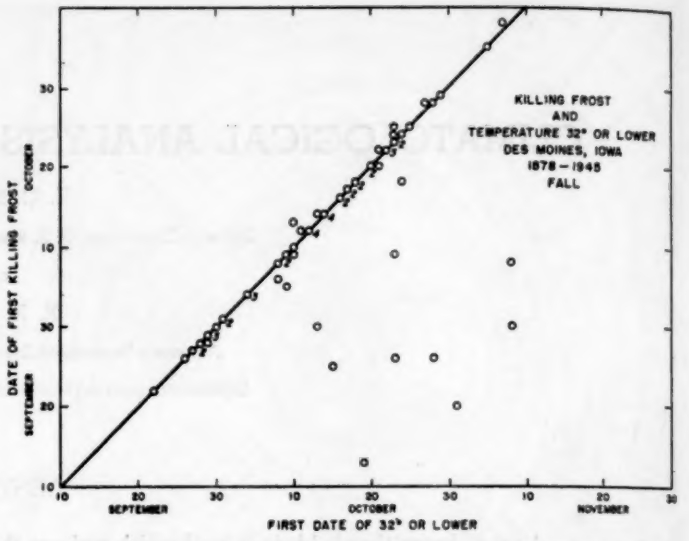

FIGURE 2.—Killing frost dates plotted against dates of 32° F. threshold in fall, Des Moines, Iowa.

Figures 1 and 2 show killing frost dates plotted against 32° F. threshold dates for Alta, a cooperative station, and Des Moines, a first order station. Note that for Alta the first killing frost date in fall comes later than the first 32° date whereas at Des Moines the 32° date comes later. An examination of several other examples showed similar inconsistencies, thus giving evidence of the shortcomings of the killing frost observation.

3. THE FREEZE SERIES

By a freeze series we mean the sequence of dates of annual occurrence of last spring or first fall freeze observed with stable instrument exposure. To apply statistical methods [10] to such a series it is necessary that an element of randomness be present. Although it never happens that this element is completely absent in a sequence of observations whatever their character, homogeneous freeze series are unconditionally random; i. e., there is no significant condition which can be imposed other than that of belonging to the class of freeze dates.

Reed and Tolley [8] evidently noted this randomness in "killing frost" series, for they compiled frequency distributions and treated frost dates as if they formed a random series. Although Reed and Tolley did not test the randomness of their frost series, the self-ordering of climatological data in time and the various extraneous effects which could introduce breaks and trends in climatological series make it good practice to apply some test for randomness. Many tests both parametric and non-parametric are available for such series, but since little is known of the power of such tests, the choice is based mostly on convenience of application. There is however, in this case the choice between a parametric and a non-parametric test, since as will be shown later, the freeze series treated here are normally distributed. In this instance then we have applied the autocorrelation test, the necessary distribution for which was derived by Anderson [1] for a normally distributed series. Grouping tests based on the tables of Swed and Eisenhart [9] have also been applied because of ease of application. In making the autocorrelation test it was assumed that the correlogram decreases from maximum values at short lags and hence only coefficients for lags one and three were computed.

The nature of the freeze series would naturally make the suspicion of non-randomness less than in other climatological series; in fact, all series tested were random on both tests. It seems, therefore, unnecessary to present results in detail although those for one station, Pocahontas, may be of interest. These are given in table 1.

The acceptance regions for ${}_LR_N$ where L is lag for number of observations N=42 and 43 may be taken directly from Anderson's table 6 for lag 1. For lag 3 the same table may be used since N/L=4 and N=4L, a criterion given by Anderson [1] for the suitability of the lag 1 table. Since the 95 percent acceptance region for N=42, 43 is approximately $(-.327<{}_1R_{42}<.278)$, it is seen that the coefficients of table 1 lie on this interval so we accept the hypothesis of randomness for both spring and fall series.

For the grouping test we again employ a two-tailed test since our alternatives to randomness are linear trend

TABLE 1.—*32° freeze autocorrelation coefficients, ${}_LR_N$, for Pocahontas, Iowa*

	Spring	Fall
Lag 1	0.224	−0.006
Lag 3	−0.032	−0.229
N	42	43
	Total Runs	
u	18	25

and location shift as well as oscillatory movement, the former giving rise to too many runs and the latter to either too many or too few. Swed and Eisenhart's [9] tables give the 95 percent acceptance region as (15, 28) approximately, for runs above and below the median with N=42, 43. The total numbers of such runs, u, for spring and fall as shown in table 1 are well within this region, and we conclude again that the series are random.

4. THE FREEZE DISTRIBUTION FUNCTION

Reed and Tolley [8] concluded that their "killing frost" series were normally distributed and fitted these series with this distribution; however, the means by which they reached this conclusion was not very powerful. The χ^2-test of goodness of fit was available at that time, but they did not report having employed it. This was perhaps just as well as this test is non-parametric and is not particularly sensitive in detecting divergence from normality. Geary and Pearson [5] have presented tests which are more sensitive in testing for non-normality. In fact Geary [4] states that these seem to be efficient tests for skewness and kurtosis for a wide range of alternatives to normality. Geary and Pearson's tests employ the statistics

$$a=\frac{\Sigma|x-\bar{x}|}{n\Sigma(x-\bar{x})^2}$$

for kurtosis, and

$$b_1=\frac{m_3}{(m_2)^{3/2}}$$

for skewness, where m_2 and m_3 are the second and third moments respectively. These were computed for a random sample of stations for 32°, 24°, and 16° freeze in spring and fall and are tabulated in tables 2 to 7 for the stations studied. The underlined values of $\sqrt{b_1}$ and a are those which fall outside of the 95 percent acceptance region. The relative infrequency of these when the reliability of the original data is considered leads us to the conclusion that the normal distribution is quite adequate for depicting freeze probability.

Since the sample mean and variance are jointly sufficient for estimating the parameters of the normal distribution, i. e., they extract all information from the sample available for fitting the normal distribution, it is only necessary to estimate these to obtain the freeze distribution function, or as we have called it, the "freeze hazard function." Values of the mean, $\bar{x}$, and variance, s^2, estimated from the various freeze series are also shown in tables 2 to 7.

Either one of two procedures may now be followed to obtain estimated probabilities for individual stations: (*a*) Employ $\bar{x}$ and s with any normal probability integral table, or (*b*) use normal probability coordinate paper for plotting the mean at 50 percent and $\bar{x}\pm 2s$ at 2.275 percent and 97.725 percent respectively. Method (*a*) may also be conveniently applied using the abbreviated normal probability table given in table 8. The results of following procedure (*b*) are shown in figure 3. A similar procedure may be applied to the 20° and 28° thresholds.

It is noted that the original data are not plotted. This is justified by the fact that plotting would involve first estimating probabilities, a procedure which is known to be much less efficient than the method of fitting described above; hence, the points would add nothing to the graphs and might actually detract from them if they tended to change the position of the lines. It may be further noted that spring freeze hazard is read from the upper scale and fall freeze hazard from the lower scale. These give the "best" estimates in the statistical sense of the

TABLE 2.—*Spring, 32° freeze. Underlined values are those which fall outside the 95 percent acceptance region*

Station	n	$\bar{x}$	s^2	s	$\sqrt{b_1}$	a	n'
Albia	30	4/28	158.8	12.6	.1197	.2065	48
Ames	30	5/1	95.3	9.8	.6182	.8327	53
Corning	29	5/2	138.5	11.8	.3681	.8163	55
Davenport	30	4/12	95.1	9.8	−.0891	.9775	73
Decorah	29	5/16	218.0	14.8	.3678	.8391	50
Denison	30	5/5	132.8	11.5	−.0614	.7926	49
Des Moines	30	4/20	134.4	11.6	.2400	.8282	68
Dubuque	30	4/19	86.1	9.3	.3177	.7993	73
Fairfield	30	4/29	121.0	11.0	.2499	.7791	46
Iowa City	30	4/28	132.6	11.5	−.0155	.7983	54
Iowa Falls	30	5/4	138.6	11.8	.1936	.8479	54
Northwood	30	5/6	130.3	11.4	.3293	.7838	51
Olin	21	5/6	146.7	12.1	.4032	.8321	44
Pocahontas	30	5/7	153.2	12.4	−.2843	.7941	42
					$g=.1257$		

TABLE 3.—*Spring, 24° freeze. Underlined values are those which fall outside the 95 percent acceptance region*

Station	n	$\bar{x}$	s^2	s	$\sqrt{b_1}$	a	n'
Albia	30	3/31	139.6	11.8	−.1756	.7962	48
Ames	30	4/6	151.8	12.3	−.0372	.7964	50
Corning	29	4/7	146.7	12.1	.2048	.8083	54
Davenport	30	3/23	174.5	13.2	−.0797	.8243	53
Decorah	30	4/20	141.4	11.9	−.0075	.8438	53
Denison	30	4/10	103.6	10.2	.0541	.9596	49
Des Moines	30	3/26	183.9	13.6	.5351	.8132	53
Dubuque	30	3/27	160.7	12.7	−.3543	.8219	47
Fairfield	30	4/2	183.9	13.6	−.3154	.7594	45
Iowa City	30	4/2	166.0	12.9	−.1393	.7825	51
Iowa Falls	30	4/10	155.9	12.5	.0903	.8218	51
Northwood	29	4/10	115.6	10.8	−.5383	.8126	51
Olin	21	4/9	99.0	9.9	.1351	.8316	33
Pocahontas	30	4/9	117.1	10.8	.2220	.8340	42
					$g=.0948$		

TABLE 4.—*Spring, 16° freeze. Underlined values are those which fall outside the 95 percent acceptance region*

Station	n	$\bar{x}$	s^2	s	$\sqrt{b_1}$	a	n'
Albia	30	3/15	114.4	10.7	.0768	.8120	49
Ames	30	3/18	106.2	10.3	−.0311	.8419	51
Corning	30	3/23	173.7	13.2	.3025	.8007	54
Davenport	30	3/9	168.0	13.0	−.4094	.7974	53
Decorah	30	3/28	175.9	13.3	.5328	.7892	54
Denison	30	3/24	129.2	11.4	.1693	.8403	49
Des Moines	30	3/13	160.6	12.7	−.1709	.7894	53
Dubuque	30	3/13	135.2	11.6	−.4098	.8312	47
Fairfield	30	3/13	161.5	12.7	.1543	.8194	46
Iowa City	30	3/17	113.4	10.6	−.0536	.8371	52
Iowa Falls	30	3/21	143.3	12.0	.0367	.8608	49
Northwood	30	3/23	159.6	12.6	−.1402	.8448	51
Olin	21	3/20	181.9	13.5	.4641	.8591	33
Pocahontas	29	3/25	174.2	13.2	−.2464	.8247	42
					$g=.0918$		

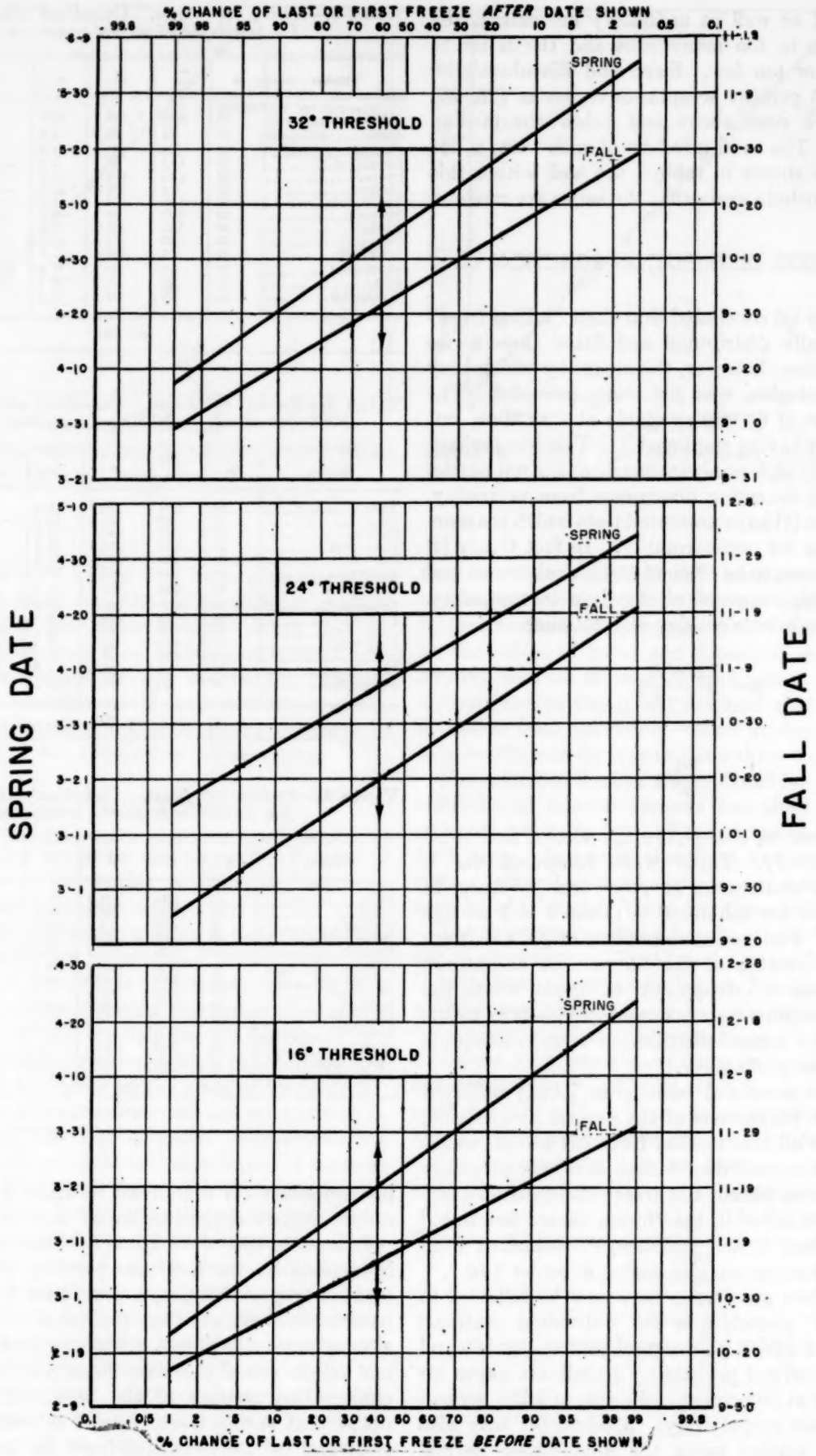
% CHANCE OF LAST OR FIRST FREEZE AFTER DATE SHOWN
99.8 99 98 95 90 80 70 60 50 40 30 20 10 5 2 1 0.5 0.1
32° THRESHOLD
SPRING
FALL
24° THRESHOLD
SPRING
FALL
16° THRESHOLD
SPRING
FALL
SPRING DATE
FALL DATE
0.1 0.5 1 2 5 10 20 30 40 50 60 70 80 90 95 98 99 99.8
% CHANCE OF LAST OR FIRST FREEZE BEFORE DATE SHOWN

FIGURE 3.—Freeze hazard at Pocahontas, Iowa, 32°, 24°, and 16° thresholds.

TABLE 5.—*Fall, 32° freeze. Underlined values are those which fall outside the 95 percent acceptance region*

Station	n	$\bar{x}$	s^2	s	$\sqrt{b_1}$	a	n'
Albia	30	10/15	149.6	12.2	.0971	.8196	48
Ames	30	10/9	194.3	13.9	.6214	.7863	54
Corning	30	10/12	168.3	13.0	.2832	.8226	54
Davenport	30	10/24	133.6	11.6	−.0558	.8178	73
Decorah	30	9/25	170.8	13.1	.2447	.7873	52
Denison	30	10/4	125.8	11.2	.3972	.8405	51
Des Moines	30	10/19	146.4	12.1	.1611	.8031	68
Dubuque	30	10/19	143.0	12.0	−.0037	.8272	73
Fairfield	30	10/10	208.5	14.4	.1579	.8470	45
Iowa City	30	10/11	191.9	13.9	.1427	.7960	53
Iowa Falls	30	10/2	79.6	8.9	.3891	.7887	54
Northwood	30	10/5	98.2	9.9	.1801	.8588	50
Olin	20	10/1	80.1	8.9	.2226	.8215	42
Pocahontas	30	10/4	119.7	10.9	.3429	.8320	43

$g = .1081$

TABLE 6.—*Fall, 24° freeze*

Station	n	$\bar{x}$	s^2	s	$\sqrt{b_1}$	a	n'
Albia	30	11/1	201.1	14.2	−.2286	.7610	49
Ames	30	10/27	127.9	11.3	−.2479	.8119	50
Corning	30	10/28	212.8	14.6	.1176	.8220	51
Davenport	30	11/13	126.7	11.3	−.1191	.7882	52
Decorah	30	10/17	211.4	14.5	−.2338	.8459	51
Denison	30	10/26	151.2	12.3	−.4701	.8326	50
Des Moines	30	11/7	121.9	11.0	−.0949	.7805	52
Dubuque	30	11/11	132.9	11.5	−.2058	.7791	52
Fairfield	30	10/28	166.7	12.9	.0482	.7985	42
Iowa City	30	10/30	160.1	12.7	.0086	.7665	52
Iowa Falls	30	10/25	139.6	11.8	−.1227	.8439	52
Northwood	29	10/27	158.2	12.6	−.2875	.8240	46
Olin	20	10/27	160.1	12.7	.2330	.7962	37
Pocahontas	30	10/23	151.3	12.3	−.1375	.8054	43

$g = .1032$

TABLE 7.—*Fall, 16° freeze*

Station	n	$\bar{x}$	s^2	s	$\sqrt{b_1}$	a	n'
Albia	30	11/23	196.5	14.0	.3515	.7517	49
Ames	30	11/15	110.9	10.5	−.2245	.8049	50
Corning	30	11/13	122.7	11.1	−.4692	.7960	51
Davenport	30	11/27	197.3	14.0	.5853	.7900	51
Decorah	30	11/9	155.5	12.5	−.3924	.7798	52
Denison	30	11/7	154.3	12.4	−.1285	.7745	51
Des Moines	30	11/25	192.4	13.9	.5127	.7735	52
Dubuque	30	11/25	176.3	13.3	.3899	.7826	52
Fairfield	30	11/22	182.2	13.5	.1082	.7882	44
Iowa City	30	11/20	125.1	11.2	−.2005	.7979	52
Iowa Falls	30	11/12	117.3	10.8	−.3577	.7948	52
Northwood	29	11/11	135.4	11.6	.1079	.8005	47
Olin	20	11/14	178.1	13.3	.1258	.8251	34
Pocahontas	30	11/8	93.8	9.7	−.1927	.7811	43

$g = .1007$

TABLE 8.—*Abbreviated table of normal probability distribution*

For probability less than $(\bar{x} \pm ts)$ read down		
$P[x<(\bar{x}-ts)]$	t	$P[x<(\bar{x}+ts)]$
.01	2.33	.99
.02	2.05	.98
.05	1.64	.95
.10	1.28	.90
.15	1.04	.85
.20	.84	.80
.25	.67	.75
.30	.52	.70
.35	.39	.65
.40	.25	.60
.45	.13	.55
.50	0	.50
$P[x>(\bar{x}+ts)]$	t	$P[x>(\bar{x}-ts)]$
For probability greater than $(\bar{x} \mp ts)$ read up		

probability of freeze occurring after a particular date in spring and before a particular date in fall.

In the above analysis n years were used to estimate the mean, variance, and standard deviation whereas the full length of record n' was used in estimating $\sqrt{b_1}$, and a. The n-year statistics came from State tabulations of freeze statistics issued to Weather Bureau Offices. These were designed according to the general principles set forth here and treated insofar as possible as a homogeneous 30-year record at cooperative stations.

5. CLIMATIC VARIATION OF THE PARAMETERS

We have seen that the two parameters of the freeze hazard distribution are the mean and standard deviation. It is quite clear from physical principles that the mean freeze date must vary with latitude and other factors. This makes it possible to draw isoline maps of mean frost (or freeze) and there are, of course, familiar examples of such maps in the literature.

While geographical variation of mean freeze date can be explained physically, there is no cogent physical basis for hypothesizing the geographical variation of the freeze date standard deviation. If, however, we think of the standard deviation as a scaling parameter, then the standard deviation of temperature is a climatological scale of temperature, and the standard deviation is a scale of freeze date. Now it is known that the climatological scale of temperature varies slowly with geographical factors, and since the freeze threshold date is a kind of inverse time function of temperature for a fixed temperature range, we might suspect that the scale of freeze threshold also changes slowly in a similar fashion. This, as we shall see, seems to be the situation.

Reed and Tolley [8] prepared isoline maps of frost threshold standard deviation which give the impression of being drawn to small islands of homogeneity rather than to some underlying geographical functions. Although they do not remark on the difficulties in drawing these isolines, they must have wondered some about drawing the same isoline value for northern North Dakota as for northern Florida. One hypothesis that could be made is that the islands are due to correlations in the random residuals. Such correlations decrease with increasing distance between stations and this, together with small climatic heterogeneities, could lead to such islands.

Although the Reed and Tolley maps give no reason to question the constancy of the freeze scale parameter over quite large areas, we did examine one possible causal factor; this was station elevation. The variances of 57 Iowa stations were correlated with station elevation. For spring this gave a correlation coefficient of only 0.1054 and for fall of only −0.0173. Neither of these is significant at the 5 percent level, leading us to the conclusion that the variance is probably not related to the station elevation.

The next logical step in our analysis of scale variation seems to be to hypothesize that the scale is essentially homogeneous over quite large areas or specifically over the

State of Iowa. To test such a hypothesis it is convenient to deal with the variance rather than the standard deviation. This is no more complicated than to consider that the variance is our population parameter rather than the standard deviation. Although there have been many tests derived for testing the homogeneity of variances, there is no test for homogeneity when there is a given correlation between the populations. We shall, therefore, use a simple test due to Cochran [2] with consideration given to the effect of dependence.

Cochran has given the distribution of g which is the ratio of the largest variance of k sample variances to the sum of the k sample variances when the k populations are independent. Extended tables for the 5 percent and 1 percent significance limits are given in reference [3]. To adjust the test for dependence we proceed as follows: Since we have only the hypothesis on the invariance of the scale, we wish to accept this hypothesis although, of course, we will not let this wish influence our decision. We note that Cochran's tables provide for k populations (stations) and sample size n (length of record in years). With Olin omitted from consideration it is seen in tables 2–7 that n is about 30 and k would be 13 if the stations were independent of each other. However, the stations are not independent and hence, k has some effective value less than 13. Now, if we examine the 5 percent limits of Cochran's table [3] we see that the g values increase with decreasing k. Consequently, if a g based on k dependent stations is not significant according to the significance limit based on k independent stations, it is all the more not significant on some smaller k resulting from the existing dependence.

The values of g for each threshold and season are entered at the bottoms of tables 2–7. Using Cochran's tables and the above reasoning with respect to dependence one can see roughly that none of these g's is significant at the 5 percent level. Again on the assumption of independence a more exact probability of exceeding $g=0.12567$ for spring 32° feeeze was computed using a normal approximation for the beta distribution. This gave a value of 0.15 which is at least this large for the true situation of dependence among the stations. Hence, the probability of exceeding $g=0.12567$ is greater than 0.15 and the probability of exceeding the g's for other thresholds is still greater. The threshold series are highly correlated (see [10]); therefore, the g's add little information to each other about heterogeneity of the variance in general. As a consequence the individual tests of the g's must be accepted as a verification of the physical hypothesis that the variances are homogeneous.

If the variances do not differ significantly over the State of Iowa, then the standard deviations cannot differ significantly, and it is a considerable simplification to assume one value of the standard deviation for the whole State. This has already been done in [11]. On the assumption of homogeneity of the variance over a large area such as a State, a much improved estimate of the variance may be obtained by taking the weighted average of the station variances. The square root of this provides a good estimate of the standard deviation. Using the standard tabulations of freeze data referred to above, table 9 was prepared. These average standard deviations may be used with any individual station mean to obtain the freeze hazard distribution for that station.

6. THE DISTRIBUTION OF FREEZE-FREE PERIOD

Since we have shown above that the freeze hazard distribution is normal, it follows from a well-known theorem in statistics that the difference between fall and spring threshold dates or freeze-free period will also be distributed in a normal distribution. This distribution will have a mean equal to the difference between the fall and spring mean dates. Its variance, however, will depend on the correlation coefficient between spring and fall freeze dates. This cannot be obtained from the statistics given above, and so must be given separate consideration.

The long time interval between spring and fall freeze dates naturally leads one to the conclusion that the correlation between them must be small. Reed [7] found

TABLE 9.—*Variances and standard deviations*

	Threshold				
	32°	28°	24°	20°	16°
	Spring				
σ^2	133.7	142.0	155.4	171.9	154.1
σ	11.6	11.9	12.5	13.1	12.4
	Fall				
σ^2	141.2	164.4	167.0	157.1	163.1
σ	11.9	12.8	12.9	12.5	12.8

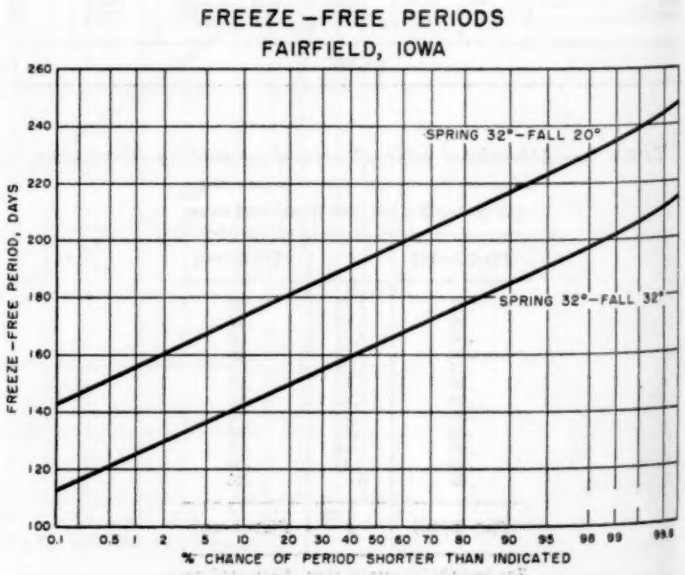

FIGURE 4.—Distribution of freeze-free period, Fairfield, Iowa.

the spring-fall correlation coefficient for one station, Keokuk, Iowa, to be −.179. Using a test which is now obsolete, he concluded correctly that this was not significantly different from zero. He made no further analysis of this correlation, and even though this single value was not significant, he included it in estimating the standard deviation of the growing season distribution. The effect of the correlation is to increase the standard deviation a little more than one day.

We have computed a number of spring-fall correlation coefficients for Iowa and found none to be significant. Two typical examples are Fairfield −.103 and Northfield −.080. Although further study of this correlation may be of interest, its small effect on the standard deviation of the freeze-free distribution makes the fruitfulness of such an effort questionable. With close approximation it may be assumed that the freeze-free period standard deviation is the square root of the sum of the spring and fall freeze variances and the mean is, of course, the difference between the fall and spring means. This gives the same statistics we had for the freeze distributions and hence, the freeze-free period distribution may be plotted on probability paper in the same manner. From the means of tables 2 and 5 and the variances of table 9, we find the spring 32°-fall 32° freeze-free period mean and standard deviation for Fairfield to be 163.9 and 16.6, respectively. The distribution is shown in figure 4.

It will be clear that the same threshold need not be used at both ends of the freeze-free period. The need for using different thresholds in spring and fall could come from either a different sensitivity of a single crop in the spring and fall or one crop being subject to the spring hazard and another to the fall hazard. Figure 4 also shows the distribution for the spring 32°-fall 20° freeze-free period which is an illustration of an application to seed corn growing. Here, the spring hazard is that of killing the tender plant, whereas the fall hazard is reduction of germination percentage. The spring and fall variances were obtained from table 9 and the mean 32°–20° freeze-free period, 195.5, from manuscript tabulations.

REFERENCES

1. R. L. Anderson, "Distribution of the Serial Correlation Coefficient," *The Annals of Mathematical Statistics*, vol. 13, 1942, pp. 14–33.
2. W. G. Cochran, "The Distribution of the Largest of a Set of Estimated Variances as a Fraction of Their Total," *Annals of Eugenics*, vol. 2, 1941, pp. 47–52.
3. C. Eisenhart et al., *Techniques of Statistical Analysis*, McGraw-Hill Book Co., Inc., New York, 1947, pp. 389–393.
4. R. C. Geary, "The Frequency Distribution of $\sqrt{b_1}$ for Samples of All Sizes Drawn at Random from a Normal Population," *Biometrika*, vol. 34, 1947, pp. 68–97.
5. R. C. Geary and E. S. Pearson, "Tests of Normality," Separate No. I from *Biometrika*, vols. 22, 27, 28, Biometrika Office, University College, London, W. C. 1, 1938.
6. H. Landsberg, *Physical Climatology*, The Pennsylvania State College, 1941, 283 pp. (p. 117).
7. W. G. Reed, "The Probable Growing Season," *Monthly Weather Review*, vol. 44, No. 9, September 1916, pp. 509–512.
8. W. G. Reed and H. R. Tolley, "Weather as a Business Risk in Farming," *Geographical Review*, vol. 2, 1916, pp. 48–53.
9. F. Swed and C. Eisenhart, "Tables for Testing Randomness of Grouping in a Sequence of Alternatives," *The Annals of Mathematical Statistics*, vol. 14, 1943, pp. 66–87.
10. H. C. S. Thom, Final Report on the Statistical Analysis of Freeze Data, U. S. Weather Bureau Contract No. Cwb 6028, Iowa State College, 1948 (Unpublished).
11. H. C. S. Thom, "What's in the Weather," *Iowa Farm Science*, Ames, Iowa, vol. 2, No. 11, 1948, pp. 3–5.
12. R. DeC. Ward, *The Climates of the United States*, Ginn and Co., Boston, 1925, 518 pp. (pp. 128–136).

RAINFALL RATES IN FLORIDA HURRICANES

BANNER I. MILLER

Weather Bureau Office, Miami, Fla.

[Manuscript Received January 9, 1958; Revised June 9, 1958

ABSTRACT

Hourly rainfall amounts from 16 hurricanes are plotted relative to the center of the storm to obtain the mean areal rainfall rates around the storm. The rates ahead of the center are greater than those to the rear, but the differences in rates between the right and left sides are not large. The frequency distributions of various hourly amounts are tabulated for stations within about 100 miles of the center. Finally, the latent heat of condensation is calculated from the mean areal rainfall data. This is found to be about 6×10^{26} ergs per day.

1. INTRODUCTION

Some of the world's heaviest rainfalls have occurred in connection with tropical cyclones; over 20 inches in 24 hours is not uncommon [7]. Several factors influence the total accumulation at a given place. Among the most important are: (1) the rate of ascent of the air within the storm's circulation; (2) the temperature and lapse rates within the area of the storm; (3) the location of the rain gage in relation to the storm's center; (4) the rate of forward motion of the storm; (5) the topography, if the storm is over land, which may greatly increase the upward motion of the air; and (6) the moisture content of the air.

Rainfall rates even in hurricanes, however, vary widely. All the factors listed above except the forward rate of movement also influence rainfall rates. Even near the center of the hurricane, in spite of the large convergence normally present, the hourly rate may be zero if the recording station chances to fall between the spiral rain bands. At the other extreme about 6 inches were recorded in about 1 hour in connection with a Florida hurricane in 1947. Relatively "dry hurricanes" are occasionally observed. In 1941 the center of a hurricane passed about 13 miles south of Miami; winds of 123 m. p. h. were observed at Dinner Key, but only 0.35 inch of rain fell at Miami during the storm. Extremely light rain was also observed as this same storm passed Nassau in the Bahamas. Such occurrences are, however, very rare.

The distribution of the rainfall around the center of the storm is also quite variable and apparently depends upon the stage of development of the hurricane, the direction of movement, the latitude at which the storm is observed, the forward speed of the center, and probably some additional factors. Many years ago Cline [1] investigated hurricane rainfall, using data mostly from storms in the Gulf of Mexico. He concluded that as long as the storm is moving the rainfall is concentrated within the right front quadrant, but that in stationary storms, much of the rainfall shifts to the rear of the center. More recently, Schoner [8] compiled some data on Gulf hurricanes and he also found a greater concentration of rainfall in the right front quadrant than in other parts of the storm. Hughes [4] computed the rainfall distribution from the mean convergence around the center as deduced from low-level aircraft reconnaissance winds and obtained a relatively symmetrical distribution around the center. This may be because there were insufficient wind observations to define an asymmetrical distribution, especially within 60 miles of the center. Dunn [2] suggests that in general the more immature the hurricane and the lower the latitude at which it is observed, the more symmetrical the rainfall from the standpoint of both intensity and area, and that it is only when the storm begins to recurve at more northerly latitudes that the greatest concentration of rainfall shifts to the front quadrants.

The purposes of this investigation were to determine the mean areal distribution of rainfall rates relative to the center of the hurricane and to establish the frequency distribution of various rates around the center. A knowledge of the mean hourly rates (by areas) might be of some use in forecasting total accumulation at any specified location, although obviously such a forecast would necessarily have to take into account the forward speed of the storm, the increased lift due to topography or frontal surfaces, and frictional influences as the storm moves over land.

2. SELECTION OF DATA

Hourly rainfall data from hurricanes whose centers crossed Florida or moved within about 300 miles of some portion of the State were used to obtain the mean areal distribution. Data from 16 hurricanes were used, and portions of their tracks during the periods for which rainfall data were tabulated are shown in figure 1. The storms which recurved off the east coast and those that moved northward in the eastern Gulf of Mexico were in-

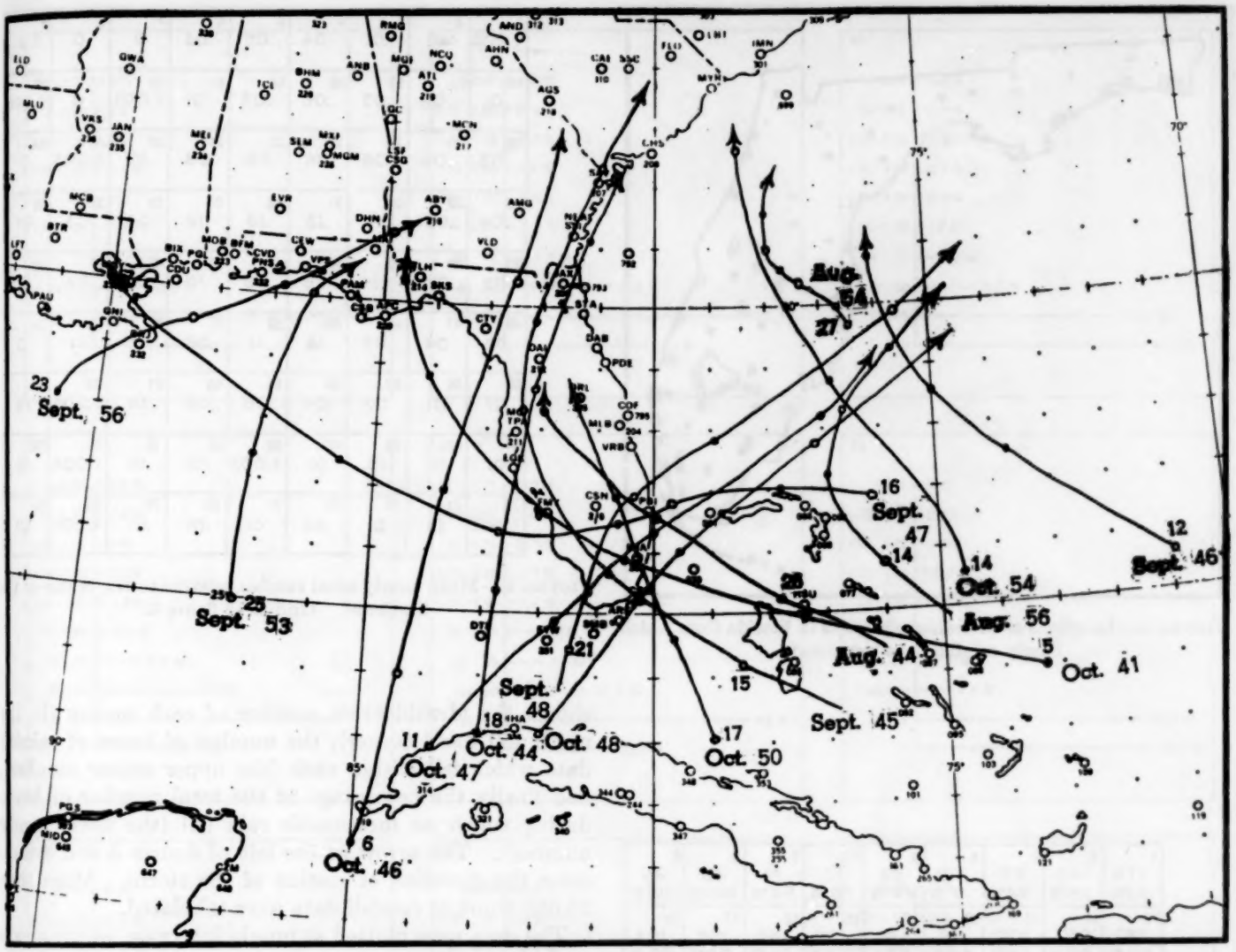

FIGURE 1.—Tracks of hurricanes used in preparation of the mean areal rainfall distribution around Florida hurricanes. Open circles indicate 7 a. m. EST positions and dark circles 7 p. m. positions. Only those portions of the tracks for the hours during which rainfall data were tabulated are shown.

cluded to obtain data for the outer edges of the hurricane. An examination of hurricane rainfall totals [7] suggests that there is little correlation between the intensity of the wind circulation and the rate of rainfall, but for this study only storms of hurricane intensity were used; i.e., as soon as the winds around the center dropped below hurricane intensity, rainfall data were no longer tabulated for that storm.

The tabulations were made from hourly rainfall amounts measured by recording rain gages in Florida from 1941 through 1956. The locations of stations for which data were available are shown in figure 2. During that period some of the earlier recording stations were closed, new ones were established, and others were moved to new locations within the same city. For these reasons, the network of stations was not constant throughout the period, but the number was reasonably stable. Most of the more important recording gages were maintained permanently throughout the entire period upon which this study is based.

Since the data are all from Florida, they are almost completely free from orographic effects and from extratropical influences. The resulting rainfall patterns are then, it is believed, as accurate a representation as can be obtained of the mean areal rainfall distribution around a hurricane, and one that is relatively free of outside influences. The increased friction as the storm moves over land undoubtedly affects the rainfall, since the angle of inflow and the resultant low-level convergence are also changed, but this factor cannot be taken into account.

3. RAINFALL RATES AND FREQUENCY DISTRIBUTION

The grid shown in figure 3 was used to tabulate the hourly rainfall amounts. The squares represent one degree of latitude on a side. In use the center of the grid (the middle of square 41) is placed over the center of the hurricane and moved with the storm. The grid extends 4.5 degrees of latitude both ahead and behind the center as well as to the right and to the left. In figure 3 are

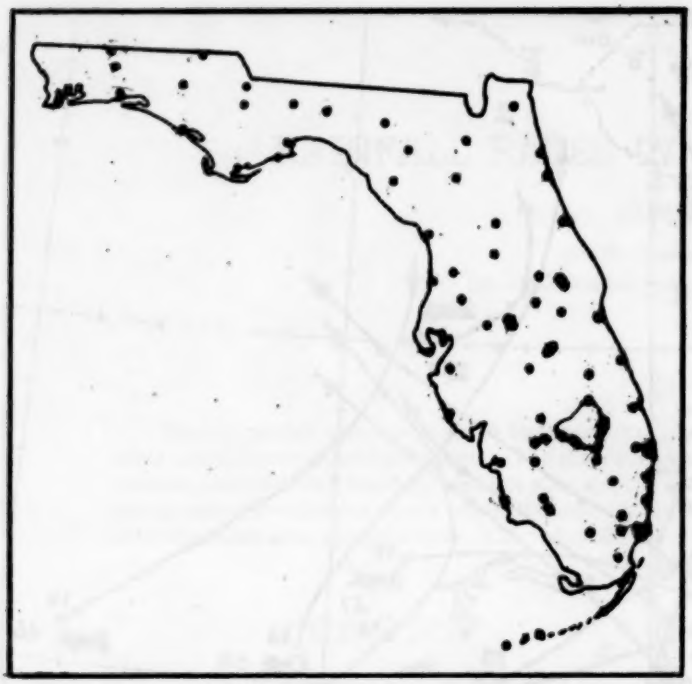

FIGURE 2.—Locations of recording rain gages in Florida from which hourly rainfall data were used.

1 176 93%	2 148 94%	3 221 92%	4 110 71%	5 59 44%	6 12 75%	7 21 96%	8 45 100%	9 69 100%
10 263 80%	11 257 80%	12 270 68%	13 191 44%	14 141 52%	15 102 68%	16 140 89%	17 213 98%	18 153 97%
19 464 67%	20 425 60%	21 414 61%	22 319 49%	23 307 47%	24 325 50%	25 415 68%	26 294 90%	27 180 97%
28 527 55%	29 614 56%	30 601 50%	31 632 32%	32 579 27%	33 561 44%	34 519 50%	35 349 79%	36 245 91%
37 583 49%	38 728 44%	39 777 38%	40 771 15%	41 748 21%	42 654 46%	43 436 60%	44 281 83%	45 173 94%
46 340 65%	47 436 50%	48 405 48%	49 439 32%	50 396 34%	51 310 51%	52 230 75%	53 171 89%	54 189 98%
55 156 73%	56 213 88%	57 205 73%	58 192 71%	59 198 69%	60 139 78%	61 154 86%	62 256 94%	63 385 96%
64 240 85%	65 354 90%	66 294 94%	67 212 88%	68 255 92%	69 234 92%	70 297 97%	71 345 96%	72 333 94%
73 312 94%	74 261 93%	75 413 93%	76 406 92%	77 424 92%	78 412 92%	79 474 92%	80 363 94%	81 234 95%

FIGURE 3.—Grid used in tabulating rainfall data. The arrow at the left indicates the direction of the storm's motion. The number in the upper left hand corner identifies the square. The number of hours of rainfall data tabulated in each square is shown in the upper center of each square, and the percentage of the total hours during which no measurable rain fell is listed in the bottom center of each square. The sides of the squares represent one degree of latitude. The hurricane is located at the middle of square 41.

1 <.005	2 .01	3 .01	4 .04	5 .05	6 .05	7 0	8 0	9 0
10 .01	11 .02	12 .03	13 .06	14 .03	15 .01	16 <.005	17 0	18 <.005
19 .03	20 .04	21 .05	22 .06	23 .08	24 .08	25 .03	26 <.005	27 0
28 .06	29 .07	30 .11	31 .13	32 .18	33 .12	34 .04	35 .03	36 .01
37 .05	38 .07	39 .14	40 .26	41 .26	42 .10	43 .05	44 .02	45 <.005
46 .02	47 .04	48 .07	49 .14	50 .11	51 .06	52 .02	53 .01	54 0
55 .01	56 .01	57 .02	58 .04	59 .06	60 .02	61 .01	62 <.005	63 .01
64 .01	65 .01	66 .01	67 .01	68 <.005	69 .01	70 .01	71 <.005	72 .01
73 <.005	74 .01	75 .01	76 .02	77 .01	78 .01	79 .01	80 <.005	81 .01

FIGURE 4.—Mean hourly areal rainfall relative to the center of the hurricane. Grid as in figure 3.

shown the identification number of each square (in the upper left hand corner), the number of hours of rainfall data which fell within each (the upper center number), and finally the percentage of the total number of hours during which no measurable rain fell (the lower center number). The arrow at the left of figures 3 and 4 indicates the direction of motion of the storm. More than 26,000 hours of rainfall data were tabulated.

The data were plotted at hourly intervals, which means that the hourly positions of the hurricane centers had to be estimated. This cannot be done with any high degree of precision, and may have resulted in some of the hourly amounts being tabulated in the wrong squares. However, such errors should be random, and with such a large sampling it appears that they can be ignored.

The mean hourly rainfall rates by 1° squares are shown in figure 4. Isohyets could of course have been added, but they would have little meaning since the values plotted at the centers of the squares represent areal means and not point values. The greatest hourly totals (0.26 inch) occur within the center square and just ahead of it. Behind the center the average rates drop off much more rapidly than they do ahead of the storm. To the right the averages are somewhat larger than they are to the left, but the differences are not considered significant. The averages of figure 4 are such that if a storm were moving directly across a rainfall station in the direction indicated by the arrow and at a speed of 10 knots, a 54-hour total of a little more than 5.5 inches would be recorded. This is about one-half the 48-hour total Hughes [4] calculated from theoretical considerations.

The percentage of the total number of hours within each square during which no measurable rainfall was

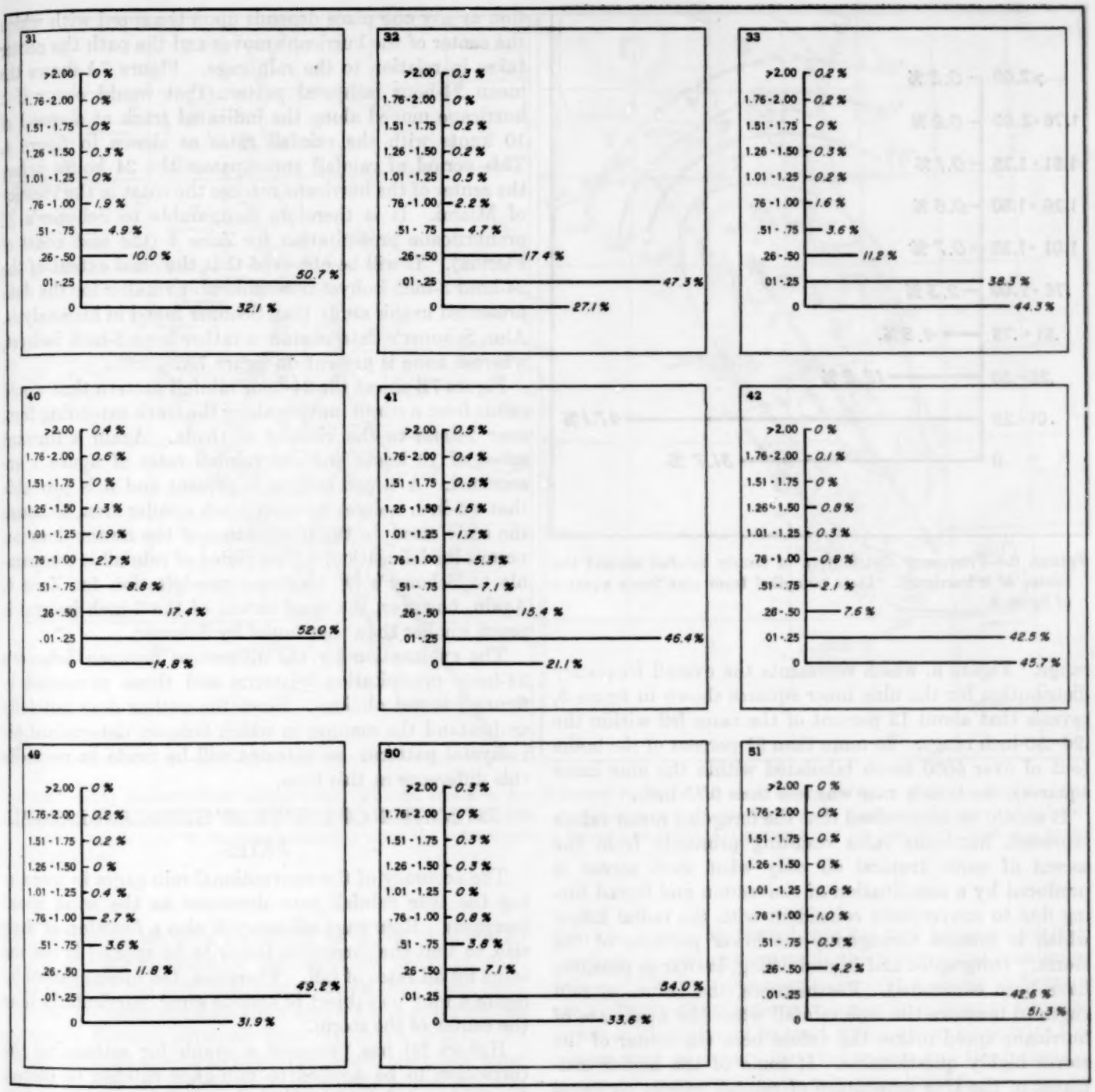

FIGURE 5.—Frequency distribution of hourly rainfall amounts around the center of the hurricane. See figure 3 for the location of the squares by number.

recorded is shown in figure 3. Along three sides of the outer edges of the grid no rain was measured in 90 to 100 percent of the hours, but along the front edge the no-rain cases drop to 49 percent. Square 40, directly ahead of the center of hurricane, has the lowest frequency of no-rain cases, 15 percent. This is even less than the percentage within the square immediately surrounding the center (square 41) in which 21 percent of the hours showed no measurable rainfall. This may reflect the tendency for the rain frequency to decrease through the rear half of the square as the center of the hurricane passes. There may also be a decrease in the rainfall rate through the rear half of this square.

Frequency distributions for other rainfall intervals are shown in figure 5. These data are plotted for the nine inner squares only, all of which lie within about 100 miles of the center of the storm. In all cases the most frequent hourly rainfall is either zero or within the .01–.25-inch

477727—58——2

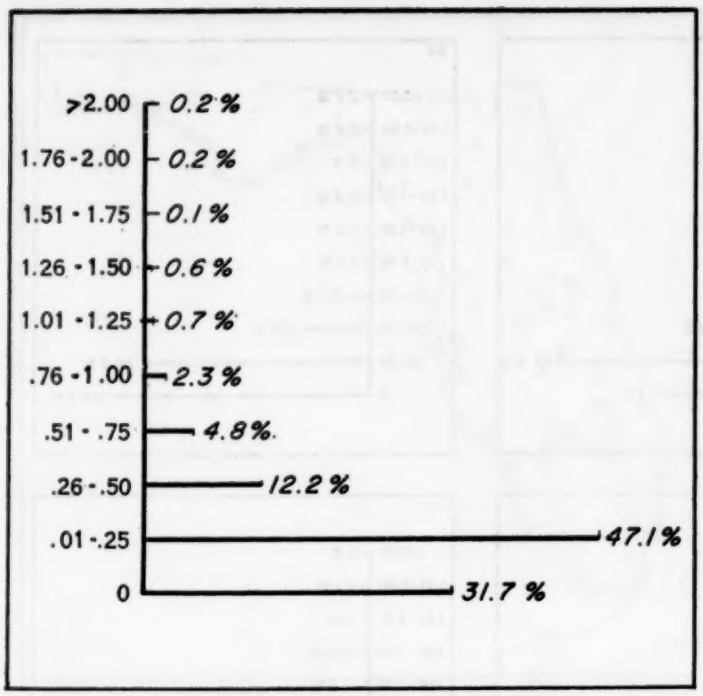

FIGURE 6.—Frequency distribution of hourly rainfall around the center of a hurricane. Data compiled from nine inner squares of figure 5.

range. Figure 6, which represents the overall frequency distribution for the nine inner squares shown in figure 5, reveals that about 12 percent of the cases fell within the .26–.50-inch range. In more than 95 percent of the hours (out of over 5000 hours tabulated within the nine inner squares), the hourly rate was less than 0.75 inch.

It should be emphasized that the foregoing mean values represent hurricane rains resulting primarily from the ascent of moist tropical air only when such ascent is produced by a combination of convection and forced lifting due to convergence coincident with the radial inflow which is present throughout the lower portions of the storm. Orographic and frontal lifting, insofar as possible, have been eliminated. Furthermore, the failure of rain gages to measure the true rainfall when the winds are of hurricane speed makes the values near the center of the storm highly questionable. If some of the higher estimates of the true percentage of rainfall caught by gages in hurricanes are correct [2], then the actual areal means near the center of the storm may be almost twice the values indicated by figure 4. Consequently any use made of the mean hourly rates for quantitative precipitation forecasting should consider at least subjectively the factors listed earlier in this paper, a combination of which may make a substantially greater contribution to the actual rainfall total than the convergence produced by the hurricane winds.

4. COMPARISON WITH EARLIER RESULTS

The rainfall rates shown in figure 4 are relative to the center of a moving hurricane, and the 24-hour accumulation at any one place depends upon the speed with which the center of the hurricane moves and the path the center takes in relation to the rain gage. Figure 7A shows the mean 24-hour isohyetal pattern that would occur if a hurricane moved along the indicated track at a speed of 10 knots with the rainfall rates as shown in figure 4. This period of rainfall encompasses the 24 hours before the center of the hurricane reaches the coast in the vicinity of Miami. It is therefore comparable to Schoner's [9] prehurricane precipitation for Zone 4 (the east coast of Florida). It will be observed that the areal extent of the 24-hour 3-inch isohyet is considerably smaller for the data presented in this study than Schoner found in his analysis. Also, Schoner's data contain a rather large 5-inch isohyet, whereas none is present on figure 7A.

Figure 7B shows the 24-hour rainfall pattern that would result from a storm moving along the track extending from near Miami to the vicinity of Ocala. Again a forward speed of 10 knots and the rainfall rates of figure 4 are assumed. A 4-inch isohyet is present and it is probable that a 5-inch isohyet covers a much smaller area, although the scale used in the preparation of the means does not permit its delineation. This period of rainfall is comparable to Schoner's [9] hurricane precipitation for Zone 4. Again, however, the areal extent of the 3-inch isohyet is much smaller than that found by Schoner.

The explanation for the differences between Schoner's 24-hour precipitation patterns and those presented in figure 7 is not obvious. Since the author does not fully understand the manner in which Schoner determined his isohyetal patterns, no attempt will be made to reconcile this difference at this time.

5. ESTIMATION OF THE "TRUE" HURRICANE RAINFALL RATES

The accuracy of the conventional rain gages in measuring the true rainfall rate decreases as the wind speed increases. Rain gage efficiency is also a function of drop size, so that the correction factor to be applied is not the same for all rates of fall. Therefore, the means shown by figure 4 may be subject to serious error, particularly near the center of the storm.

Hubert [3] has prepared a graph for estimating the correction to be applied to rain-gage catches to correct for the losses due to high winds. For heavy rain, which Hubert defines as a rate greater than 0.11 inch per hour, no distinction is made between shielded and unshielded gages, and the correction varies from zero for no wind to a factor of nearly 1.4 for winds of 100 m. p. h. For rainfall rates less than 0.11 inch per hour, two curves are presented. One is for unshielded and the other for shielded gages. For the shielded gage, the correction factor for light to moderate rain reaches a value of about 2.5 for wind speeds of 100 m. p. h. For unshielded gages the correction factor is even greater.

Hubert does not claim much in the way of accuracy, only that the corrections are in the right direction and bear approximately the proper relation to one another.

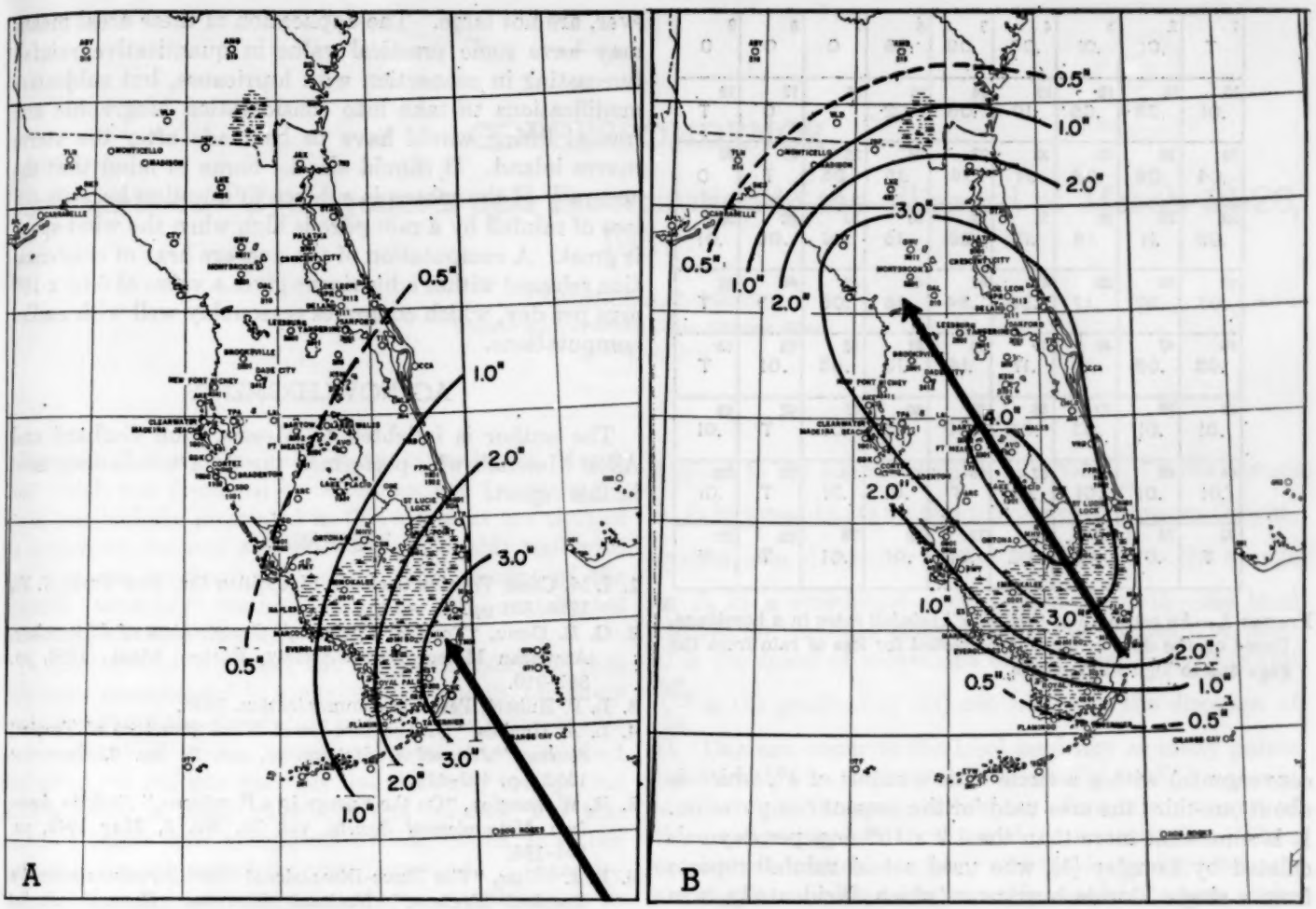

FIGURE 7.—(A) Pre-hurricane precipitation: 24-hour accumulation obtained by using the rates shown in figure 4 as the center of the hurricane moves along the indicated track at a speed of 10 knots. Period ends as the center crosses the coast near Miami. (B) Hurricane precipitation: 24-hour accumulation using the rates shown in figure 4 as the center moves along the indicated track at a speed of 10 knots.

He has labeled the area for winds in excess of about 65 m. p. h. as very doubtful for both light and heavy rainfall.

An attempt has been made to estimate the "true" rainfall rates by using the data from figure 4 and applying the correction factors obtained from Hubert's graph. To obtain the wind speeds at rain-gage levels, the mean wind field by layers, as presented in an earlier report [6], was used. Curves were fitted to the vertical distribution of the wind speeds for various radial distances from the center of the storm. These were then extrapolated from a level of 500 meters (assumed to be represented by the 0–1 km. layer) which is approximately the height of the top of the average rain gage. These reduced values, while probably not too accurate, were used to correct the rates shown in figure 4.

The corrected values, which are offered as an estimate of the "true" mean rainfall rate within Florida hurricanes are shown in figure 8. A comparison with figure 4 shows that the rainfall pattern has become slightly more asymmetrical than before. This is a reflection of the asymmetry in the mean wind field [6]. It will also be noted that the maximum "true" rate has now become 0.34 inch per hour in comparison with the uncorrected maximum value of 0.26 inch per hour. The rates shown in figure 8 are probably slightly more accurate than those of figure 4; however, they should be used with caution since both the factors used to correct for wind speeds and the reduction of the 500-meter winds to rain gage heights are open to question.

6. RELEASE OF LATENT HEAT

Several order-of-magnitude calculations [4, 5] have indicated that the latent heat of condensation released within a hurricane is of the order of 2 to 4×10^{26} ergs per day. The present data afford an opportunity to check these computations by use of the mean data obtained from an unusually large number of cases. Using the entire grid and the means of figure 4, a computation of the latent heat of condensation gives 2.51×10^{25} ergs per hour or 6.02×10^{26} ergs per day. This compares well with the value of 4.36×10^{26} ergs per day obtained by Hughes [4], who based his computation on the rainfall (calculated from low-level

1 T	2 .01	3 .01	4 .06	5 .08	6 .08	7 0	8 0	9 0
10 .01	11 .03	12 .05	13 .10	14 .05	15 .02	16 T	17 0	18 T
19 .04	20 .06	21 .08	22 .11	23 .16	24 .15	25 .05	26 T	27 0
28 .08	29 .11	30 .14	31 .17	32 .25	33 .16	34 .06	35 .05	36 .01
37 .07	38 .10	39 .17	40 .33	41 .34	42 .18	43 .08	44 .03	45 T
46 .03	47 .05	48 .10	49 .17	50 .14	51 .10	52 .03	53 .01	54 T
55 .01	56 .01	57 .03	58 .06	59 .09	60 .03	61 .01	62 T	63 .01
64 .01	65 .01	66 .01	67 .01	68 T	69 .01	70 .01	71 T	72 .01
73 T	74 .01	75 .05	76 .02	77 .01	78 .01	79 .01	80 T	81 .01

FIGURE 8.—An estimate of the "true" rainfall rates in a hurricane. Based on the data of figure 4 corrected for loss of rain from the gage due to high wind speeds.

convergence) within a circle with a radius of 3°, which is about one-third the area used for the present computation. It is somewhat more than the 1.9×10^{26} ergs per day calculated by Longley [5], who used actual rainfall reports from a single Florida hurricane (which, incidentally, was used in determining the areal means of figure 4). All values, however, are close enough to establish reasonably the mean value of the heat of condensation released within an average hurricane. Individual storms, however, will obviously vary greatly.

7. SUMMARY

On the average, rainfall rates within Florida hurricanes are greater ahead of than behind the center of the storm. Differences between rates on the right and left sides, however, are not large. The application of these areal means may have some practical value in quantitative rainfall forecasting in connection with hurricanes, but subjective modifications to take into consideration orographic and frontal lifting would have to be made after the storm moves inland. It should also be borne in mind that the accuracy of the means is subject to question because the loss of rainfall by a rain gage is high when the wind speed is great. A computation of the average heat of condensation released within a hurricane gives a value of 6.02×10^{26} ergs per day, which compares reasonably well with earlier computations.

ACKNOWLEDGMENTS

The author is indebted to Messrs. Don Gerhard and Allen Marshall who performed the data tabulations used in this report.

REFERENCES

1. I. M. Cline, *Tropical Cyclones*, MacMillan Co., New York, N. Y., 1926, 301 pp.
2. G. E. Dunn, "Tropical Cyclones," *Compendium of Meteorology*, American Meteorological Society, Boston, Mass., 1951, pp. 887–910.
3. L. F. Hubert, Personal communication, 1958.
4. L. A. Hughes, "On the Low-Level Wind Structure of Tropical Storms," *Journal of Meteorology*, vol. 9, No. 6, December 1952, pp. 422–428.
5. R. W. Longley, "On the Energy in a Hurricane," *Bulletin American Meteorological Society*, vol. 30, No. 5, May 1949, pp. 194–195.
6. B. I. Miller, "The Three-Dimensional Wind Structure around a Tropical Cyclone," *National Hurricane Research Project Report*, No. 15, 1958, 41 pp.
7. R. W. Schoner and S. Molansky, "Rainfall Associated with Hurricanes," *National Hurricane Research Project Report* No. 3, 1956, 305 pp.
8. R. W. Schoner, Frequency and Distribution of Areal Rainfall Averages Associated with Tropical Storms Entering the Texas Coast. Unpublished manuscript, Hydrologic Services Div., U. S. Weather Bureau, Washington, D. C., 1957, 9 pp.
9. R. W. Schoner, Characteristic and General Isohyetal Patterns for Gulf and East Coast Hurricanes. Unpublished manuscript, Hydrologic Services Div., U. S. Weather Bureau, Washington, D. C., 1957, 18 pp.

CORRESPONDENCE

Comments on "Cyclogenesis and Precipitation in the Blizzard of March 21-26, 1957"

LAWRENCE A. HUGHES
Weather Bureau Forecast Center, Chicago, Illinois
January 12, 1958

Recently I reexamined the storm situation of March 1957 which was discussed by McQueen and Loopstra [1]. I was particularly interested in this storm at the time of its occurrence because this office did reasonably well with the forecasts involved and because the concept of the 500-mb. tendency method (Hughes [2]) contributed materially to those forecasts.

In their article McQueen and Loopstra indicated that they were unsuccessful in applying the 500-mb. tendency method. From the description in the article I was unable to discover just where, when, and how it was applied so I could not tell whether they had difficulty in applying it or whether it really gave incorrect results. For this reason I made new computations and found that the method indicated essentially what happened. I therefore feel that I failed to supply an adequate explanation in my published article. I will attempt to clarify those points which from their article I judge were misunderstood.

The formula allows computation of the local quasi-instantaneous 500-mb. height tendency from the surface pressure tendency and the mean temperature advection from 1000 mb. to 500 mb. The computation can be averaged over any time interval for which a pressure tendency can be obtained, since the portion due to the advection is instantaneous. Since pressure tendencies are customarily reported for a 3-hour period, this time interval is convenient and usually small enough so that the entire computation can be considered as instantaneous.

It is also convenient, however, to express the result in terms of a 12-hour tendency. It is important, though, to see that this does not change the character of the tendency, for it is still essentially instantaneous. However, now it is in more familiar units and can be compared with the 12-hour height changes from successive radiosonde reports. Because these reports yield a 12-hour average tendency, this comparison must be done with care.

In applying or verifying the results of a computation one must keep in mind some of the things considered in Petterssen's rules of pressure kinematics at sea level. This is done through consideration of the operator

$$\frac{\delta}{\delta t}=\frac{\partial}{\partial t}-C\frac{\partial}{\partial x}$$

applied to the 500-mb. height Z_s. Now $\frac{\delta Z_s}{\delta t}$ is the change in Z_s in a coordinate system moving with pressure (height) system—the deepening tendency—and $\frac{\partial Z_s}{\partial t}$ is the change in Z_s in a coordinate system fixed to earth—the local change, in this case computed by the tendency method. C is the speed of movement of the pressure system and $\frac{\partial Z_s}{\partial x}$ is the gradient of 500-mb. height in the direction of C. One can compute the local tendency at many points but its value to the forecaster is usually small, because it is difficult to interpret, unless the effect of movement of the pressure system is removed or nonexistent. When this is done the local tendency and the deepening tendency are the same. This can occur in essentially two ways: (1) where C is zero, and (2) when $\frac{\partial Z_s}{\partial x}$ is zero in the direction of C. The second occurs mainly in low centers and on trough and ridge lines (lines of maximum or minimum curvature) when C is perpendicular to the line. We can always evaluate C perpendicular to the trough line, in fact that is what we usually mean as C. Thus, if we want the computation to indicate the amount of deepening of a trough, we must compute it only on the trough line.

This, of course, means that the computed tendency is usually appropriate only for a very short time locally, i. e., at any one point on earth, since the condition $\frac{\partial Z_s}{\partial x}=0$ usually will not persist for very long at that point. Thus in order to verify a computation it is necessary to make the comparison with the real height changes computed in a coordinate system moving with the trough, the $\frac{\delta}{\delta t}$ coordinate system, such as would be done in verifying the deepening of a surface low center.

To indicate how the technique worked in the March 1957 case at hand, the 500-mb. height tendency was computed each 12 hours from 2130 CST March 20 to 0930 CST March 23. Prior to these times the surface pressure tendencies could not be quantitatively evaluated as the trough was over the Pacific Ocean. The results of these computations are given below:

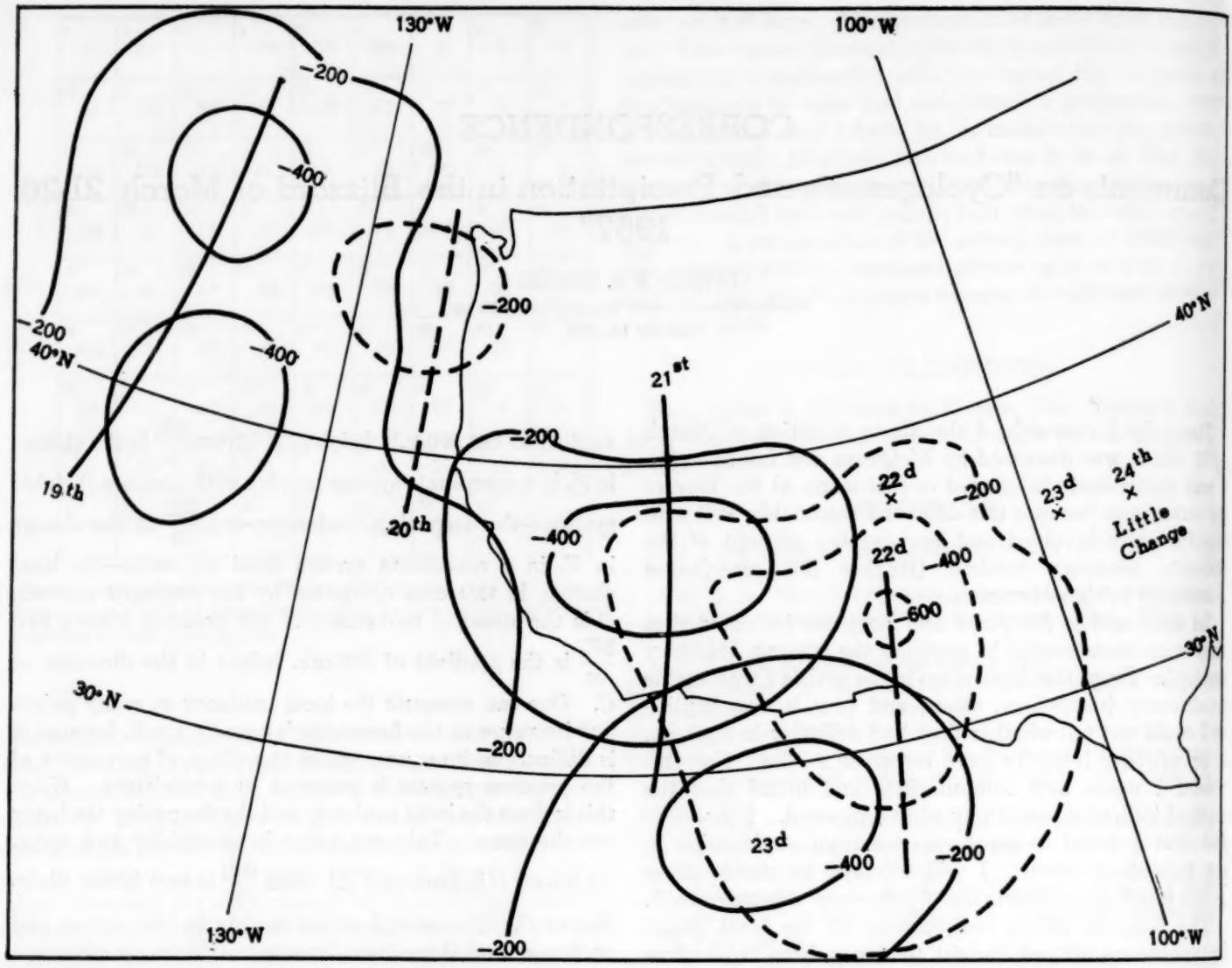

FIGURE 1.—Twenty-four-hour 500-mb. height changes in feet (2100 to 2100 CST) for March 1957 computed in a coordinate moving eastward with the speed of the trough line (the low center was used for the last two days). The position of the trough line at the end of each tendency interval is indicated by the more or less vertical lines. The position of the low center on the last three days, when the trough was becoming ill-defined, is indicated by an "X". Only the changes related to this one trough were computed.

Date—Time (CST)		Net 500-mb. height change (ft./12 hr.)	Area of computation
March 20	2130	−200	Oregon coast.
March 21	0930	−200	Northern California.
March 21	2130	−100	Southern Nevada.
March 22	0930	−400	Arizona.
March 22	2130	−300	New Mexico.
March 23	0930	−500	Mexico, south of Arizona and New Mexico (questionable data).

The above computations were made from the routine maps of the Chicago forecast center mainly because they were current with the upper-air charts and had a good amount of surface pressure tendency data. Computations from the facsimile copies would differ but little. A *preselected* "K" factor was used; 0.5 for the first three computations, 0.4 for the computations over Arizona and over New Mexico, and 0.3 over Mexico. The values other than 0.5 were used to allow mainly for orographically induced downslope motion.

Verification was done rather easily in this case since the trough was oriented essentially north-south throughout the period and it was merely necessary to superimpose

two charts, rotate one about the North Pole until the trough lines under consideration became superimposed, and then perform a graphical subtraction. The results are given in Figure 1.

A low center formed on the 22d so the coordinate system was allowed to shift southward from the 22d to the 23d to follow this center, thus reducing the falls for the 23d from what they would have been otherwise. A 24-hour tendency was used for verification because the 12-hour tendencies were small for a 200-ft. contour spacing and too much overlapping would occur in the figure. For comparison just halve the verifying values.

It can be easily seen that the trough deepened slowly and rather uniformly for four straight days up to 2100 CST on the 22d. This was followed by deepening in the southwestern portion which deformed the trough, then deepening stopped. The relatively small amount of deepening shown for the 20th could easily be due to an error in analysis on either the 19th or the 20th since the trough during this 24-hour interval was west of the good data network of the United States. If the error were mainly on the map of the 20th, the amount of deepening shown for the 21st would be somewhat too high. The amount of deepening shown for the 22d is also somewhat excessive since the trough had some tilt from north at the time and the coordinate system should have been moved slightly southward but was moved due east. These changes would make the deepening appear even more uniform and closer to that indicated by the computations. Incidentally, the suggested method of making the computation gives a mean value of the tendency over an area usually the size of an average State and not the peak value. Considering that these computations were mostly made over regions where both the 1000-mb. geostrophic wind and the 1000–500-mb. thickness is fictitious, the verification indicated is as good as one should expect.

One must keep in mind when using this tendency method that it indicates essentially what is happening at the moment and thus can catch the beginning of new trends which, because of the relative frequency of surface charts with respect to upper-air charts and the time lag for transmission of the latter, may give up to about 21 hours advance warning of the new trend over that indicated by the upper-air chart alone. It cannot, however, indicate a trend that is not occurring at the time. This last, however, is characteristic of practically all, if not all, forecasting techniques.

REFERENCES

1. H. R. McQueen and J. F. Loopstra, "Cyclogenesis and Precipitation in the Blizzard of March 21–26, 1957," *Monthly Weather Review*, vol. 85, No. 3, Mar. 1957, pp. 99–111.
2. L. A. Hughes, "On the Determination of 500 mb. Height Tendencies," *Bulletin of the American Meteorological Society*, vol. 38, No. 4, Apr. 1957, pp. 221–225.

THE WEATHER AND CIRCULATION OF JULY 1958[1]

Heavy Precipitation Associated With a Trough in Central United States

CARLOS R. DUNN

Extended Forecast Section, U. S. Weather Bureau, Washington, D. C.

1. 30-DAY MEAN CIRCULATION

The outstanding feature of the monthly mean circulation pattern at 700 mb. for July 1958 was the large-amplitude wave which extended from the central Pacific to central North America (fig. 1). The circulation in the remainder of the Northern Hemisphere was characterized by blocking over the North Atlantic, with the westerlies strong and displaced well to the south. Over Eurasia a weak flow of rather chaotic nature existed with many truncated troughs and ridges.

Another striking characteristic of this July's circulation was the large percentage of troughs and ridges which were located in climatologically infrequent positions. Klein and Winston [2] have showed that 30-day mean troughs and ridges have climatologically preferred regions of occurrence (fig. 2). A prominent aspect of their statistics is the small longitudinal width of the bands of high frequency, and the rather extensive in-between areas where very few, if any, troughs or ridges were observed during their period of study. In order to compare this July with the long-period frequencies, the 30-day mean trough and ridge locations for July 1958 (taken from fig. 1) have been superimposed on figure 2A and 2B, respectively. This July a minority of the troughs and ridges were located in the preferred areas, namely, the troughs over California, northeastern Canada, southern Russia (between the Black and Caspian Seas), and eastern Siberia. On the other hand, this is the first July since the records began in 1933 that a trough has been observed in the eastern Bering Sea. The activity in this trough is attested by the high incidence of cyclones in that area (Chart X). Furthermore, the troughs which were observed in the central United States, Atlantic, and western Siberia were located in relatively unfavored areas. Quite similar statements may be made about the ridges. Most important to the Western Hemisphere were the unusually located ridges over New England and just off the Washington-British Columbia coast. Because so many of its major components were not in their usual regions, the mean circulation of July 1958, taken over the entire Northern Hemisphere, was of a type seldom observed in midsummer.

The pronounced nature of the trough and ridge systems in the central and eastern Pacific, together with their location in climatologically unfavored areas, resulted in major height departures from normal. The largest of these were a positive center (260 ft.) just off the British Columbia coast and a strong negative anomaly in the central Pacific which affected both the circulation and weather over the United States. Vorticity flux from out of this Pacific wave was strong and persistent enough to produce cyclonic flow and below normal heights (and temperatures) over most of the central United States, in spite of the continental (thermal) factors which normally support anticyclonic conditions aloft in this area during July.

The circulation in June 1958 [5] was more typical of summertime with a trough along each coast and a ridge over the Rocky Mountains. During the month of June, the trend was toward filling of the west coast trough and more cyclonic flow over central United States. This trend continued into July, as illustrated by the anomalous height rises along each coast and falls over the Plains (fig. 3). Confluence, which had been prominent in June [5], still existed over the United States, even though the California trough was weaker and the branch of southerly flow therefore diminished.

Downstream in the Atlantic blocking was prominent, as shown by the positive anomaly over Greenland and the large area of negative anomaly to the south (fig. 1). The westerlies were depressed and cyclonically curved from the United States to Europe. A major cyclone track was associated with these westerlies, resulting in a very stormy July over central Europe. The cyclones which formed over central and eastern North America had west to east paths which converged near Newfoundland and formed this major storm track across the Atlantic to Great Britain (Chart X).

2. TRANSITION WITHIN THE MONTH

The mean circulation for the month was made up of essentially two regimes. The primary pattern, which is exemplified by a 5-day mean 700-mb. chart (fig. 4), was characterized by a stronger than normal Bermuda High,

[1] See Charts I–XVII following p. 284 for analyzed climatological data for the month.

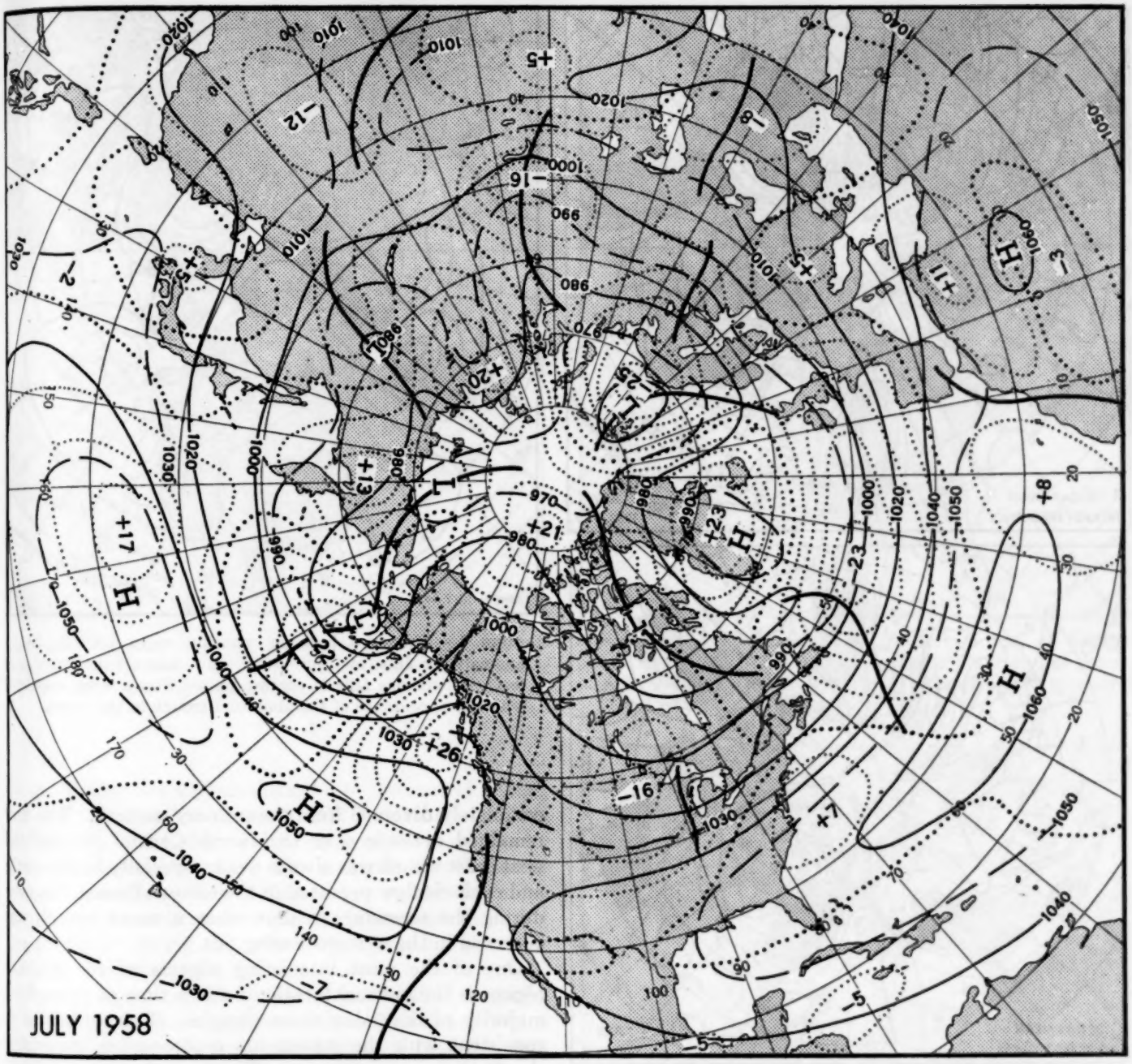

FIGURE 1.—Mean 700-mb. contours (solid) and height departures from normal (dotted) (both in tens of feet) for July 1958. Important feature was the large-amplitude wave extending from the trough in the central Pacific to the trough in the central United States.

a major trough through the central United States, and an abnormally weak trough along the west coast. There was a pronounced ridge in the eastern Pacific and western Canada, a low center in the eastern Bering Sea, well east of the normal location, and a center of cyclonic activity in eastern Siberia near 60° N., 120° E.

The secondary circulation regime of July 1958, which is illustrated by another 5-day mean chart (fig. 5), differed from the primary regime over the United States in that the west coast trough was deeper and the center of cyclonic activity, previously over central United States, shifted to the east coast. These dissimilarities are attested by the height change between the two 5-day mean charts (fig. 6), with rises in central United States flanked by falls along both coasts. Upstream there was a shift of the major area of cyclonic activity from the eastern to the western section of the Bering Sea and a marked weakening of the low center in eastern Siberia as the blocking High over northern Siberia moved eastward (fig. 6). Most of the month the primary pattern prevailed,

477727—58——3

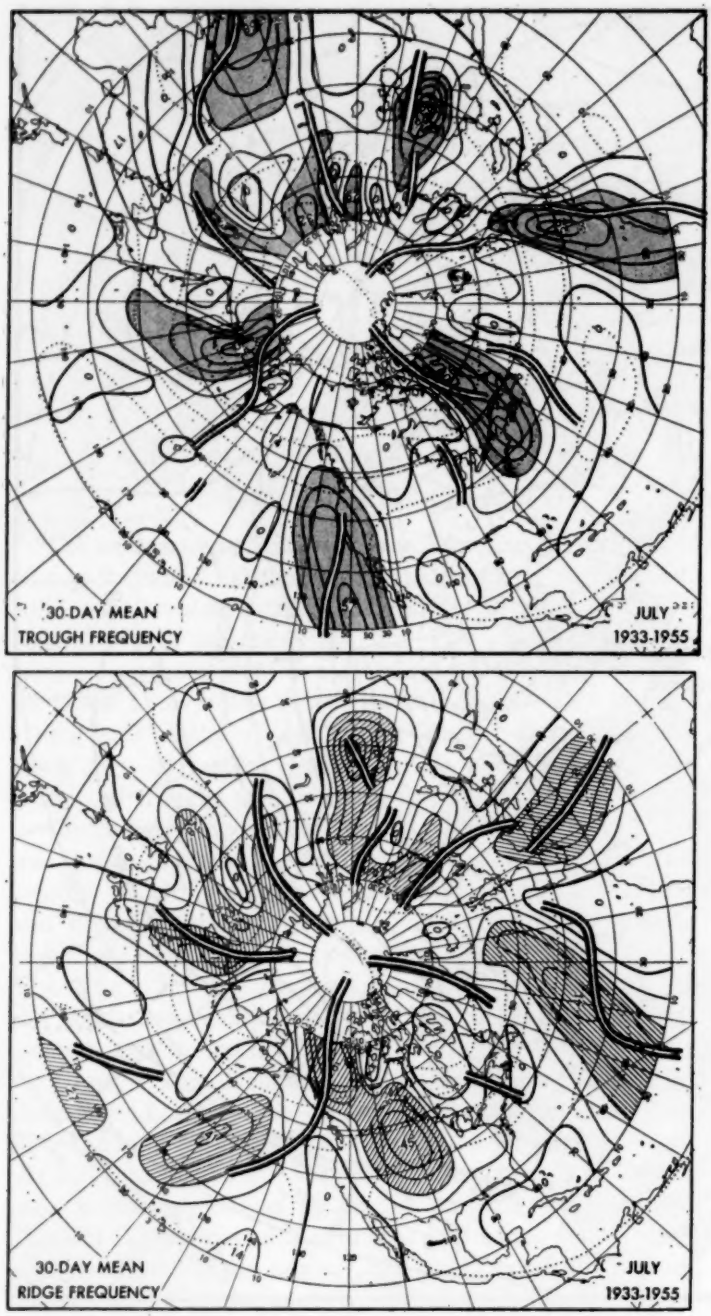

FIGURE 2.—Percent of time that troughs (A) and ridges (B) on 30-day mean 700-mb. charts were located within 10° longitude intervals at latitudes from 20° N. to 70° N. for July, for the period 1933–1955. The data were adjusted to an equivalent basis with 10° at 50° N. as the unit. The lines of equal frequency are drawn at intervals of 10 percent, with the zero line heavier. Areas with frequency greater than 20 percent are shaded. The light dotted lines are the normal 700-mb. contours for July. The 30-day mean troughs and ridges for July 1958 from figure 1 have been superimposed (double track lines) on the proper chart for comparison.

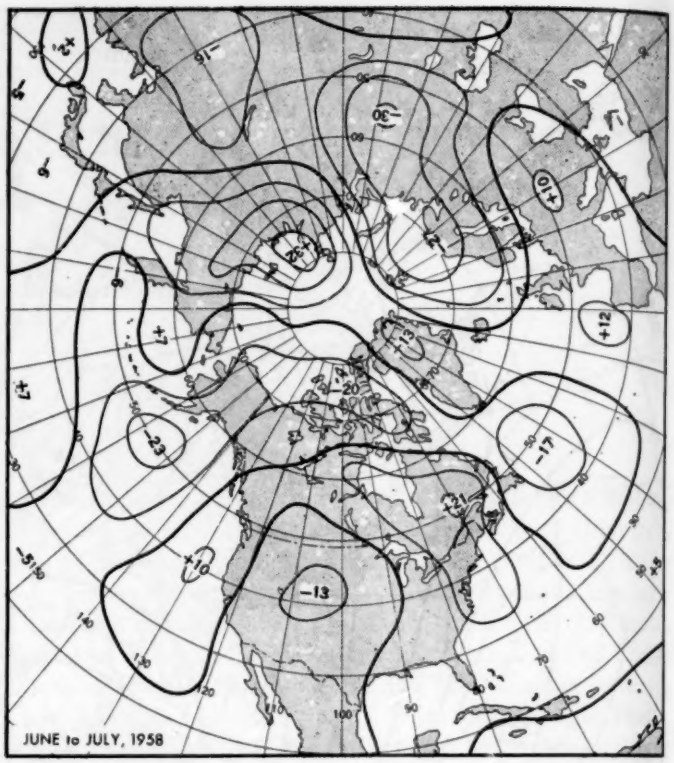

FIGURE 3.—Difference between monthly mean 700-mb. height anomaly for June and July 1958 (July minus June) in tens of feet. Anomalous falls in central United States were associated with the appearance of the abnormal trough in that area.

and the secondary one existed for only approximately one week beginning immediately after the middle of July. It should be emphasized that a complete reversal of the flow pattern did not take place, and the circulation was never completely divorced from the primary pattern. The flow remained cyclonic over the North Central States; the west coast trough was always weak, especially in the north, and cyclonic flow persisted in the eastern Bering Sea even during the secondary regime when a mean trough was observed in the western Bering Sea.

One of the most interesting aspects of the primary regime is the unusual location for this time of year of the majority of the 5-day mean troughs. This, of course, is consistent with the statements made earlier concerning the 30-day mean troughs. The investigation by Klein and Winston [2] further showed that 5-day mean troughs, as well as 30-day mean troughs, occur in climatologically preferred regions (fig. 7A). To show the persistent aspect of the abnormality of the mean circulation, the geographical frequencies of occurrence of 5-day mean troughs this July were computed and are displayed in a manner identical to that used in the aforementioned study (fig. 7B). Troughs were counted which appeared on the twelve 5-day mean charts for July that are routinely computed three times per week and centered two or three days apart. The normally high frequency of occurrence over New England and along the east coast of the United States was supplanted this July by maxima in adjacent areas, namely the eastern Atlantic and central United States. The latter was a significant departure from recent years. Equally anomalous were the high trough frequency in the

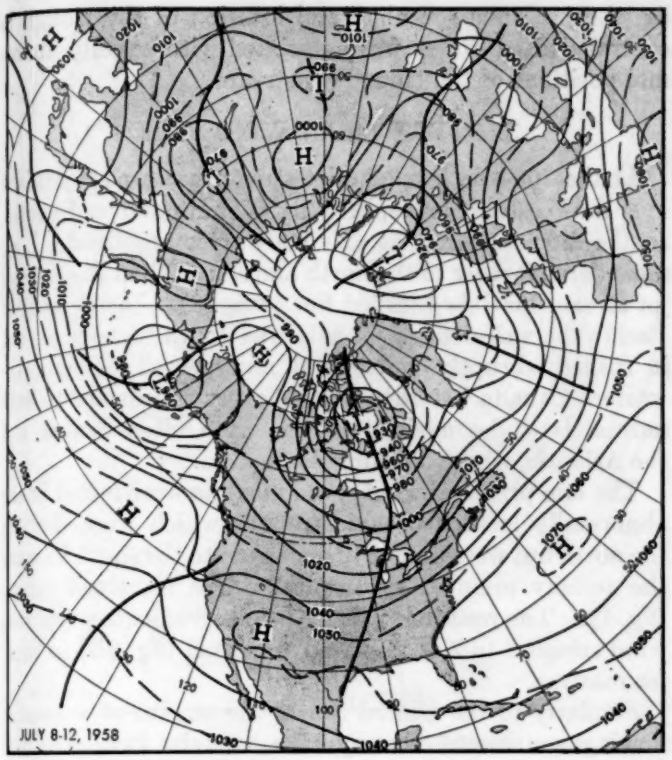

FIGURE 4.—5-day mean 700-mb. contours in tens of feet for July 8–12, 1958. The trough in central United States was a characteristic of the primary regime of July.

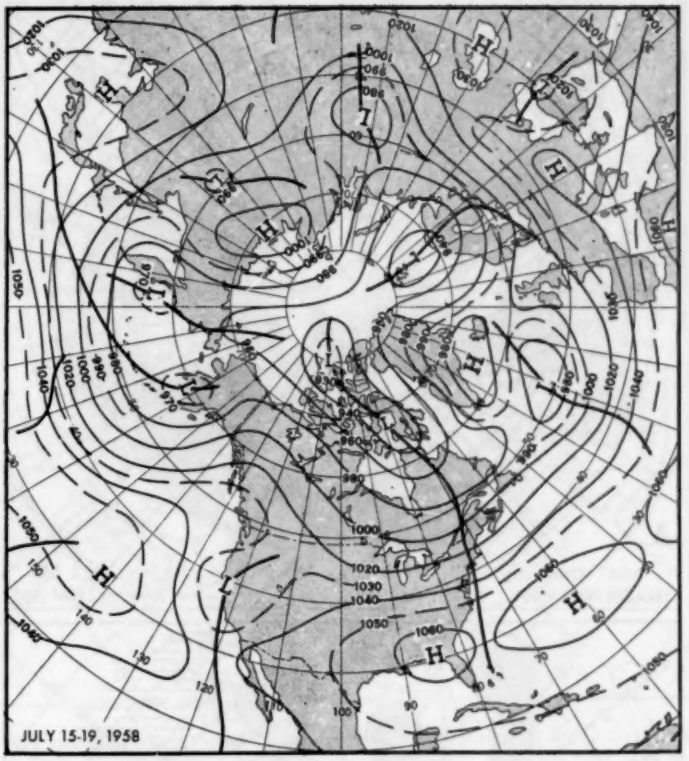

FIGURE 5.—5-day mean 700-mb. contours in tens of feet for July 15–19, 1958. This chart is typical of the secondary regime of July—troughs observed along the coasts but not in central United States.

eastern Bering Sea and southward into the central Pacific, and also the sharp maximum at 60° N. latitude between 120° E. and 130° E. longitude. Some of the troughs were located in favorable areas. For example, the California trough, although weak, was observed on most 5-day mean charts, and the occurrence of troughs in the western Bering Sea primarily during the secondary regime is discernible in the frequency chart.

It is of interest to seek out "teleconnections," or spatial relationships, between features of the circulation. During July 1958 there was a strong suggestion that the high incidence of troughs at 50°—60° N. latitude between 120° and 130° E. longitude, an unfavorable area in recent years for troughs, played an important role in forming the abnormal pattern downstream. In accordance with the familiar wavelength considerations and spatial distribution of percentage frequency of sign of height anomalies [3], troughs and subnormal heights in this area supported troughs located downstream in the *eastern* Bering Sea rather than in the more favored western section of the Sea near Kamchatka. In turn, the eastward displacement of the Bering Sea trough suppressed the trough along the west coast of the United States and supported cyclonic activity in central United States. Inspection of the series of 5-day mean 700-mb. charts for July 1958 revealed that in every case the trough in the western Bering Sea occurred only when the trough at 120°—130° E. filled as the Siberian blocking High shifted

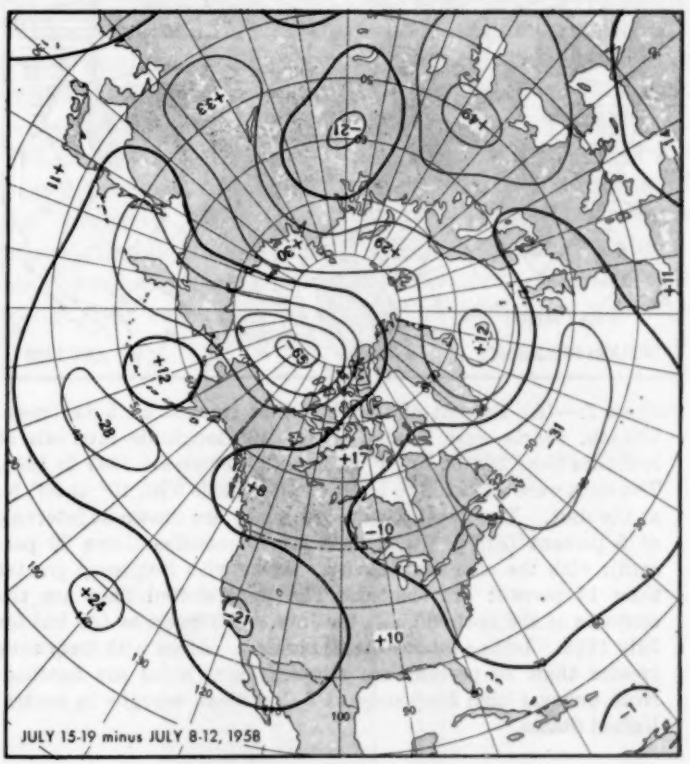

FIGURE 6.—Height difference between the 5-day mean charts for July 8–12 (fig. 4) and July 15–19, 1958 (fig. 5) (July 15–19 minus July 8–12) in tens of feet. Isoline interval is 200 feet. Heights increased in central United States but decreased in the East and West as the circulation changed to a pattern more typical of summer.

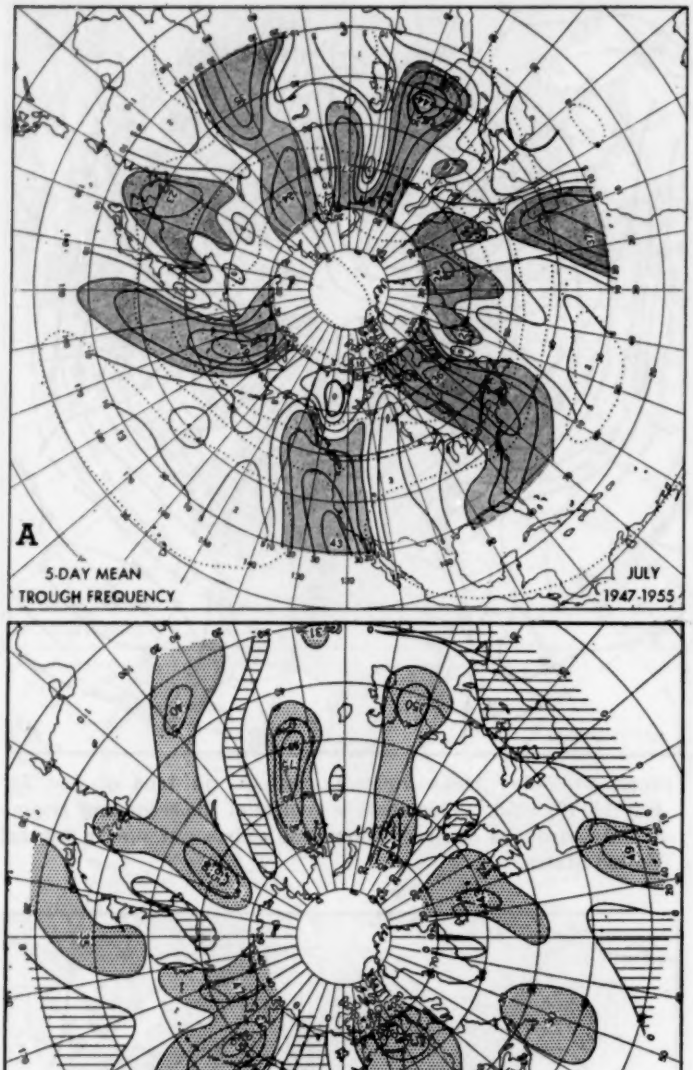

FIGURE 7.—(A) Percent of the time that troughs on 5-day mean 700-mb. charts were located within 10° longitude intervals at latitudes from 30° N. to 70° N. for July for period 1947 to 1955. The data were adjusted to an equivalent basis with 10° at 50° N. as the unit. The lines of equal frequency are drawn at intervals of 5 percent (except 10 percent for frequencies above 20 percent), with the zero line heavier. Areas with frequency greater than 15 percent are shaded. The light dotted lines are the contours of the normal chart for July. (B) Same as (A) but for July 1958. Isoline interval is 20 percent. Areas with frequency greater than 20 percent are stippled; zero areas are hatched. Note unusual high frequency of 5-day mean troughs in central United States.

eastward. Thus the abnormal location of the trough in central United States was associated with equally abnormal positions of the troughs upstream.

3. 30-DAY MEAN WIND FIELD

At the 700-mb. level the jet stream was well organized over the Western Hemisphere (fig. 8), but not over Eurasia. In the former region its axis had larger amplitude, i. e., meandered farther to the north and south, than the normal jet stream for July (dashed line in fig. 8). In the central Pacific the well-defined jet axis was south of normal, but it turned abruptly northward and passed over northwestern Canada before dipping sharply southward to subnormal latitudes again over eastern United States and the Atlantic, where blocking dominated.

The two principal wind speed maxima were found in the abnormally located oceanic troughs which were deep in the north but were unable to penetrate to the south because the zonally oriented subtropical ridges remained strong (fig. 1). The resultant intense height gradients supported wind speeds 3 to 7 m. p. s. above normal (fig. 8B) in these jet maxima.

Similarly in the United States the stream of westerlies flowing southward through the trough, located where ridges are more commonly found, resulted in supernormal winds over most areas of the central and eastern States.

Weaker than normal winds in the northeastern Atlantic were a manifestation of the blocking in that area. And subnormal wind speeds over northwestern United States, associated with the weaker than normal trough in that area, were noteworthy for their pronounced effect on the local weather (see section 5).

4. AIRMASSES AND DAILY FRONTAL POSITIONS

The planetary wave of large amplitude centered over western North America resulted in frequent advection of cool, polar airmasses into the central United States, and the temperature of the lower layers of air averaged below normal in this area during July (fig. 9). Several Highs had tracks extending from western Canada into the northern Plains and then eastward across United States (Chart IX). The frequency of anticyclone passages was computed (within 5° latitude-longitude "boxes" at 45° N.) for July 1958 over the Western Hemisphere, and seven Highs, the maximum for the entire area, passed through the box centered over Lake Michigan. The pronounced 700-mb. ridge in the West and the weak ridge in the East were attended by warm air masses and few anticyclonic centers at sea level.

Since the cool airmasses repeatedly penetrated unusually far south in central United States, an active frontal zone was frequently located at rather low latitudes for July along an east-west band from the Middle Atlantic States to the southern Rocky Mountain States (fig. 10). Quite often in July, fronts remain farther north than this along the northern tier of States. This

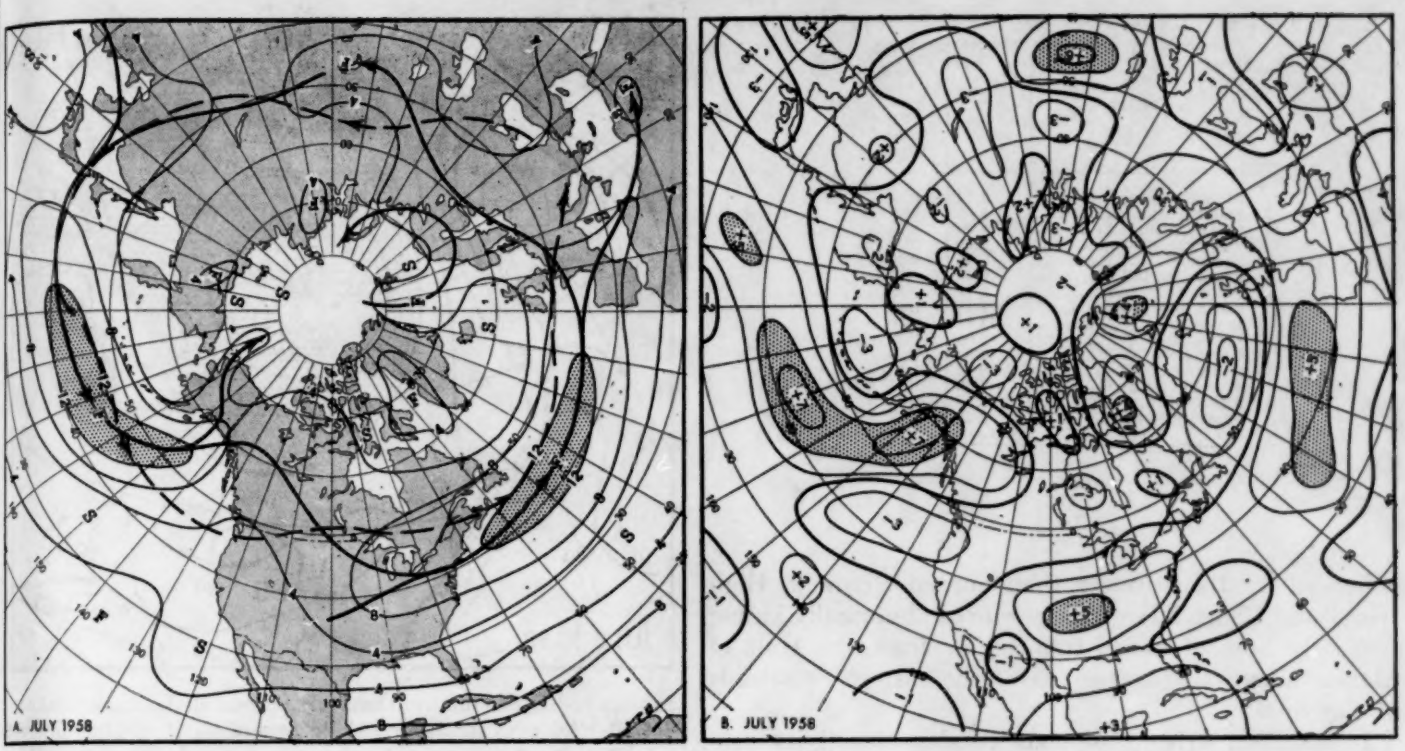

FIGURE 8.—(A) Mean 700-mb. isotachs and (B) departure from monthly normal wind speed (both in meters per second) for July 1958 Solid arrows in (A) indicate principal areas of maximum winds and dashed arrows their normal July positions. Regions with speeds greater than 12 m. p. s. have been stippled. Jet maxima were located over the Pacific and Atlantic oceans, and wind speeds were above normal over central and eastern United States.

July, fronts were observed on 15 or more days in the middle latitudes of the United States, with an extreme of 24 days with fronts in the Kansas-Missouri region.

This month we had an excellent illustration of the expected simultaneous relationship of several meteorological parameters. Extending from the central United States to the Northeast, there existed a confluence zone (fig. 1) and jet stream with attendant super-normal winds (fig. 8). Associated with these circulation features were a strong north-south temperature gradient (fig. 9) and narrow band of high frequency of days with fronts (fig. 10) Along this active zone, showers were frequent, and the total precipitation for the month was large.

5. WEATHER OF THE MONTH

PRECIPITATION

July was a wet month over most of the United States (Chart II, Chart III A, B). Vast areas received more than the normal amount, and some regions reported 3 to 5 times the usual July rainfall (Chart III–B). In the central areas of the United States and in the Northeast extreme amounts from 5 to 15 inches (Chart II) established many new station precipitation records. No less than eleven stations in this area, which have long periods of record, reported all time high precipitation amounts for July (table 1). Springfield, Mo. and Parkersburg, W. Va. even had their wettest calendar month on record. Other stations, although not reporting record-breaking amounts, had more rainfall than any July in recent years—many since the turn of the century (table 2). The inclusion of Billings, Mont., in table 2 indicates the heavy precipitation regime which occurred in parts of the northern Rocky Mountain States. This July's heavy rainfall, besides being associated with the abnormally cyclonic flow, confluence, jet stream, and frequent fronts over central areas of the United States, was also

TABLE 1.—*New precipitation records made in July 1958*

Station	Total monthly precipitation (inches)	Date records start
Lincoln, Nebr.	11.40	1878
Columbia, Mo.	11.45	1889
Springfield, Mo.	18.75	1887
Akron, Ohio	11.43	1887
Columbus, Ohio	10.07	1878
Toledo, Ohio	6.71	1870
Youngstown, Ohio	7.41	1942
Parkersburg, W. Va.	12.05	1888
Williamsport, Pa.	8.30	1873
Baltimore, Md.	11.50	1871
Nantucket, Mass.	7.45	1886
Tucson, Ariz.	5.20	1892
Mount Shasta, Calif.	1.77	1888

TABLE 2.—*Unusually large precipitation amounts for July 1958*

Station	Total July precipitation	Latest previous year with larger amount
Billings, Mont.	3.12	1912
Duluth, Minn.	8.51	1909
Omaha, Nebr.	9.60	1875
Valentine, Nebr.	5.39	1929
Peoria, Ill.	8.42	1860
Evansville, Ind.	9.69	1910
Indianapolis, Ind.	8.11	1875
South Bend, Ind.	7.18	1896
Lexington, Ky.	10.64	1875
Louisville, Ky.	7.05	1922
Charleston, W. Va.	9.36	1938
Columbia, S. C.	8.70	1936
Washington, D. C.	7.15	1945
Middletown, Conn.	8.14	1938
Providence, R. I.	6.29	1938

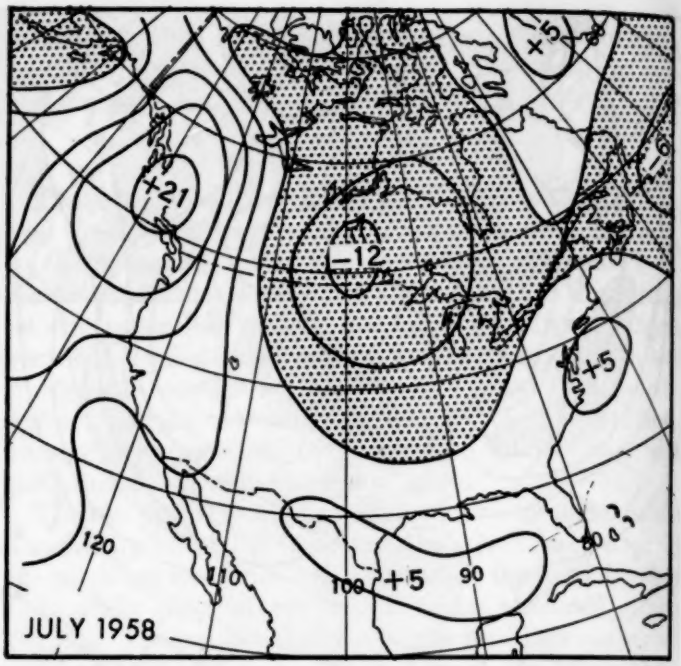

FIGURE 9.—Departure from monthly normal of the mean thickness (700–1000 mb.) for July 1958 (in tens of feet). Isoline interval is 50 feet. Below normal values are stippled. Cool conditions dominated the central United States while warm airmasses occupied the Northwest and Southeast.

enhanced by the stronger than normal Bermuda High (fig. 1 and Chart XI) which produced abnormally strong southerly flow of moist tropical air from the Gulf of Mexico northward over much of the eastern two-thirds of the country.

In southern Arizona pronounced shower activity produced above normal rainfall (Chart III–B), and Tucson reported the wettest July on record. Northern California and southern Oregon, usually dry at this time of year, had precipitation totaling more than one inch. Mount Shasta, Calif., established a new July record of 1.77 inches.

Because of the highly favorable regime for rainfall, dry conditions were reported from only small areas in the United States. The extreme west coast where downslope flow prevailed (note anomalous flow from northeast in fig. 1), received little or no rainfall. Seattle, Wash., with no measurable precipitation, had the driest July on record, and Tatoosh Island, Wash., measured only 0.24 inch, their smallest amount since 1922. A large area of the Great Basin was also arid, but there was no organized drought in the United States. The few stations that did report record dry weather were widely scattered. In addition to those stations already mentioned, Winslow, Ariz. with 0.17 inch and Cape Hatteras with 0.45 inch reported the driest July on record. Grand Junction, Colo., and Albuquerque, N. Mex , had their driest July since 1898 and 1900 respectively. Over the United States as a whole there was a paucity of significant dry-weather reports, but many precipitation and cloudiness records were broken, and July 1958 will be recorded as an extremely wet month in most areas.

TEMPERATURE

In the central portion of the United States, where the heavy rainfall was noted, temperatures averaged very cool for July. However extreme southern parts of the Plains, and Rocky Mountain States were warm with some areas reporting much-above normal temperatures (Chart I). Hot weather also was observed in the Far Northwest, in coastal regions of California, and in the Middle and Southern Atlantic States.

From June [5] to July there was a westward shift of the temperature pattern, associated with the retrogression of the planetary trough from the east coast to the central United States. In the central Plains and Rocky Mountain States temperatures cooled by 2 to 3 classes from June to July, while an equal amount of warming took place in the Middle Atlantic States (fig. 11). Little change occurred in between over the Central States where temperatures remained below normal.

This month's temperature pattern is, in most areas, easily related to the mean flow. The ridge with above normal heights in western Canada and the trough with subnormal heights over central United States (fig. 1) were accompanied by stronger than normal northerly flow over western North America. This encouraged frequent invasions of cool airmasses over the central Plains of the United States. The eastern ridge remained flat, especially in the north, under the domination of the Atlantic blocking, so that the cool airmasses frequently pushed eastward and kept northern New England cool.

The cool weather in States bordering the eastern Gulf of Mexico seemed to be associated with cyclonic flow at 500 mb. (not shown), and the cloudiness and precipitation which occurred in the first half of July.

In the Great Basin the subnormal temperatures, which have been so characteristic of Julys since 1953, are not easily explained. The records at Winnemucca and Ely,

for example, indicate that both the maximum and minimum temperatures were below normal, while the amounts of cloudiness and sunshine were very close to normal. Precipitation could not have suppressed the temperatures since it was below normal, and in fact the warmest and cloudiest days tended to occur together. The California trough was weak, and there was little advection of cool Pacific air into the Basin. The 700–1000-mb. thickness averaged above normal (fig 9). However, at 700 mb. the anomalous flow was from the north-northeast (fig. 1), indicating that on the average cooler than normal air was advected into this area at the higher levels. This cool air aloft could have maintained a steep lapse rate, thus holding the surface temperatures below normal. But this seems hardly an adequate explanation for the much below normal temperatures that were observed. An extreme of −6.1° at Winnemucca is over three times the standard deviation—a rare event indeed. Perhaps these extreme anomalies are tied in with the currently used normal temperature.

Temperatures in the Great Basin have been cool, relative to surrounding areas, since 1953 when the normal temperatures were adjusted for different periods of record, changes of station locations, etc. Because past records have been so heterogeneous, establishing the proper normal is a very difficult problem. Therefore, it is possible that the negative anomalies during recent Julys in this area are partially a result of the new normal temperatures, which are higher than those used prior to 1953. For example, the July normal temperatures used after 1952 were higher than the previous normals by 3.6° F. at Winnemucca, Nev., 4.9° F. at Ely, Nev. 3.4° F. at Las Vegas, Nev., and 3.8° F. at Yuma, Ariz. At neighboring stations the normals also increased but by smaller amounts. After checking the records at a few of these pertinent stations it was found that the monthly mean temperature anomaly at Winnemucca has been negative every July since 1953 and also negative at Ely since 1955. For every 5-day period during July 1958 the anomaly at Winnemucca was negative, and at Ely the anomaly reached +1 for only two 5-day periods, which, incidentally, were overlapping.

Admittedly certain regimes are known to persist for considerable lengths of time, and the cool weather relative to past years in the Great Basin may be entirely real or at least partly so. But the associated circulation anomalies (incidentally based on normals for a different period than the temperature normals) for this July do not support the extreme temperature anomalies in that area. More light will probably be shed on this problem when new normals are computed in 1960.

The warmth in the Middle Atlantic States was associated with the persistent Bermuda High and southerly anomalous flow at sea level (Chart XI) and at 700 mb. (fig. 1). The only time cool, dry air really penetrated this area was during the secondary regime (fig. 5) immediately after mid-month. In the Northwest the strong ridge (fig. 1), with absence of westerlies (fig. 8), and accompanying cool Pacific airmasses, prolonged the record-breaking heat wave previously reported in June [5]. Olympia and Seattle, Wash., and Eugene and Pendleton, Oreg. had the warmest July on record.

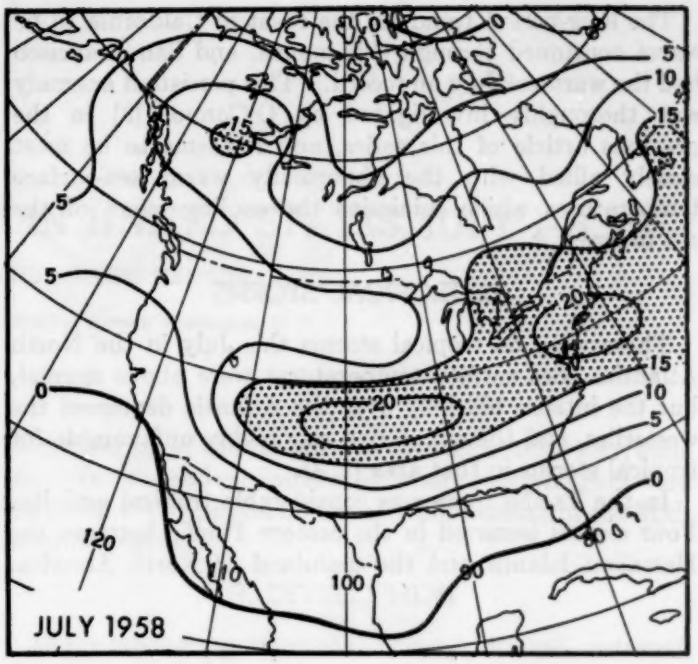

FIGURE 10.—Number of days in July 1958 with fronts of any type within unit squares (with sides approximately 500 miles). All frontal positions are taken from *Daily Weather Map*, 1:00 p. m., EST. Areas with 15 or more days with fronts are stippled. Fronts were frequently located in central and northeastern United States, separating the cool polar airmasses from the maritime tropical airmasses.

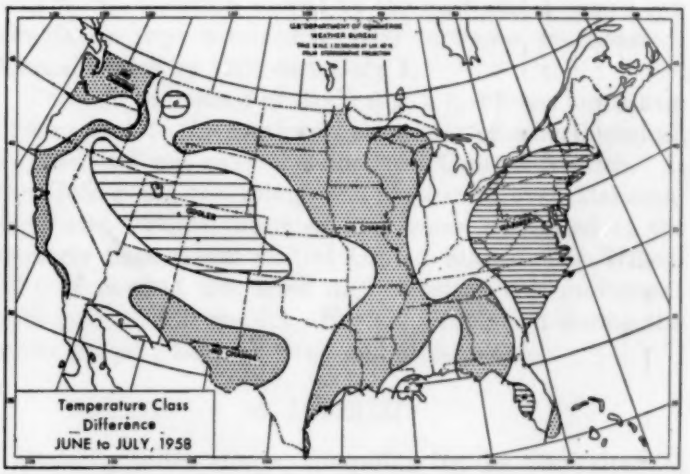

FIGURE 11 —Number of classes the anomaly of temperature changed from June to July 1958. Areas where the anomaly in July was 2 or 3 classes cooler are stippled, 2 or 3 classes warmer are fine hatched, and areas of no change in anomaly are coarse hatched. The East was warmer and the interior areas of the West were cooler in July than in June.

The long-period trend for the coast of California to be warm continued through this month, and San Francisco had the warmest July on record. This persistent anomaly was thoroughly investigated by O'Connor [5] in the previous article of this series, and it seems to be most closely allied with the abnormally warm sea-surface temperatures which minimize the cooling effect of the sea breeze.

6. TROPICAL STORMS

There were no tropical storms this July in the North Atlantic. Sea-surface temperatures were above normal, but the intense blocking over the Atlantic depressed the westerlies, and the circulation was highly unfavorable for tropical storms in that area [1, 4].

In the Pacific there was considerable tropical activity. Four storms occurred in the eastern Pacific between the Hawaiian Islands and the mainland of North America. Two of these cyclones reached hurricane intensity. In the western Pacific six tropical storms were reported, and all but one reached typhoon intensity.

REFERENCES

1. E. M. Ballenzweig, "Relation of Long-Period Circulation Anomalies to Tropical Storm Formation and Motion," *Journal of Meteorology* (To be published).
2. W. H. Klein and J. S. Winston, "Geographical Frequency of Troughs and Ridges on Mean 700-mb. Charts," to be published in *Monthly Weather Review*, vol. 86, 1958.
3. [D. E. Martin], "Atlas of 700-mb. Five-Day Mean Northern Hemisphere Anomaly Charts," Air Weather Service, *Technical Report* No. 105–100/2, July 1955, 39 pp.
4. J. Namias, "Long-Range Factors Affecting the Genesis and Paths of Tropical Cyclones," *Proceedings, UNESCO Symposium on Typhoons, 9–12 November 1954, Tokyo*, pp. 213–219.
5. J. F. O'Connor, "The Weather and Circulation of June 1958—Record Cold in Northeast and Warmth in Northwest," *Monthly Weather Review*, vol. 86, No. 6, June 1958, pp. 229–236.

THE COLD LOW OVER SOUTHEASTERN UNITED STATES, JULY 1–6, 1958

EDMUND A. DI LORETO AND MASARU HAMADA

National Weather Analysis Center, U. S. Weather Bureau, Washington, D. C.

1. INTRODUCTION

During the summer months anticyclonic circulation persists at the surface over southeastern United States. The airmass is usually either convectively unstable or in the process of becoming so, due to strong day-to-day insolation and the availability of moisture from the Gulf of Mexico and the Atlantic Ocean.

Because frontal systems and surface cyclonic circulation are lacking, showers and thunderstorms that occur in this airmass have been attributed to the release of conditional instability by surface heating regardless of the extent of the activity. Studies by Byers and Rodebush [1], and others, indicate that thermal instability, though a necessary condition, is not in itself sufficient cause for the development of widespread cloudiness and thunderstorm activity. Baum's study [2] indicated that the occurrence of thunderstorms in Florida cannot be determined purely from the standpoint of thermodynamics, even when the moisture parameter is taken into consideration. Widespread cloudiness and shower activity are always associated with relatively large-scale zones of convergence that are dynamically induced.

In this study an attempt will be made to explain on the basis of dynamically induced convergence the cloud and precipitation pattern that developed with the upper cold Low circulation over southeastern United States, July 1–6, 1958.

2. ANTECEDENT CONDITIONS

During the last week of June a cold front moved across the eastern United States. The portion of this cold front that had extended across northern Florida dissipated and by the last day of the month a high pressure system dominated the weather over southeastern United States. The air behind the cold front was a comparatively cool and dry Canadian type.

Aloft, at 500 mb. and 250 mb., a large-amplitude trough associated with the surface frontal system extended from a Low centered near Sable Island south-southwestward across the extreme western Atlantic Ocean, across the northern border of Florida and into the Gulf of Mexico. With the zone of strong westerlies extending across extreme southern Canada, the portion of the trough north of 36° N. continued moving eastward. The southern portion, with generally light circulation, tended to remain stationary. This shearing of the trough was evident at 0000 GMT, June 30. Warm air advection and generally rising heights were indicated over the Northeast and the northernmost Mid-Atlantic States.

3. DEVELOPMENT

As the northern portion of the trough sheared eastward, warm air advection aloft across New England and the northernmost Mid-Atlantic States brought height rises over these areas. This was evident at 500 mb. (fig. 1 A and B) and to a greater degree at 250 mb. (fig. 2 A and B).

As a result of building of the 250-mb. heights to the north of the stationary portion of the trough with little change to the south, there was an increase of cyclonic vorticity south of the height rises. Winds over Virginia and North Carolina veered to the east and a closed low circulation was established over extreme southeastern United States by 1200 GMT, July 1.

Through the period of study (fig. 2 A–F), the low center drifted first to the southwest across extreme northwestern Florida and out over the northern Gulf of Mexico. It then followed a recurving path northward over Alabama, then east-northeastward as it became imbedded in the westerly flow across central United States. The Wilson [3] grid method was tried in forecasting this movement with good to fair results. Surface circulation during the entire period remained weak and anticyclonic.

4. STABILITY

Stability index charts, computed by the Showalter [4] method for obtaining a measure of conditional instability (fig. 3 A–F), indicated that in general the air over southeastern United States was convectively stable during the first day of the period. This is not surprising in view of the Canadian origin of this air. The air over southern Florida, a mixture of Canadian and tropical maritime airs, was conditionally unstable.

The changes in stability index, progressing through the period, are attributed, in part, to heating and the addition of moisture in the low levels of the relatively cool air, and to cold air advection associated with the moving cold Low in the high levels. Comparison of the soundings on the vertical cross sections (figs. 4 and 5) shows that this differential advection, heating below and cooling aloft,

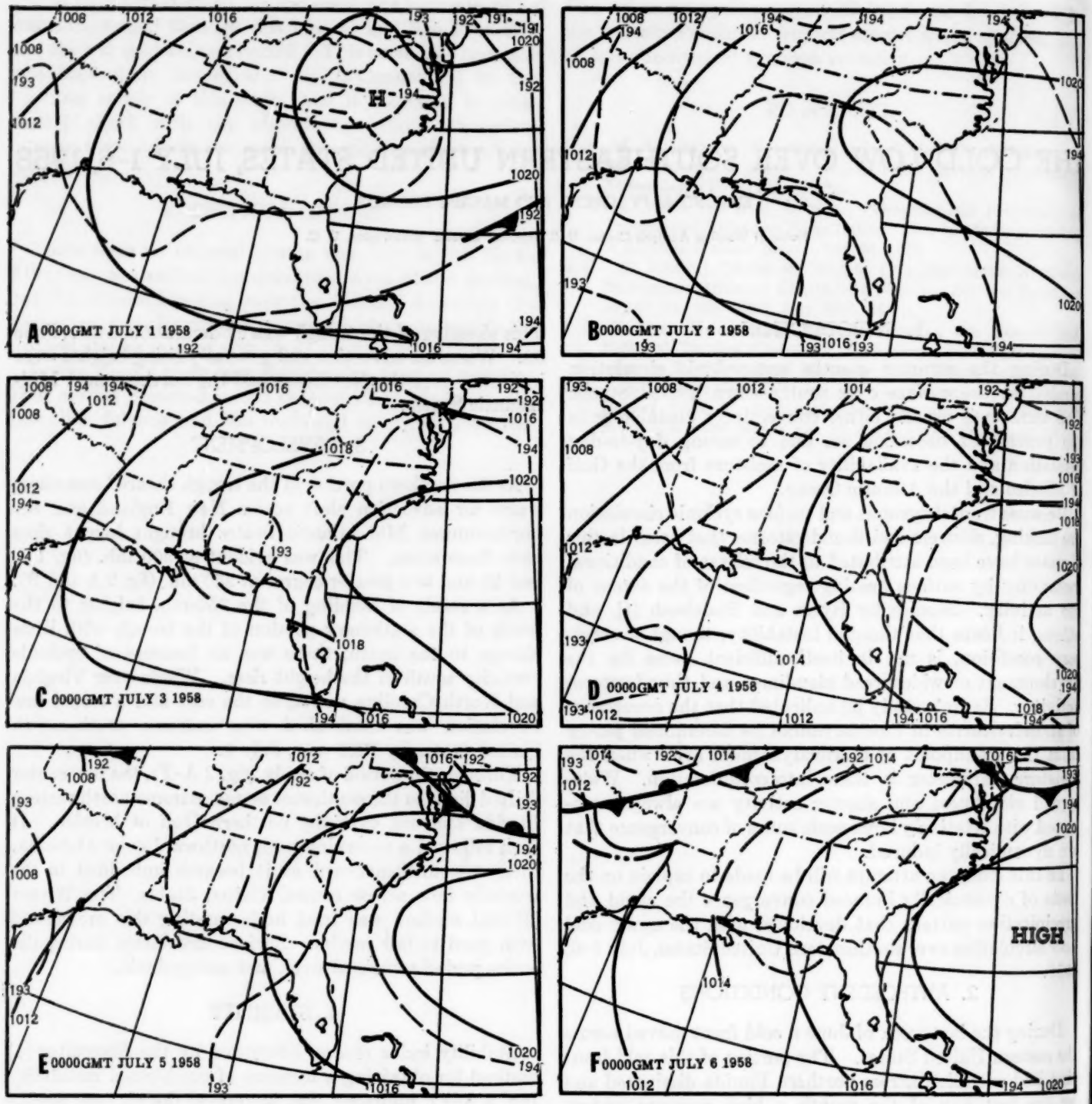

FIGURE 1.—Sea level isobars (solid lines) and 500-mb. contours (dashed lines) for 0000 GMT, July 1 to July 6, 1958. 500-mb. contours are in hundreds of geopotential feet.

resulted in packing of the isotherms and indicated decreasing stability. In the vertical cross sections, Bellamy D values [5] are used to illustrate the vertical structure of the atmosphere. The rate of change of D values also indicates stability condition; i. e., cooling is depicted by increasing negative departures or decreasing positive departures.

The stability index at Montgomery, Ala., decreased from +3, July 2 to −2, July 4, as the cold Low moved from just south of Panama City, Fla., to near the Mobile, Ala., area. Jackson, Miss., during the same period, showed a stability index decrease from +4 to +1.

The change in stability index at Montgomery resulted from an increase in temperature and moisture at the

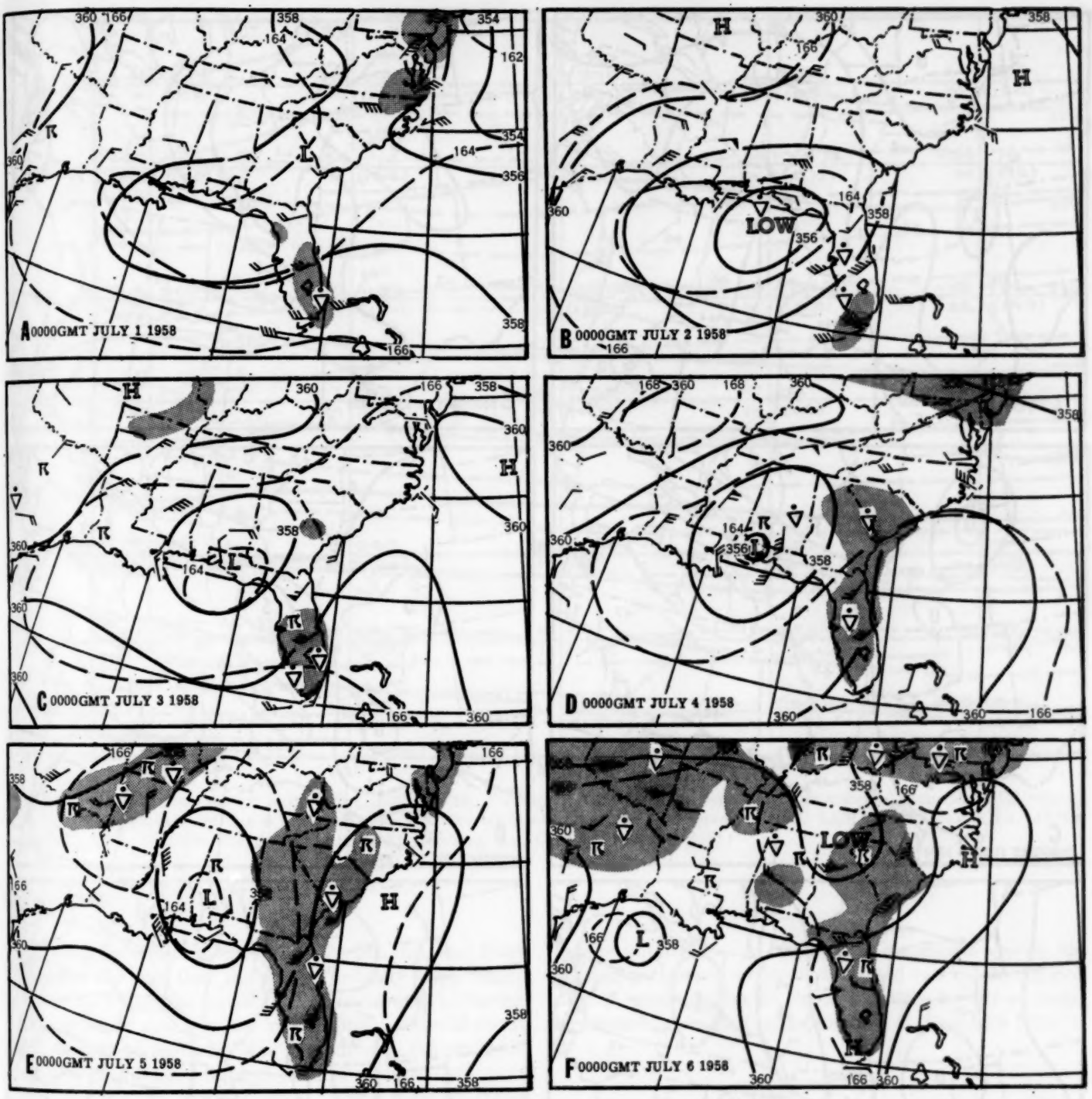

FIGURE 2.—250-mb. maps for 0000 GMT, July 1 to July 6, 1958 with 500–250-mb. thickness lines (dashed). Current cloudiness is shown by shading, and areas of precipitation by symbols.

850-mb. level and cooling at the 500-mb level. At Jackson, the change was due only to an increase in temperature and moisture at the 850-mb. level since the 500-mb. temperature was unchanged.

Farther to the east of the upper low center, Athens, Ga., showed a decrease in stability index from +4 to −1, attributable to increased temperature and moisture at the 850-mb. level with no change in temperature at the 500-mb. level. Lake Charles, La., to the west of the Low, showed a slight increase in stability.

It is noteworthy that to the east of the Low (figs. 4 and 5) marked moisture increases were indicated up through the 500-mb. level, whereas to the west the increases were slight and occurred only in the lowest levels.

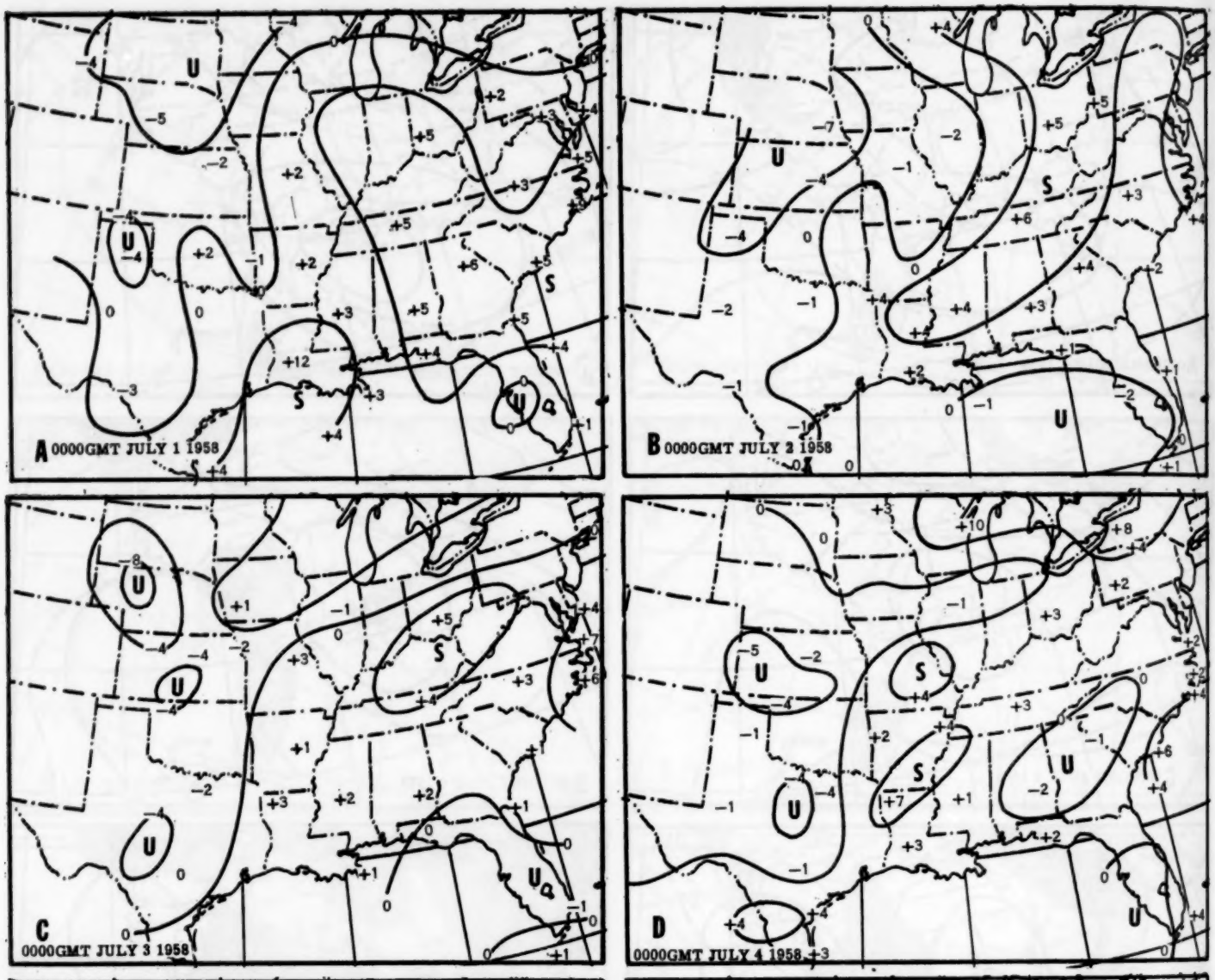

FIGURE 3.—Showalter stability index for 0000 GMT, July 1 to July 6, 1958.

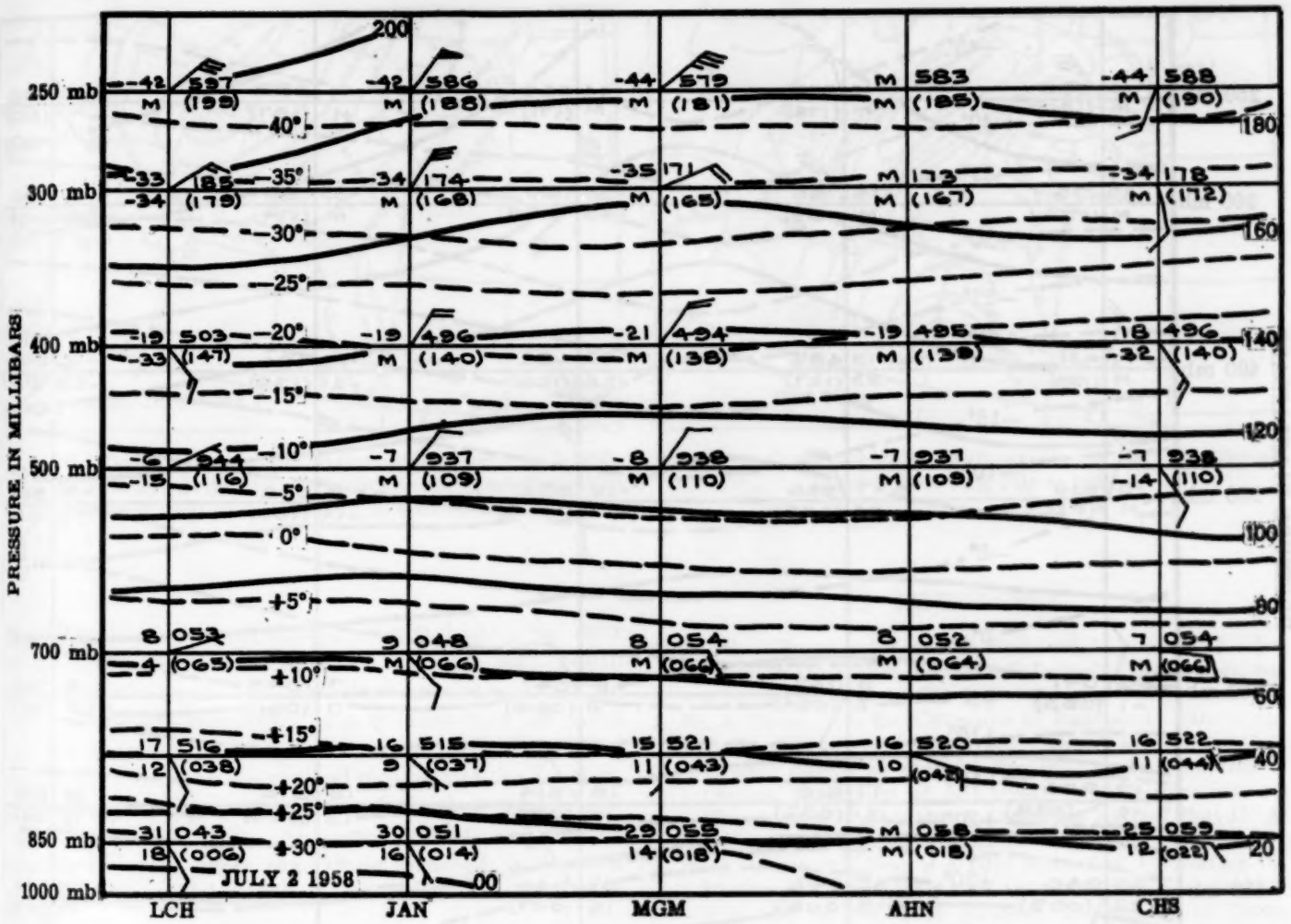

FIGURE 4.—Vertical cross section at 0000 GMT, July 2, 1958. Figures in parentheses are departure from standard atmosphere (D values). Isolines of D values (solid) are in hundreds of feet. Isotherms (dashed lines) are at intervals of 5° C. LCH=Lake Charles, La., JAN=Jackson, Miss., MGM=Montgomery, Ala., AHN=Athens, Ga., CHS=Charleston, S. C.

The generally weak circulation at the 500-mb. and lower levels and the fact that the air was initially fairly homogeneous rule out the possibility of horizontal advection as the cause of this increase in moisture. Since the only likely source of moisture was the surface, the observed changes indicate the extent of vertical motion.

Vertical motion has the effect, other than of transporting moisture aloft, of stretching the air column in the vertical and decreasing absolute stability. Vertical motion cannot be determined directly from observations but can be related to vorticity and divergence. The Joint Numerical Weather Prediction Unit was preparing vertical motion charts during this period while experimenting with a two-level baroclinic model. These charts (not shown) indicated a weak positive vertical velocity over all of southeastern United States and, of course, did not explain the variation in distribution of moisture aloft. This could be because of the general weakness of the circulation up through the 500-mb. level and the result of smoothing out of small-scale features which can be locally important. In the x, y, p coordinate system the vertical p-velocity, $\omega \equiv dp/dt$, is related to wind divergence, $\mathrm{div}_p\, \mathbf{V}$, measured on an isobaric surface by the equation of continuity written in the form (c. f., Panofsky [6]):

$$\frac{\partial \omega}{\partial p} = -\mathrm{div}_p\, \mathbf{V}$$

Although it is possible to evaluate divergence from reported winds, this is difficult because the greatest contribution to divergence is made by wind deviations from the geostrophic wind. For the purpose of this discussion, only the sign of the vertical motion is required to explain its contribution to change in stability and the weather.

We can approximate the vertical distribution of divergence from the vorticity theorem and from this distribution and the equation of continuity we can determine the sign of the vertical motion. (Note that although ω and w, the real vertical motion, have opposite signs, $\partial\omega/\partial p$ and $\partial w/\partial z$ have the same sign.) The isobaric horizontal

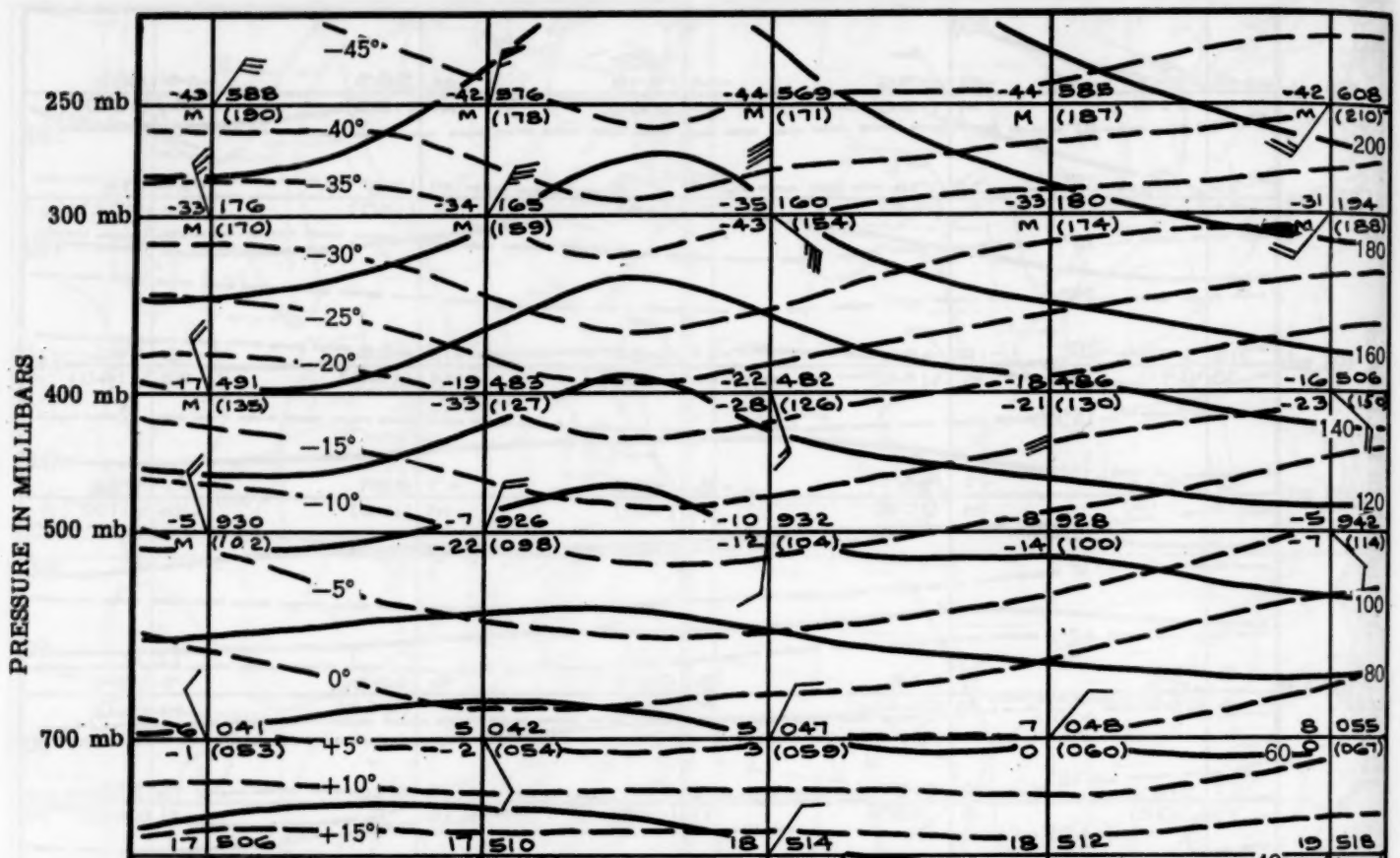

FIGURE 5.—Vertical cross section at 0000 GMT, July 4, 1958.

divergence $\text{div}_p \mathbf{V}$ is given by the vorticity equation written in the form:

$$\text{div}_p \mathbf{V} = -\frac{1}{\zeta + f}\left(\frac{d\zeta}{dt} + \beta v\right)$$

where ζ is the relative vorticity, f the Coriolis parameter, t time, β the rate of change of f along the y axis, and v the component of the wind along the y axis (positive northward).

If the relative vorticity is negative at ridges and positive at troughs, and the air moves faster than the system (Panofsky [6]), $d\zeta/dt$ will be negative east of troughs and positive east of ridges. The βv term is positive east of troughs and negative east of ridges but is relatively less important than $d\zeta/dt$ at high speeds. At high levels, therefore, we can expect divergence east of troughs and conversely convergence east of ridges. At low levels, with slower winds, the βv term becomes more important; if the winds are slower than the system, $d\zeta/dt$ has the same sign and therefore also contributes to convergence ahead of troughs and divergence east of ridges. Hence, from the equation of continuity, we can expect ascending motion east of the upper trough and descending motion west of the trough.

Horizontal divergence charts for July 4 (figs. 6 and 7), prepared as described by Saucier [7], give the distribution of the horizontal divergence at 2,000 ft. and the 250-mb. level, and agree favorably with what has been discussed. The resulting vertical motion explains the occurrence of the unstable areas (fig. 3 A–F) east of the low center and the tendency for stabilization to the west.

The following paragraph discusses the association of weather with vertical motion and changes in stability.

5. PRECIPITATION

During the first day of the period, precipitation, in the form of showers, and cloudiness were confined to the unstable area over southern Florida (fig. 2A). By July 4

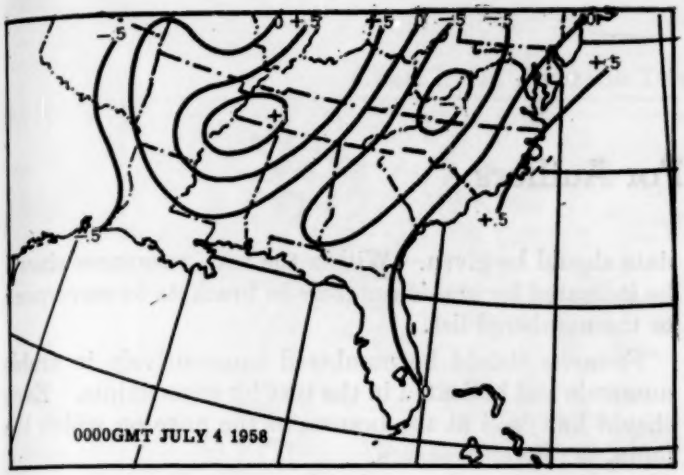

FIGURE 6.—Computed horizontal divergence (10^{-5} sec^{-1}) for 2000-ft. level at 0000 GMT, July 4, 1958. Positive areas indicate horizontal divergence and negative areas horizontal convergence.

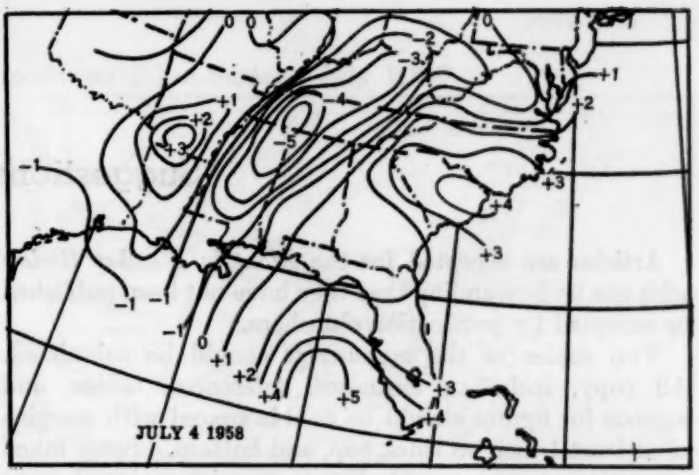

FIGURE 7.—Computed horizontal divergence (10^{-5} sec^{-1}) for 250-mb. level at 0000 GMT, July 4, 1958.

(fig. 2D), cloudiness and shower activity had spread over all of northern Florida, most of Georgia, and South Carolina, but west of the Low clear skies continued and no precipitation was reported. It is evident that the cloud and precipitation pattern obtaining through the period was closely related to the vertical motion and the development of instability to the east of the low center and stability to the west. Showers and thunderstorms reported in areas other than those enclosed in figure 2 appeared to be widely scattered.

6. CONCLUSION

The review of this storm brought forth an appreciation of the effects of dynamically induced divergence and vertical motion on stability and the weather. These effects and the weather could only be explained when the comparatively stronger high-level cyclonic circulation was considered, since at the surface the circulation remained weakly anticyclonic during the entire period. This dynamic lifting served the twofold purpose of increasing and releasing convective instability.

REFERENCES

1. Horace R. Byers and Harriet R. Rodebush, "Causes of Thunderstorms of the Florida Peninsula," *Journal of Meteorology*, vol. 5, No. 6, Dec. 1948, pp. 275–280.
2. W. A. Baum, "On the Utilization of Radiosonde Data in the Study of Thunderstorm Thermodynamics," *Report to the U. S. Weather Bureau on Research Performed by the University of Chicago, Department of Meteorology in Connection with the Thunderstorm Project*, Oct. 1, 1946–June 30, 1947 Part IV–A, University of Chicago, Aug. 1947.
3. H. P. Wilson, "A Test of a Grid Method of Forecasting the Motions of Lows at 500 mb. in Arctic Regions," *Circular* 2539 TEC 194, Meteorological Division, Department of Transport, Canada, Oct. 4, 1954.
4. A. K. Showalter, "A Stability Index for Thunderstorm Forecasting," *Bulletin of the American Meteorological Society*, vol. 34, No. 6, June 1953, pp. 250–252.
5. J. C. Bellamy, "The Use of Pressure Altitude and Altimeter Correction in Meteorology," *Journal of Meteorology*, vol. 2, No. 1, Mar. 1945, pp. 1–79.
6. Hans Panofsky, *Introduction to Dynamic Meteorology*, The Pennsylvania State University, University Park, Pa., 243 pp. (pp. 90–91 and 115–117).
7. Walter J. Saucier, *Principles of Meteorological Analysis*, University of Chicago Press, Chicago, Ill., 1955, 438 pp. (pp. 321–322).

Suggestions For Authors

Articles are accepted for the *Monthly Weather Review* with the understanding that they have not been published or accepted for publication elsewhere.

Two copies of the *manuscript* should be submitted. All copy, including footnotes, references, tables, and legends for figures should be double spaced with margins of at least 1 inch on sides, top, and bottom. Some inked corrections are acceptable but pages with major changes should be retyped. The style of capitalization, abbreviation, etc., used in the *Review* is governed by the rules set down in the Government Printing Office Style Manual.

Tables should be typed, each on a separate page, with a title provided. They should be numbered consecutively in arabic numerals.

In *equations* conventional symbols in accordance with the American Standards Association Letter Symbols for Meteorology should be used. If equations are written into the manuscript in longhand, dubious-looking symbols should be identified with a penciled note.

References should be listed on a separate sheet and numbered in the order in which they occur in the text; or, if there are more than 10, in alphabetical order according to author. The listing should include author, title, and source (if the source is a magazine, the volume, number, month, year, and complete page numbers should be listed; if the source is a book, the publisher, place and date of publication, and the page numbers of the reference). If reference is made to a self-contained publication, the author, title, publisher, place of publication, and date should be given. Within the text, references should be indicated by arabic numbers in brackets to correspond to the numbered list.

Footnotes should be numbered consecutively in arabic numerals and indicated in the text by superscripts. Each should be typed at the bottom of the page on which the footnote reference occurs.

Illustrations. A list of legends for the illustrations should be typed (double spaced) on a separate sheet. Each illustration should be numbered in the margin or on the back outside the image area. To fit into the *Review* page, illustrations must take a reduction not to exceed 3½″ x 9″ (column size) or 7½″ x 9″ (page size). Map bases should show only political and continental boundaries and latitude and longitude lines, unless data are to be plotted, when station circles will also be needed. Usually the less unnecessary detail in the background the better will be the result from the standpoint of clear reproduction. Line drawings and graphs should also be uncluttered with fine background grids unless the graph demands very close reading. It is not necessary to submit finished drawings, as drafting work can be done at the time the paper is prepared for publication.

Photographs should be sharp and clear, with a glossy surface. Bear in mind that marks from paper clips or writing across the back will show up in the reproduction. Drawings and photographs should be protected with cardboard in mailing.

U. S. GOVERNMENT PRINTING OFFICE: 1958

Chart I. A. Average Temperature (°F.) at Surface, July 1958.

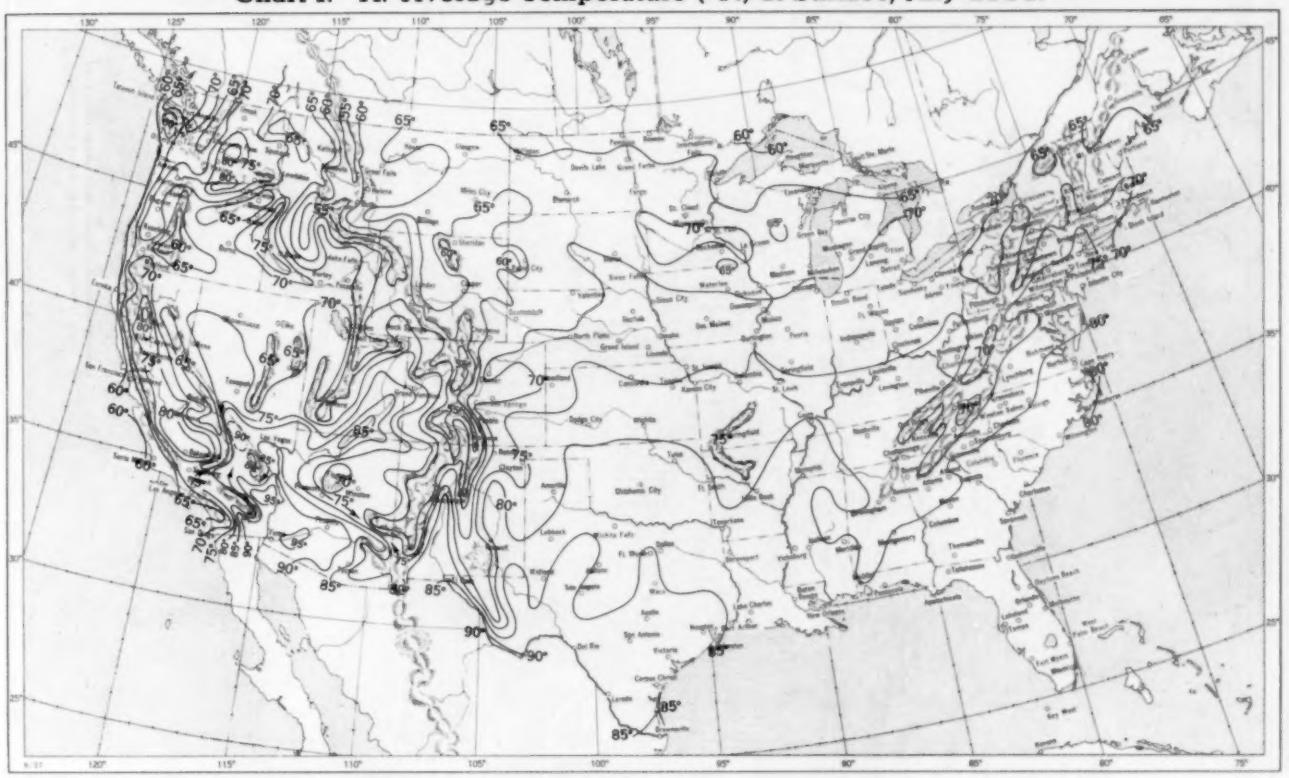

B. Departure of Average Temperature from Normal (°F.), July 1958.

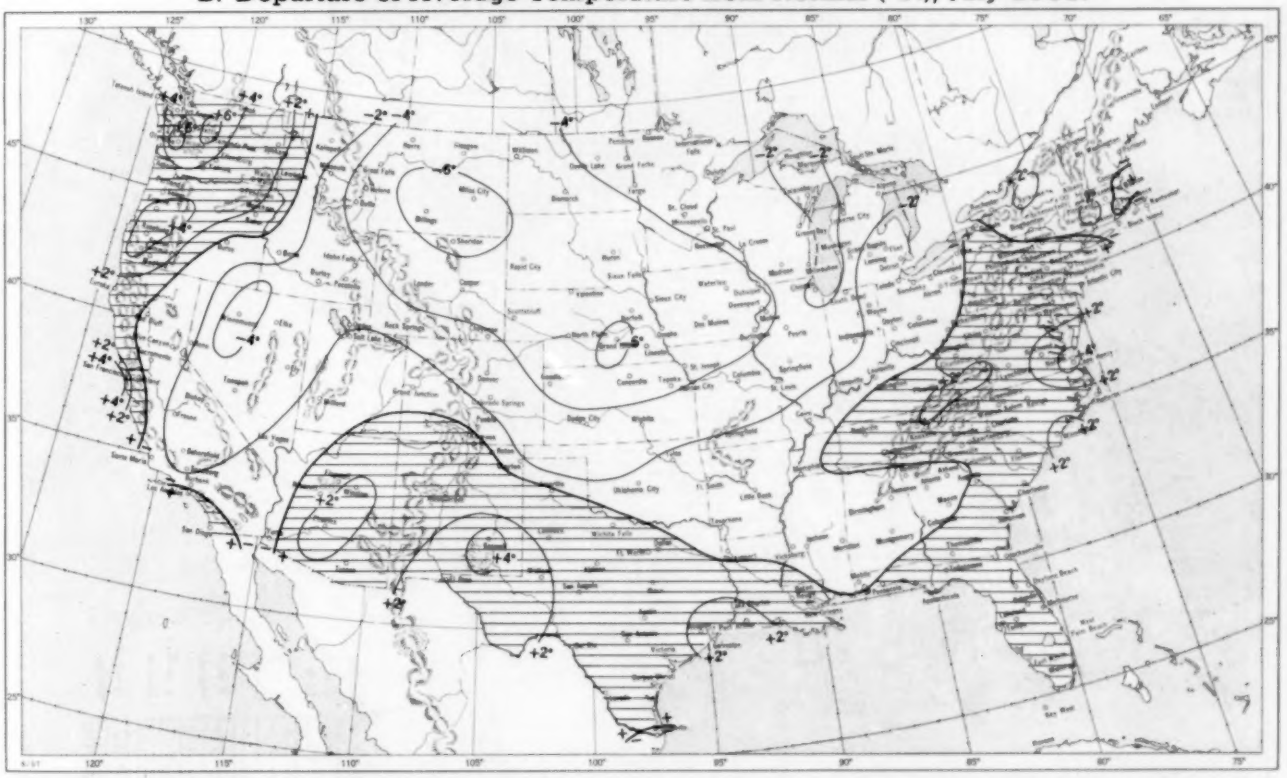

A. Based on reports from over 900 Weather Bureau and cooperative stations. The monthly average is half the sum of the monthly average maximum and monthly average minimum, which are the average of the daily maxima and daily minima, respectively.

B. Departures from normal are based on the 30-yr. normals (1921-50) for Weather Bureau stations and on means of 25 years or more (mostly 1931-55) for cooperative stations.

Chart II. Total Precipitation (Inches), July 1958.

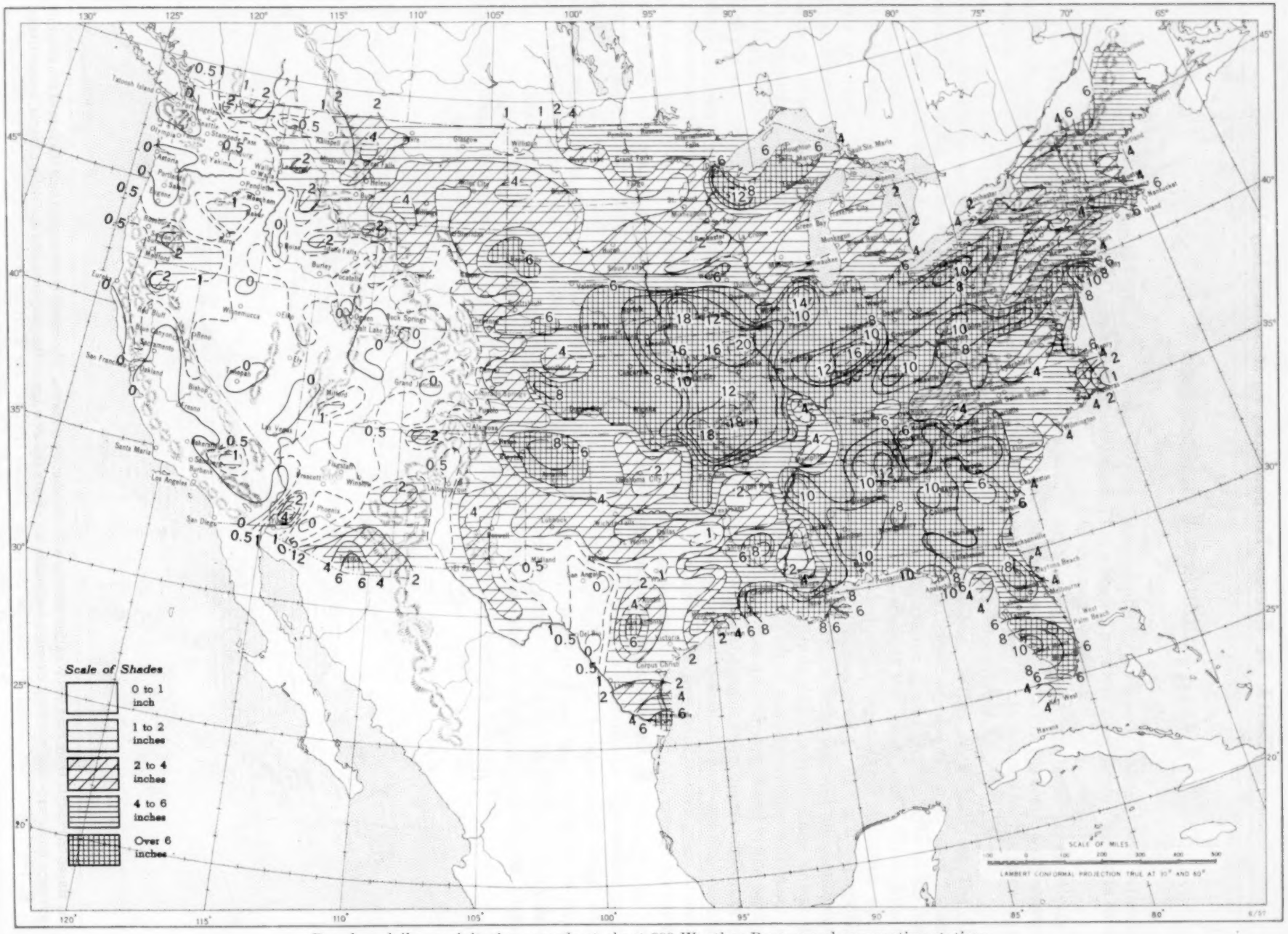
Scale of Shades
0 to 1 inch
1 to 2 inches
2 to 4 inches
4 to 6 inches
Over 6 inches
SCALE OF MILES
LAMBERT CONFORMAL PROJECTION TRUE AT 33° AND 45°

Based on daily precipitation records at about 800 Weather Bureau and cooperative stations.

Chart III. A. Departure of Precipitation from Normal (Inches), July 1958.

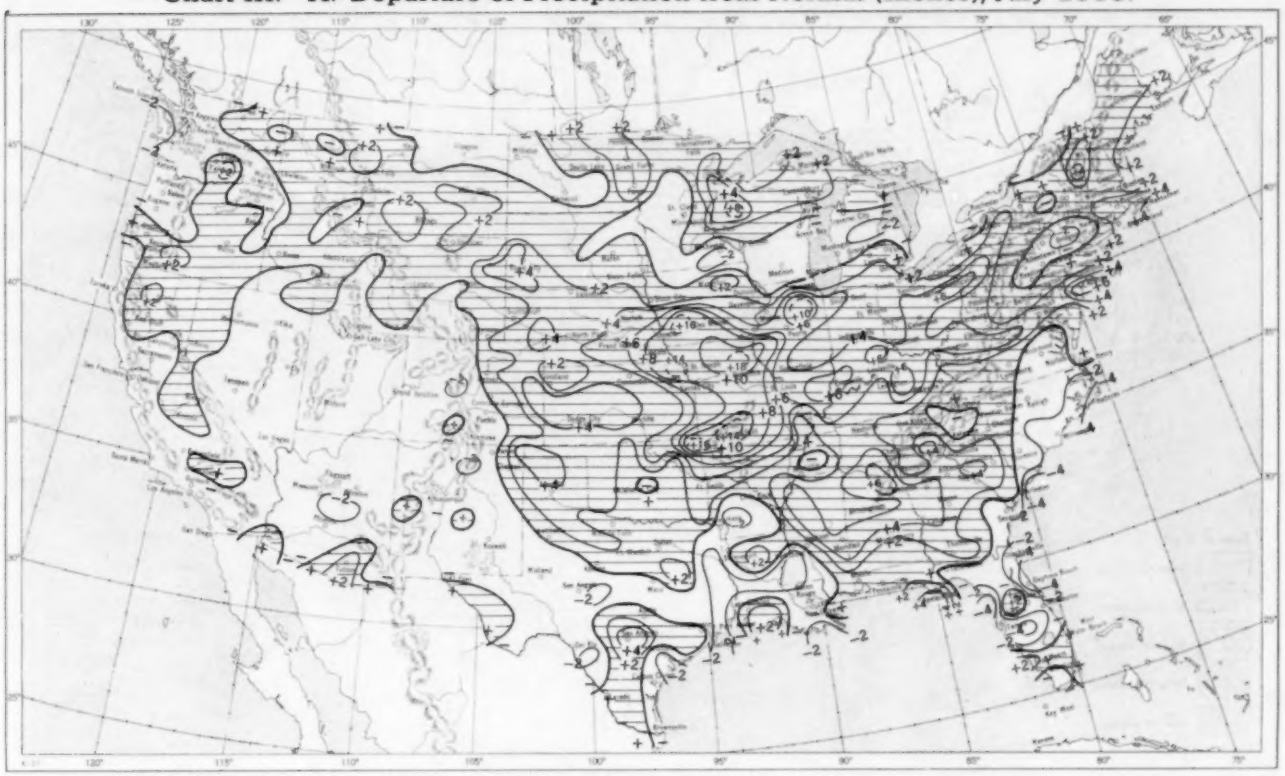

B. Percentage of Normal Precipitation, July 1958.

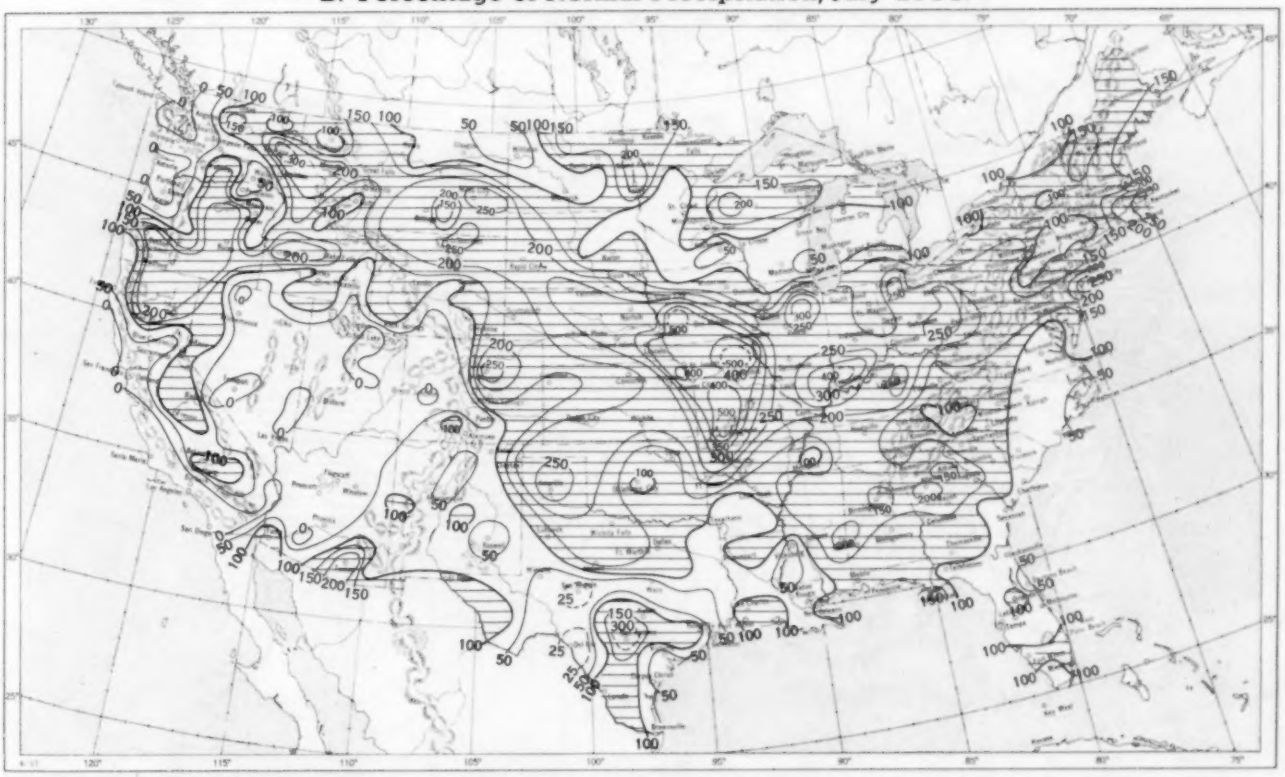

Normal monthly precipitation amounts are computed from the records for 1921-50 for Weather Bureau stations and from records of 25 years or more (mostly 1931-55) for cooperative stations.

Chart VI. A. Percentage of Sky Cover Between Sunrise and Sunset, July 1958.

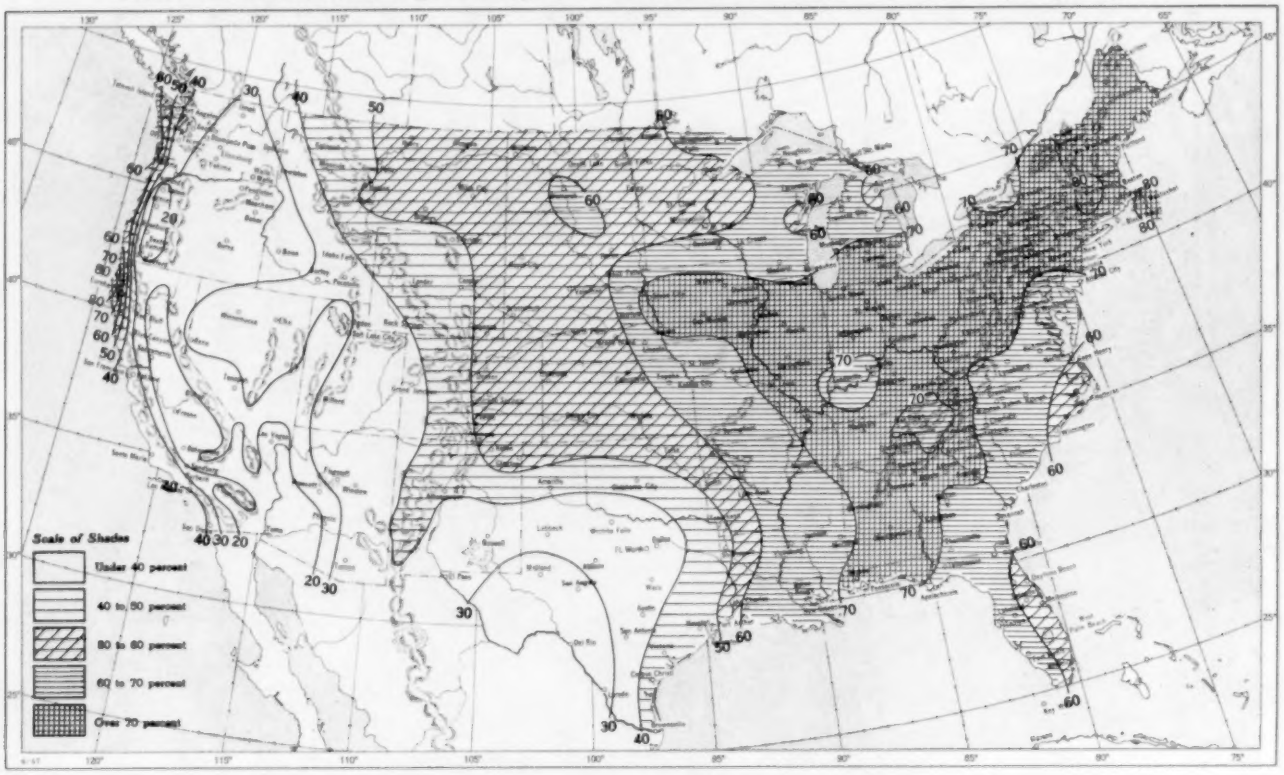

B. Percentage of Normal Sky Cover Between Sunrise and Sunset, July 1958.

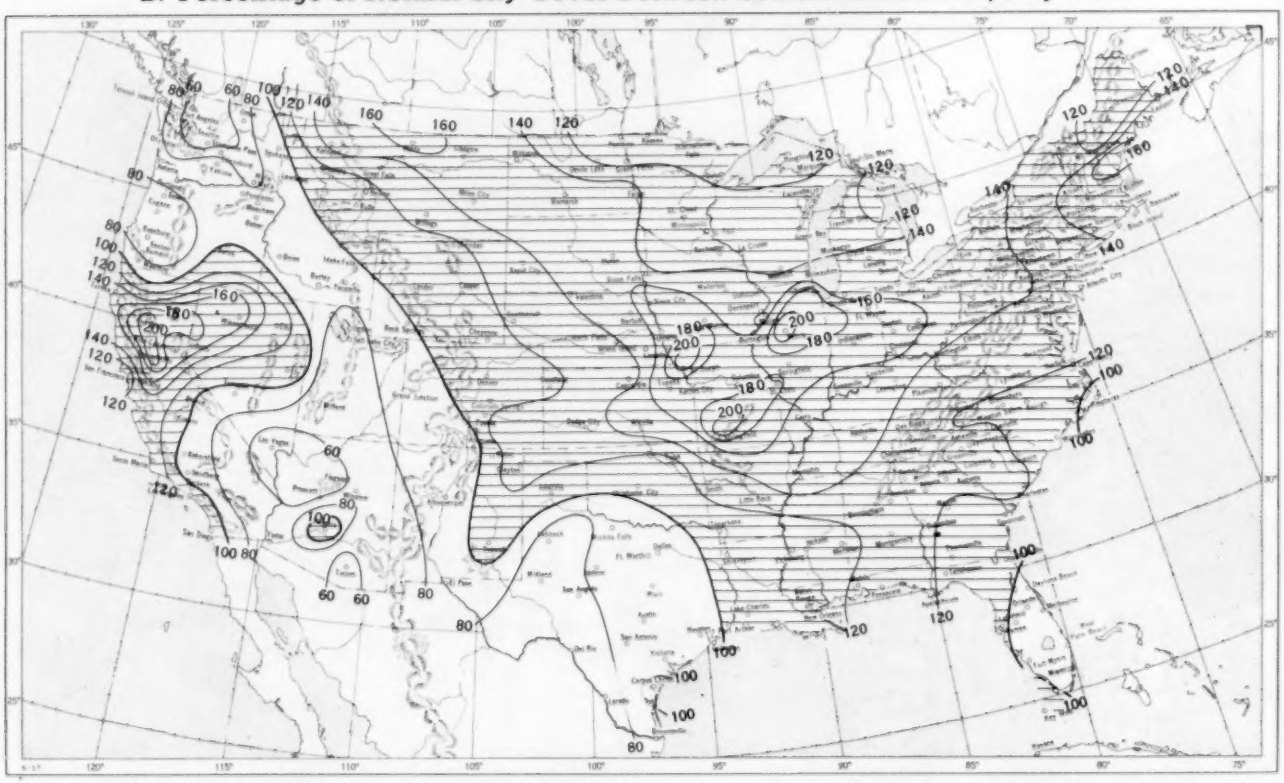

A. In addition to cloudiness, sky cover includes obscuration of the sky by fog, smoke, snow, etc. Chart based on visual observations made hourly at Weather Bureau stations and averaged over the month. B. Computations of normal amount of sky cover are made for stations having at least 10 years of record.

Chart VII. A. Percentage of Possible Sunshine, July 1958.

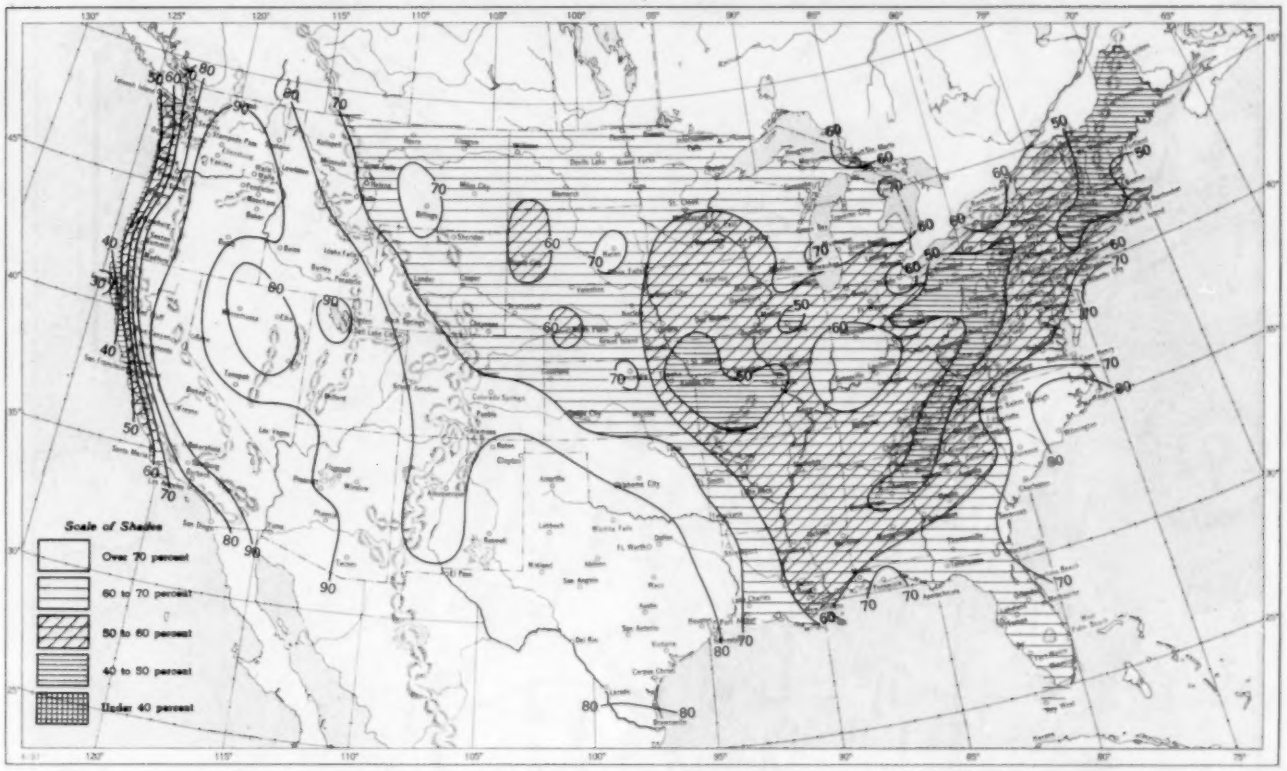

B. Percentage of Normal Sunshine, July 1958.

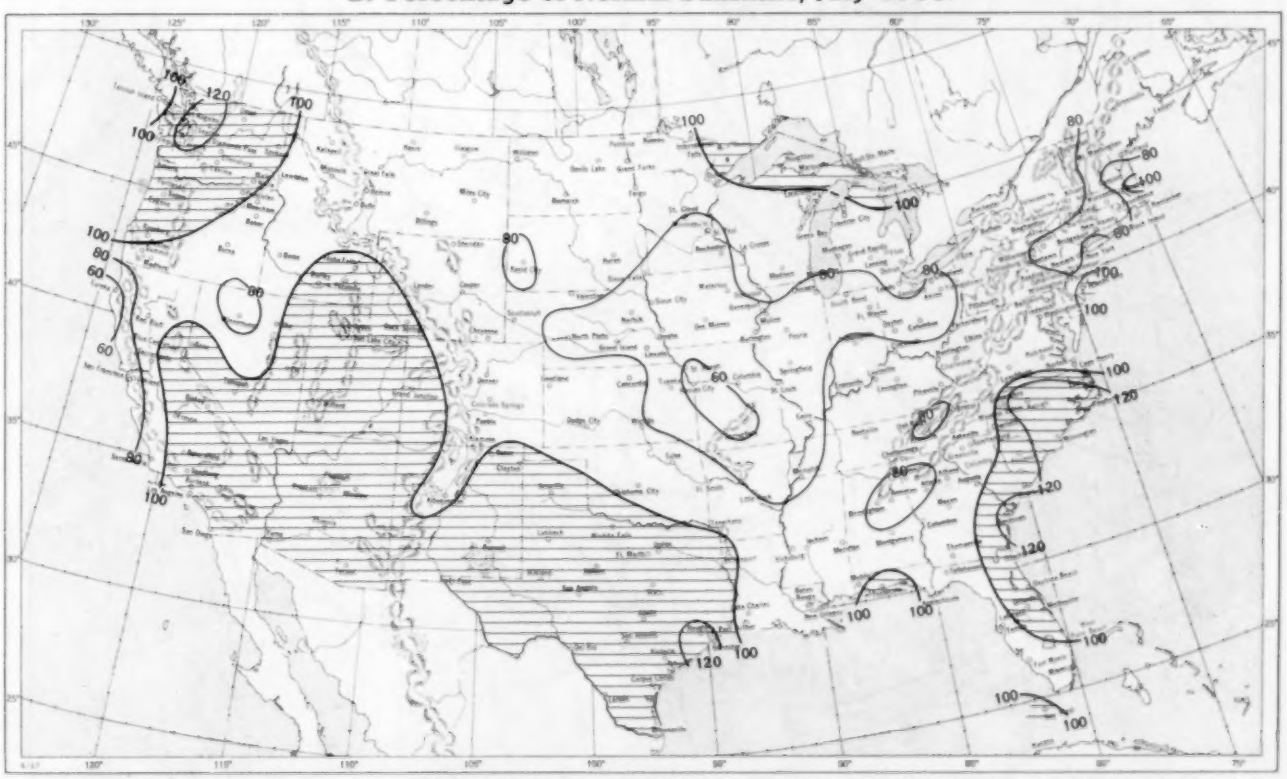

A. Computed from total number of hours of observed sunshine in relation to total number of possible hours of sunshine during month. B. Normals are computed for stations having at least 10 years of record.

Chart VIII. Average Daily Values of Solar Radiation, Direct + Diffuse, July 1958. Inset: Percentage of Mean Daily Solar Radiation, July 1958. (Mean based on period 1951-55.)

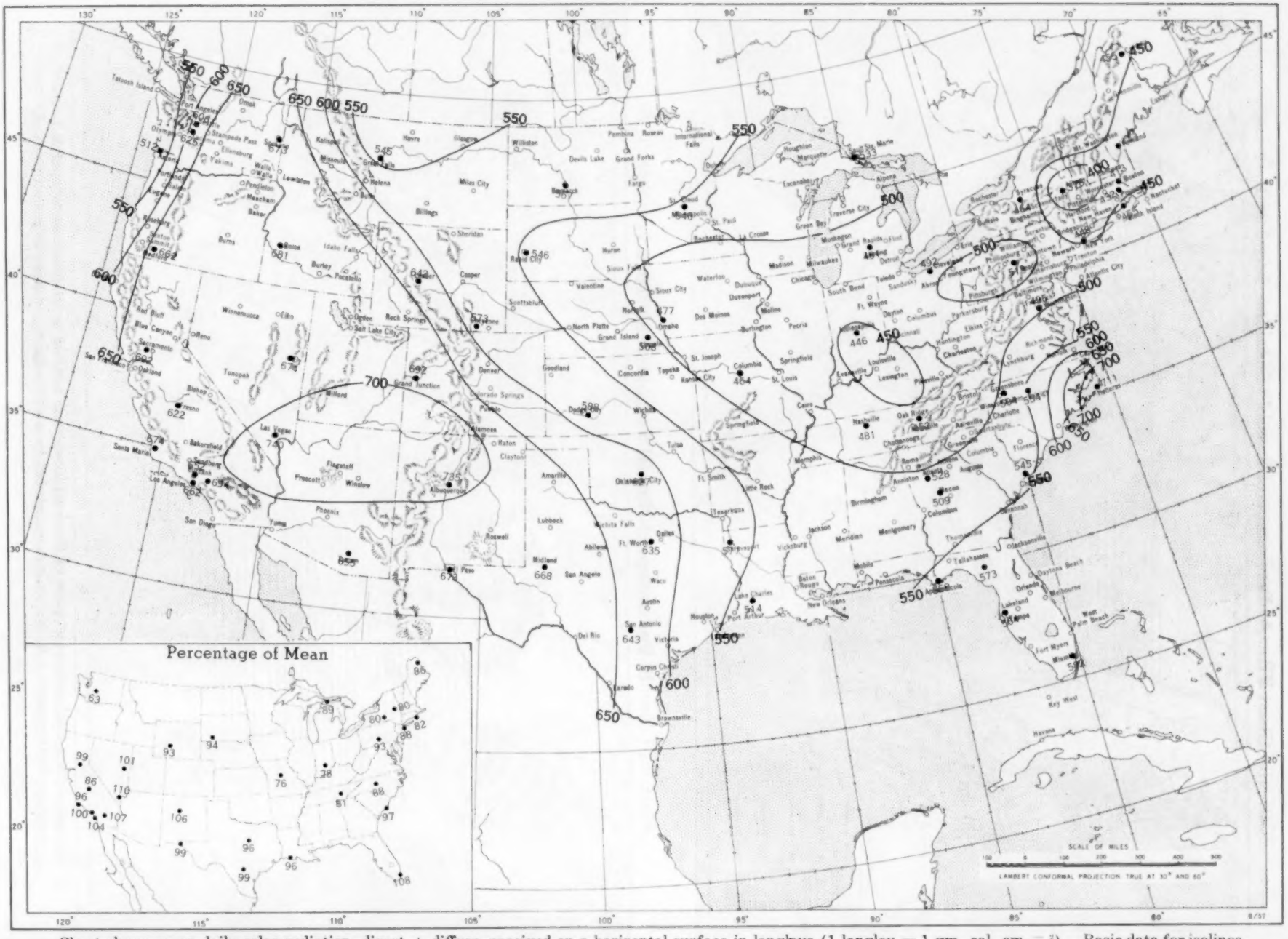

Chart shows mean daily solar radiation, direct + diffuse, received on a horizontal surface in langleys (1 langley = 1 gm. cal. cm. $^{-2}$). Basic data for isolines are shown on chart. Further estimates are obtained from supplementary data for which limits of accuracy are wider than for those data shown. The inset shows the percentage of the mean based on the period 1951-55.

Chart IX. Tracks of Centers of Anticyclones at Sea Level, July 1958.

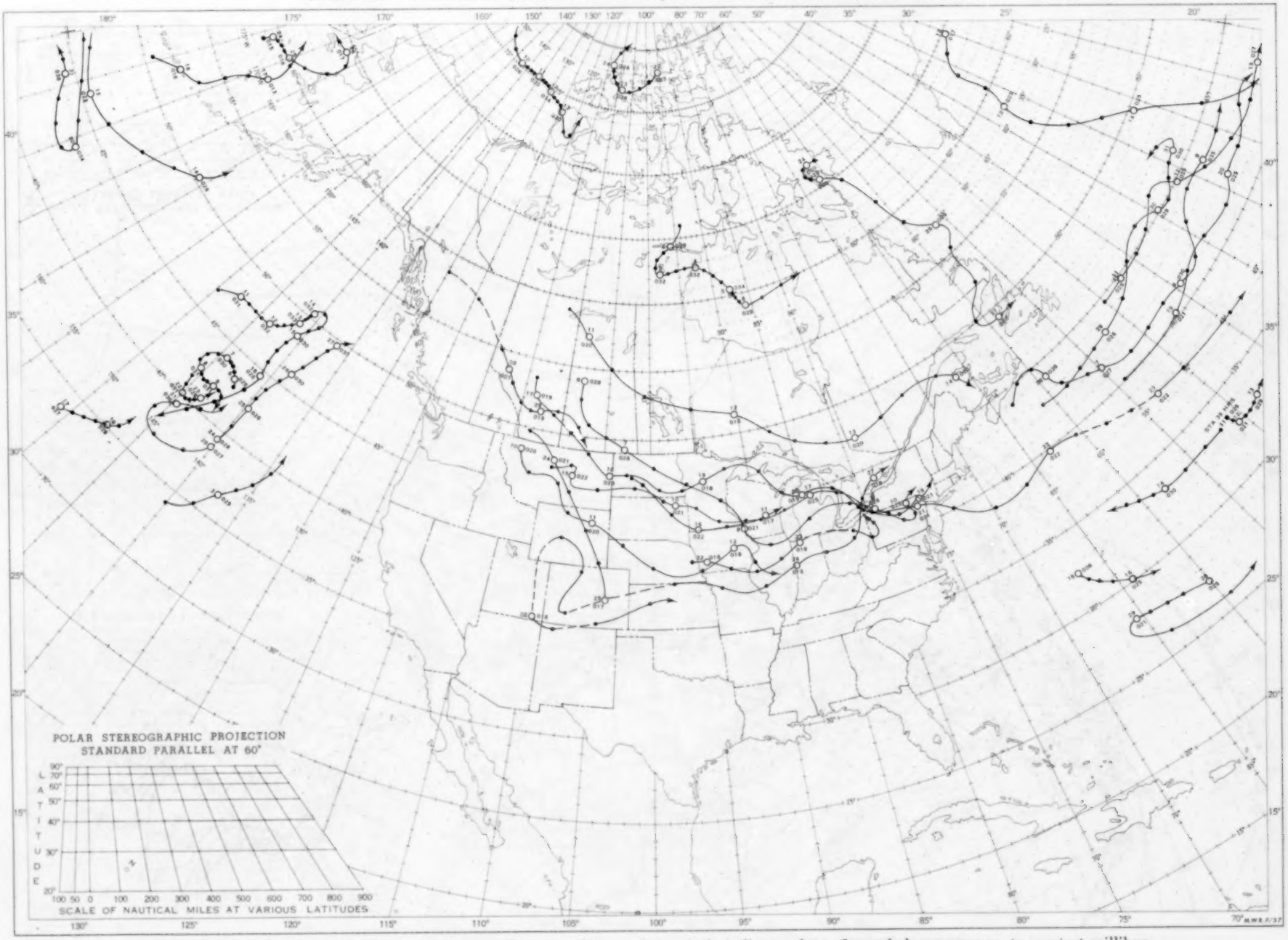

Circle indicates position of center at 7:00 a. m. E. S. T. Figure above circle indicates date, figure below, pressure to nearest millibar. Dots indicate intervening 6-hourly positions. Squares indicate position of stationary center for period shown. Dashed line in track indicates reformation at new position. Only those centers which could be identified for 24 hours or more are included.

Chart X. Tracks of Centers of Cyclones at Sea Level, July 1958.

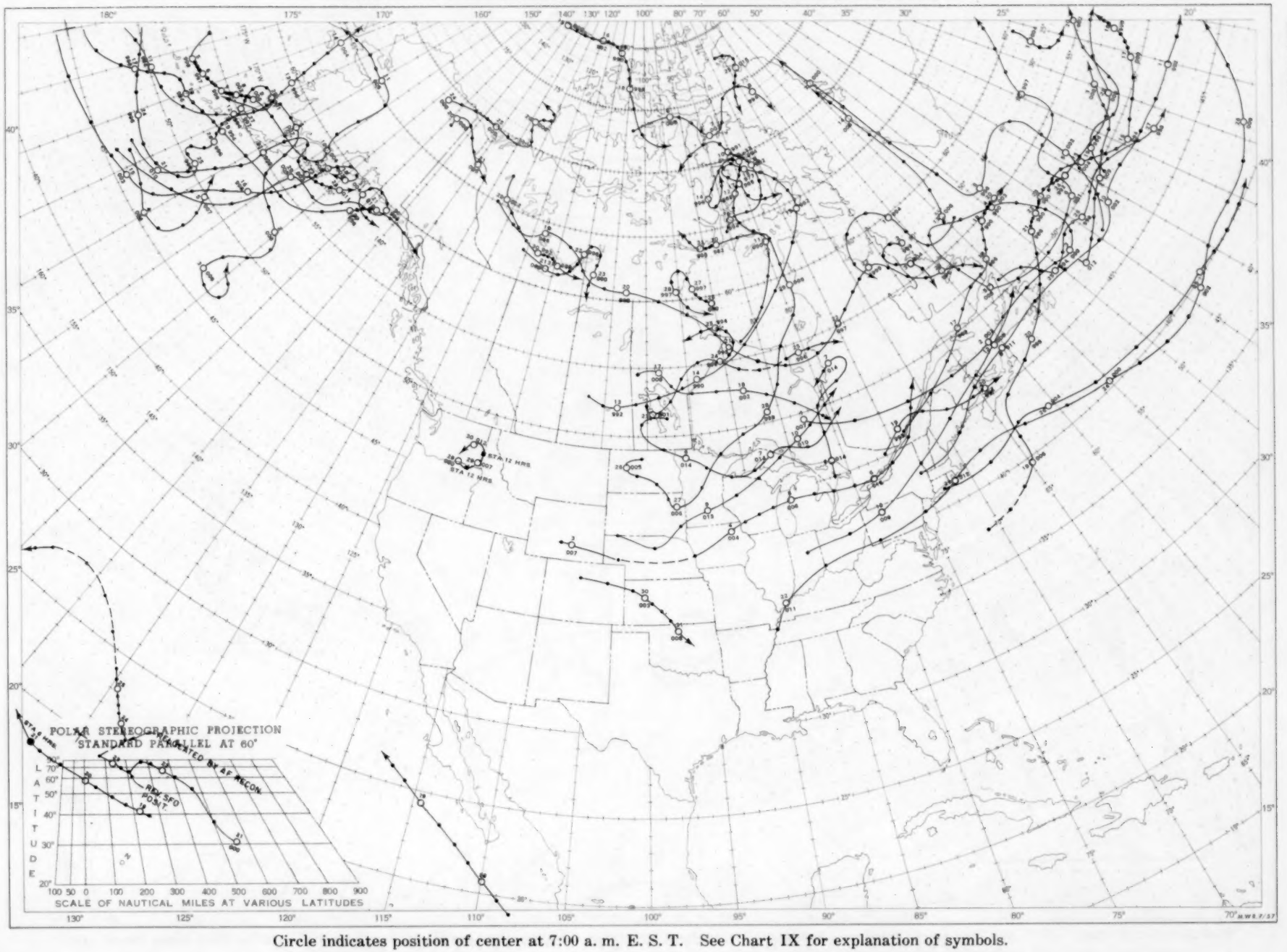

Circle indicates position of center at 7:00 a. m. E. S. T. See Chart IX for explanation of symbols.

Chart XI. Average Sea Level Pressure (mb.) and Surface Windroses, July 1958. Inset: Departure of Average Pressure (mb.) from Normal, July 1958.

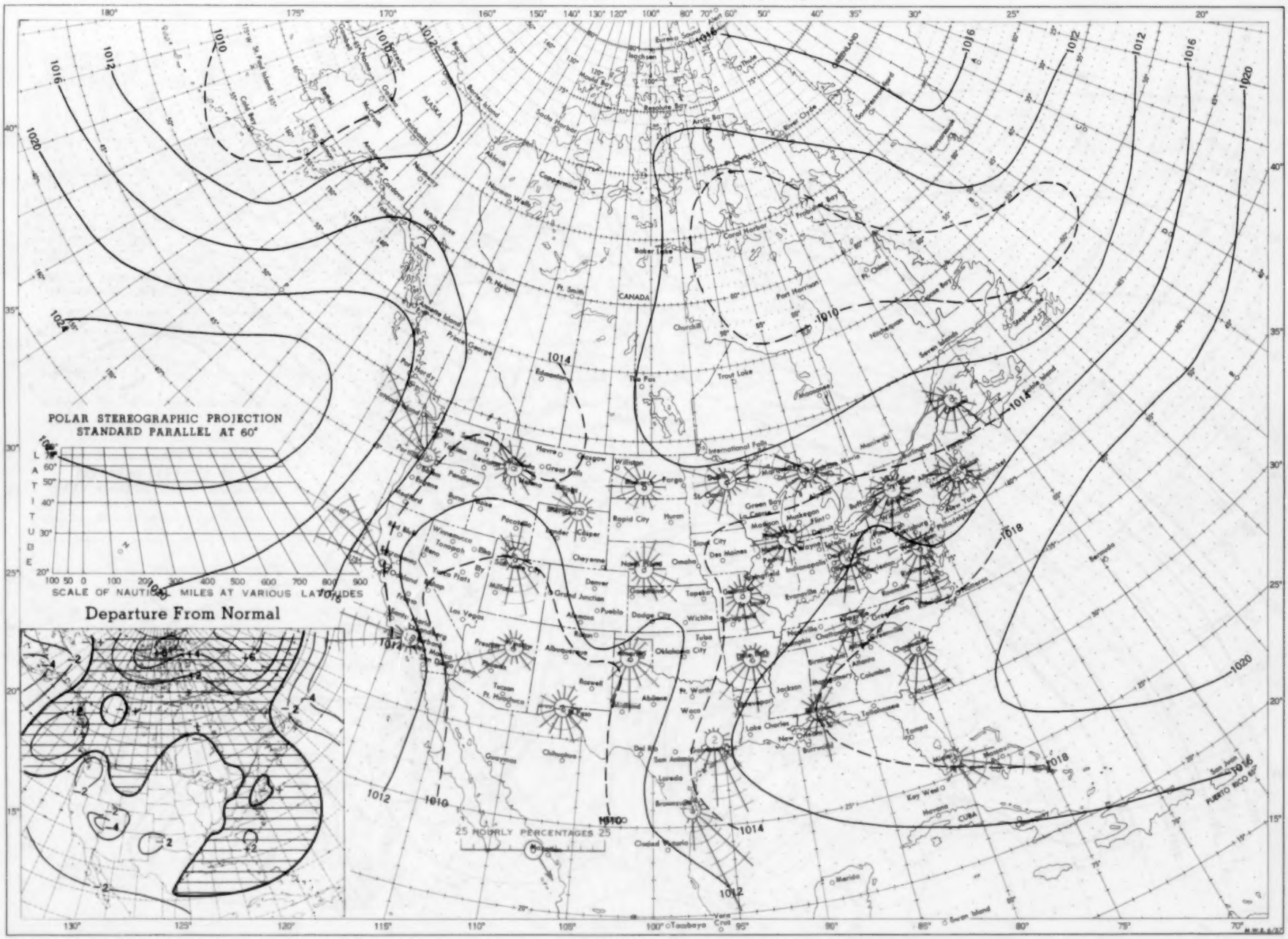

JULY 1958

Average sea level pressures are obtained from the averages of the 7:00 a. m. and 7:00 p. m. E. S. T. readings. Windroses show percentage of time wind blew from 16 compass points or was calm during the month. Pressure normals are computed for stations having at least 10 years of record and for 10° intersections in a diamond grid based on readings from the Historical Weather Maps (1899-1939) for the 20 years of most complete data coverage prior to 1940.

Chart XII. 850-mb. Surface, 1200 GMT, July 1958. Average Height and Temperature, and Resultant Winds.

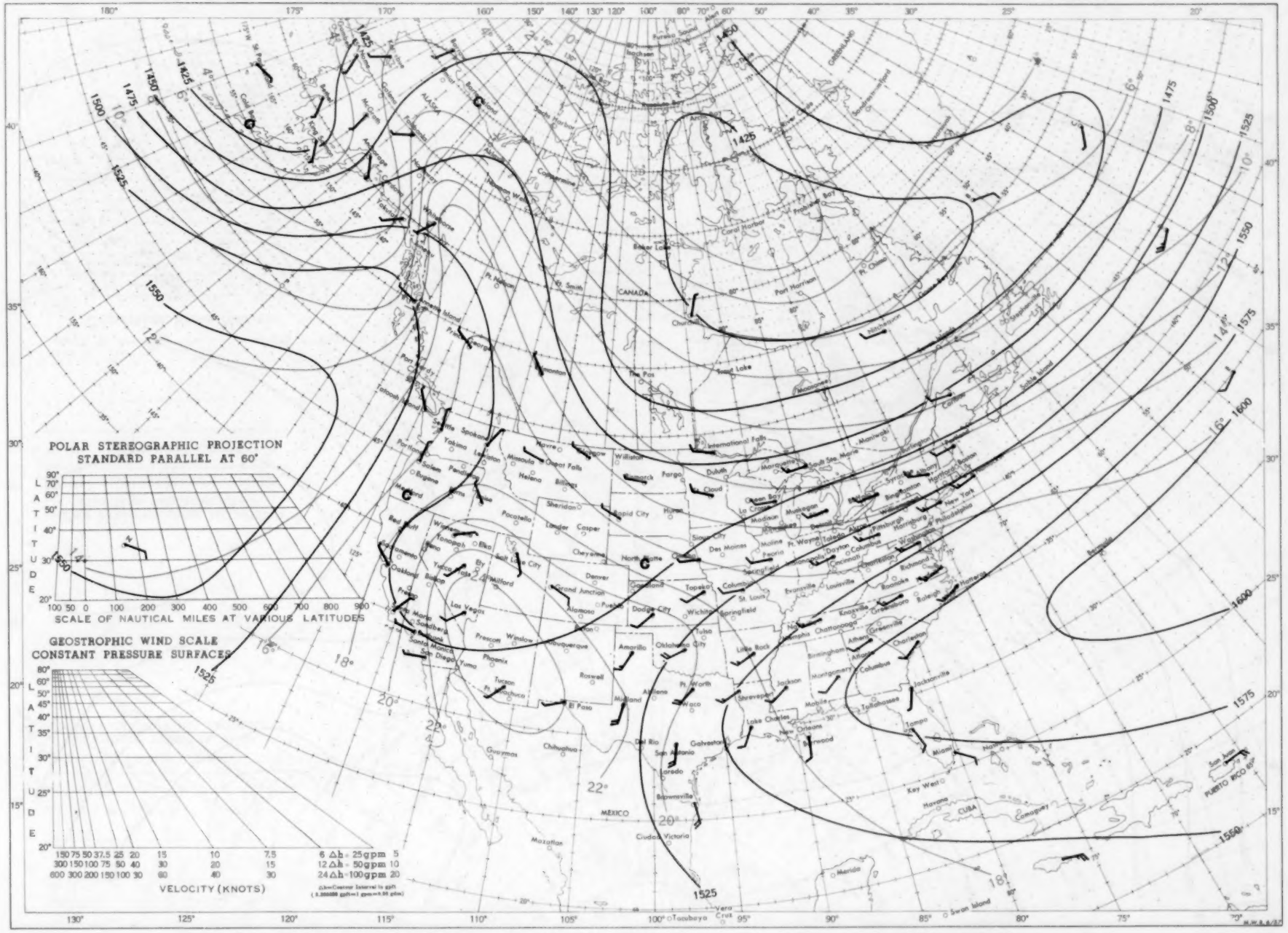

Height in geopotential meters (1 g.p.m. = 0.98 dynamic meters). Temperature in °C. Wind speed in knots; flag represents 50 knots, full feather 10 knots, and half feather 5 knots. All wind data are based on rawin observations.

Chart XIII. 700-mb. Surface, 1200 GMT, July 1958. Average Height and Temperature, and Resultant Winds.

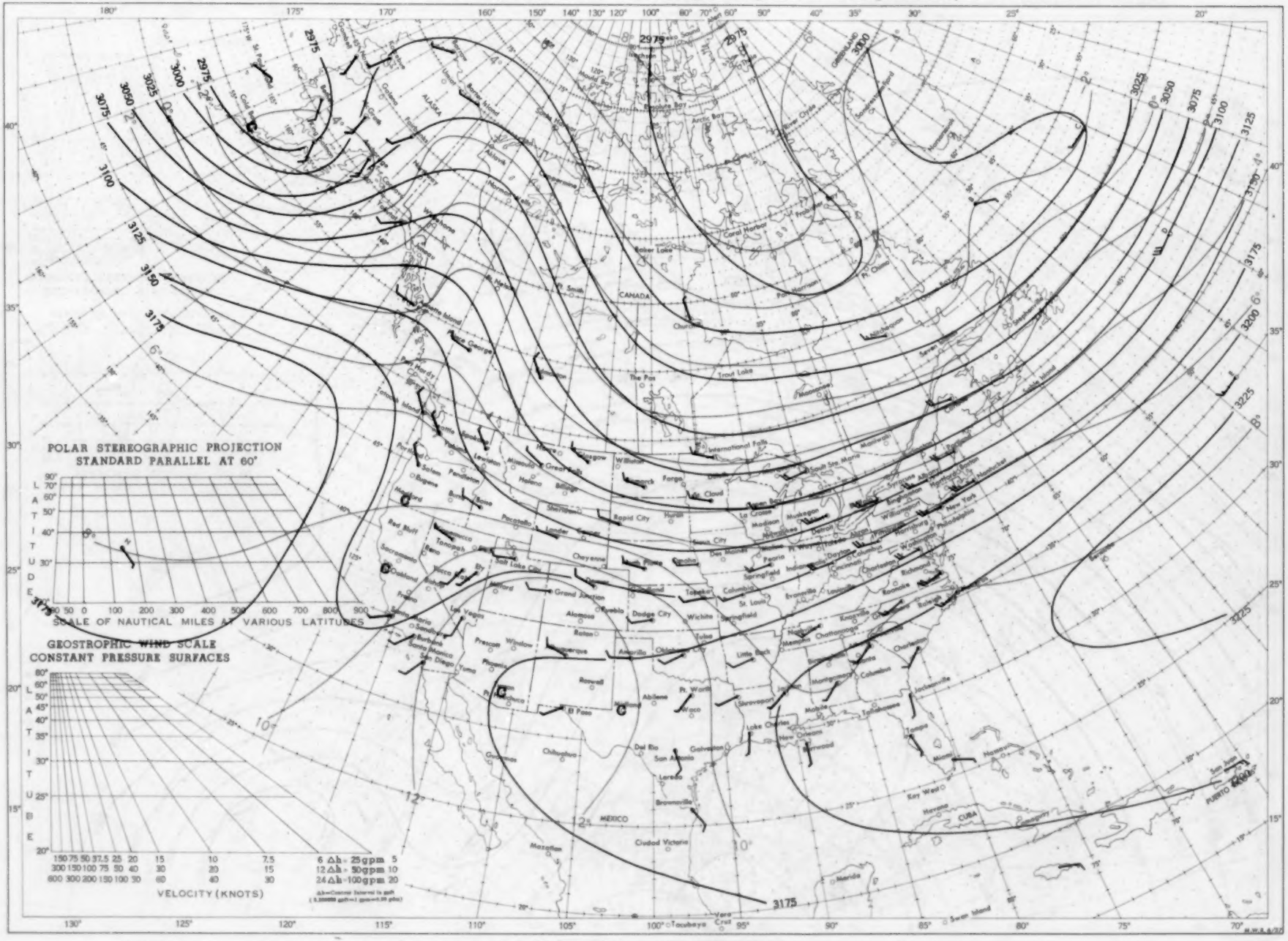

See Chart XII for explanation of map.

Chart XIV. 500-mb. Surface, 1200 GMT, July 1958. Average Height and Temperature, and Resultant Winds.

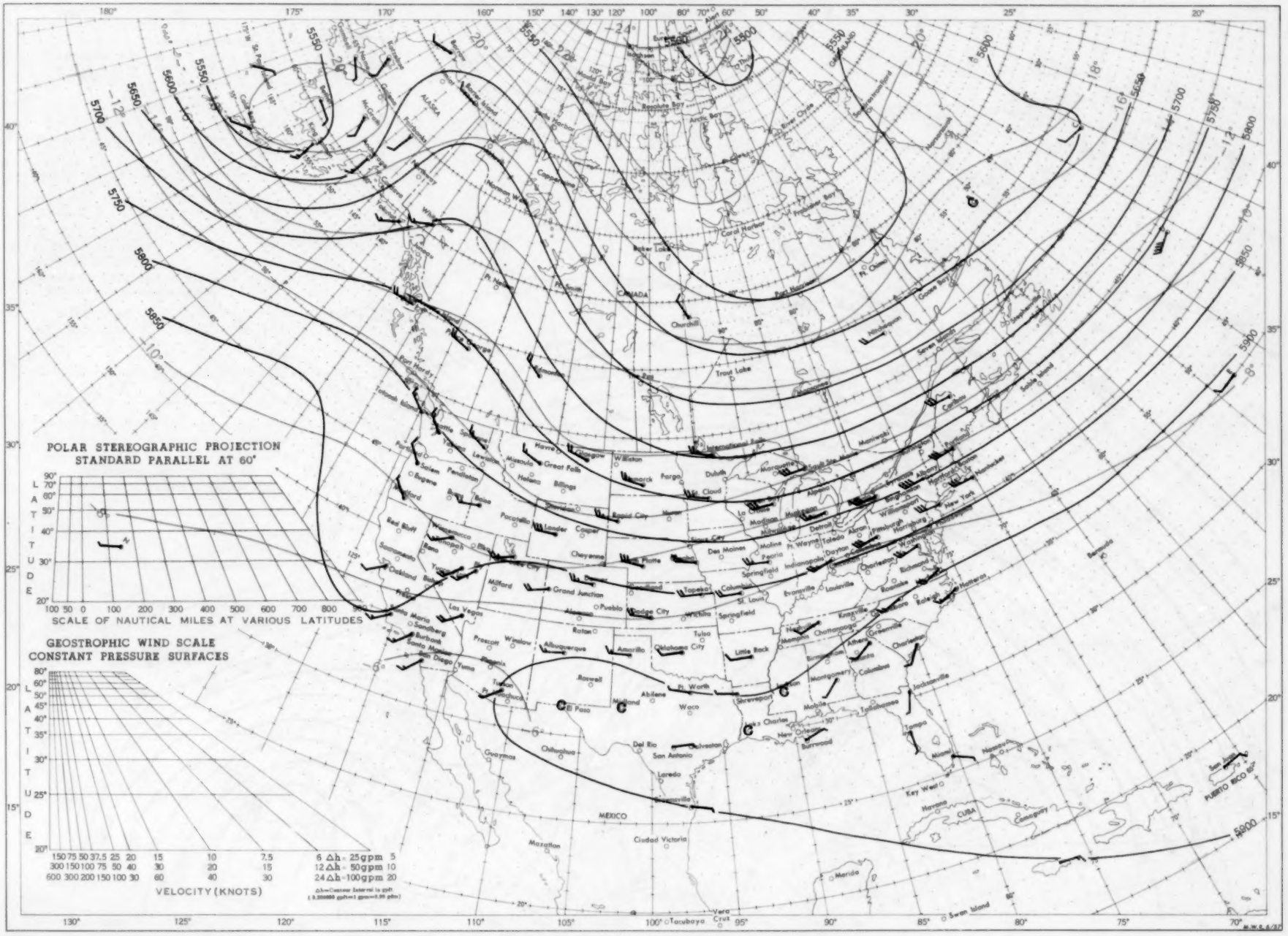

See Chart XII for explanation of map.

Chart XV. 300-mb. Surface, 1200 GMT, July 1958. Average Height and Temperature, and Resultant Winds.

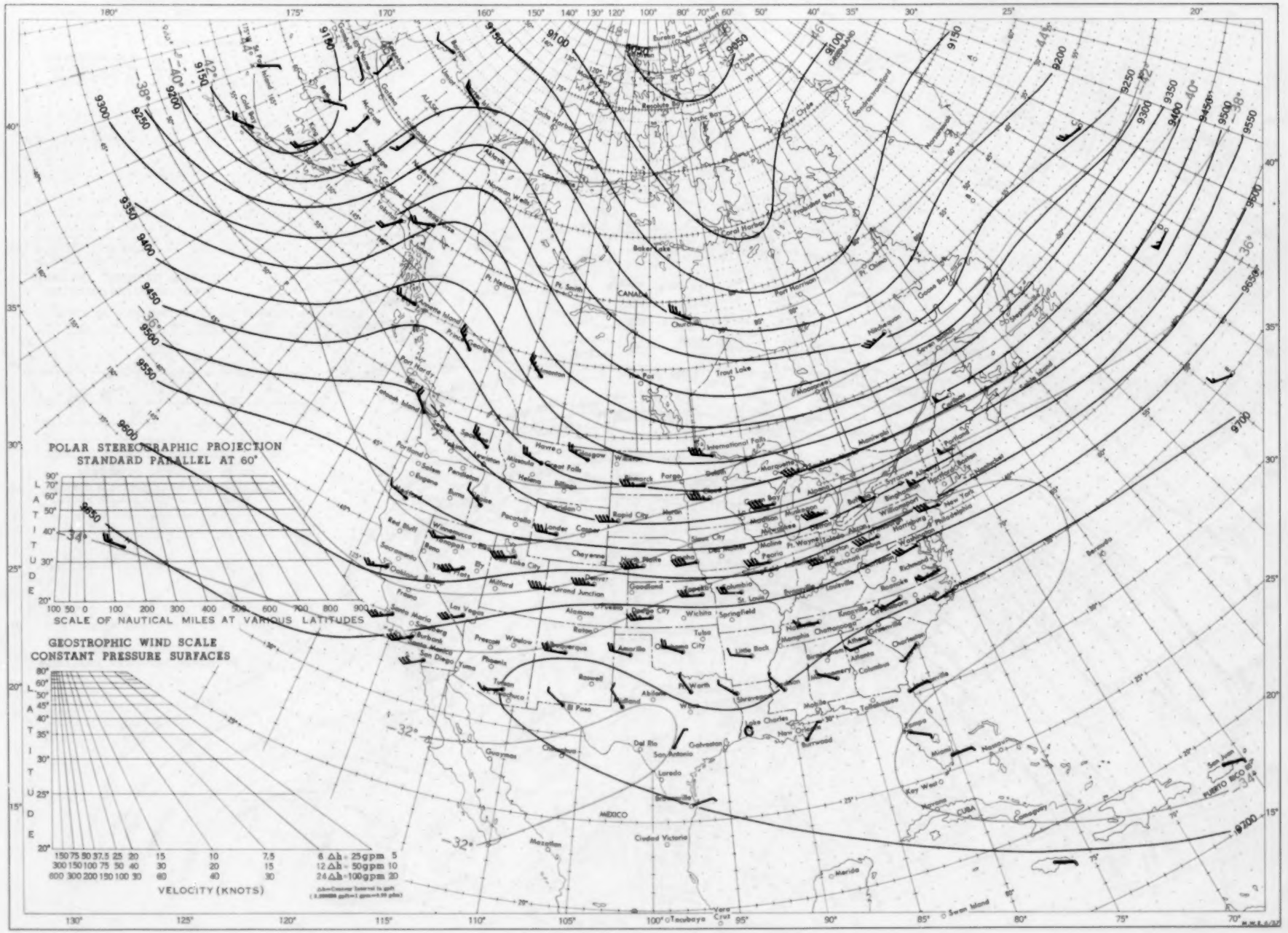

See Chart XII for explanation of map.

Chart XVI. 200-mb. Surface, 1200 GMT, July 1958. Average Height and Temperature, and Resultant Winds.

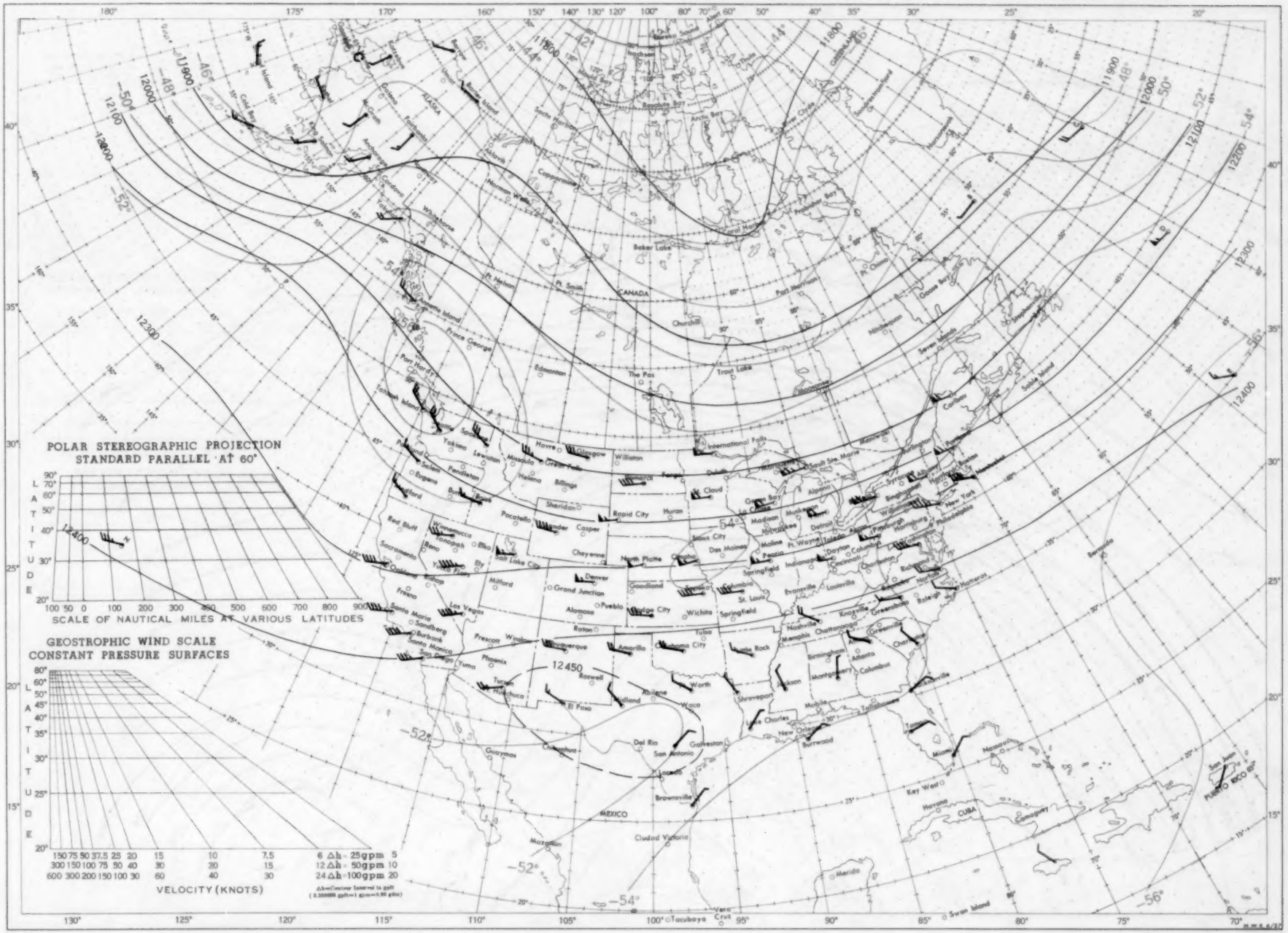
POLAR STEREOGRAPHIC PROJECTION
STANDARD PARALLEL AT 60°
LATITUDE
90° 70° 60° 50° 40° 30° 20°
100 50 0 100 200 300 400 500 600 700 800 900
SCALE OF NAUTICAL MILES AT VARIOUS LATITUDES
GEOSTROPHIC WIND SCALE
CONSTANT PRESSURE SURFACES
LATITUDE
80° 60° 50° 45° 40° 35° 30° 25° 20°
150 75 50 37.5 25 20 15 10 7.5
300 150 100 75 50 40 30 20 15
600 300 200 150 100 30 60 40 30
VELOCITY (KNOTS)
6 Δh = 25gpm 5
12 Δh = 50gpm 10
24 Δh = 100gpm 20
CANADA
MEXICO
CUBA
PUERTO RICO
Bermuda

See Chart XII for explanation of map.

Chart XVII. 100-mb. Surface, 1200 GMT, July 1958. Average Height and Temperature, and Resultant Winds.

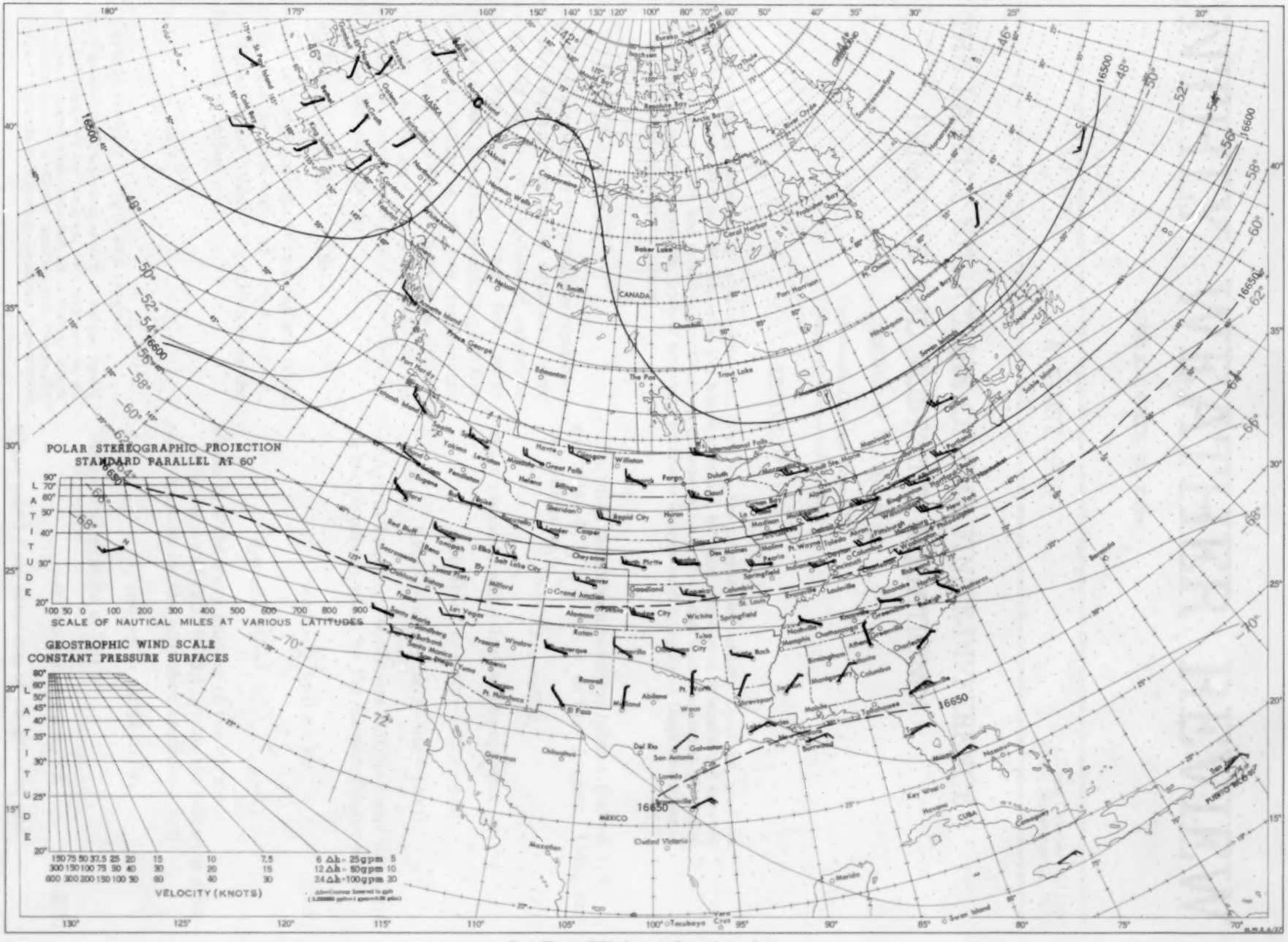

See Chart XII for explanation of map.